AN EXPERIMENTAL STUDY ON WGS CATALYSTS: RELATING PERFORMANCE UNDER REALISTIC FEED WITH OXYGEN HOLDING CAPACITY

by

Gözde Öztürk

B.S., Chemical Engineering, Middle East Technical University, 2015

Submitted to the Institute for Graduate Studies in
Science and Engineering in partial fulfillment of
the requirements for the degree of
Master of Science

Graduate Program in Chemical Engineering
Boğaziçi University

2018

to my family

ACKNOWLEDGEMENTS

First of all, I would like to state my truthful thanks to my thesis supervisor Prof. Ahmet Erhan Aksoylu for his patience, encouragement and guidance. It was a privilege for me to work with him since I have learned a lot from his wisdom and broad knowledge on catalysis and reaction engineering.

I wish to express my heartfelt gratitude to Dr. Burcu Selen Çağlayan for her profound guidance throughout my study and also for her expertise in XPS and Raman Spectroscopy analyses.

I would also like to thank the members of dissertation committee, Prof. Hüsnü Atakül and Prof. Ramazan Yıldırım, for accepting to be a member of the committee and for allocating their precious time to read and comment on my thesis.

My heartfelt thanks to Merve Eropak and Ali Uzun for their endless effort and leading me during my work. This accomplishment would not have been possible without them.

Very special thanks are for my dearest friends Canan Ezgi Doğan, Dilek Yiğit and Nazlı Urgav for their unceasing encouragement, help and joyful memories we shared. Deepest thanks to Orhun Acar Özdoğan for his encouragement, unfailing support and understanding. He has always been there to support me and cheer me up whenever I was need in.

I would like to thank Melek Selcen Başar and Burcu Acar for their help in the experimental systems. I also wish to express my gratitude to Cihat Öztepe for his willing to help without any hesitation. Thanks for the all members of KB 411-A, I feel very lucky to work with the CATREL team.

Intimate thanks for Bilgi Dedeoğlu for his technical assistance and also Melike Gürbüz, Başak Ünen, Yakup Bal and Murat Düzgünoğlu for their friendly approach. I also wish to thank to Bilge Gedik Uluocak for her effort in SEM analyses conducted at Boğaziçi University Advanced Technologies Research and Development Center.

Finally, I would like to express my sincere thanks and appreciation to my family, my mother Şükran Öztürk and my father İbrahim Öztürk, for their never-ending patience, encouragement and lasting care throughout my whole life. They have always been there to support me for every decision I made.

Financial support for this study was provided by TÜBİTAK through project 214M170. The financial support provided for both Gözde Öztürk and lab infrastructure by Republic of Turkey Ministry of Development through project 2016K121160 is greatly acknowledged.

ABSTRACT

AN EXPERIMENTAL STUDY ON WGS CATALYSTS: RELATING PERFORMANCE UNDER REALISTIC FEED WITH OXYGEN HOLDING CAPACITY

The present work is a part of an ongoing study aiming to design and develop high performance, steam tolerant, non-pyrophoric WGS catalyst(s) to be used in a demo-scale fuel processor (DFP) producing PEM grade hydrogen for PEM fuel cells. The current work mainly focuses on developing a reliable methodology for determination of oxygen storage capacity (OSC) of the catalysts through the use of *operando* IGA-MS analysis; and establishing a relation between WGS activity and OSC. In this context, Pt-Re-V/CeO_2 catalysts were prepared, characterized and tested in WGS performance tests for two realistic feed compositions at 300, 350, 400 and 450 °C for fixed GHSV at 120,000 ml g_{cat}^{-1} h^{-1}. The freshly reduced and spent samples were characterized by SEM, XPS, Raman spectroscopy and CO Chemisorption. The results of the catalytic tests indicated that 1Pt-1Re-1V sample having superior performance may be a great candidate to be used in a fuel processor with its high activity, selectivity and stability. The OSC values of the samples were determined through a novel *operando* IGA-MS methodology under two realistic feed compositions at 350 °C by fixed GHSV as 40,000 ml g_{cat}^{-1} h^{-1}. Additional OSC tests were also conducted at 400 and 450 °C over the sample having superior performance. The combined evaluation of WGS performance and *operando* OSC results point out that; there are two types of OSCs, structural (S-OSC) and effective (E-OSC), having prominent effect on WGS performance; increasing reaction temperature was found to have a negative effect on E-OSC; and the surface groups determined in S-OSC measurements have significant roles, *especially at the time when reactive mixture first contacts the catalyst*, in water activation, while, after surface concentrations and redox mechanism reach steady state, E-OSC becomes the primary factor affecting WGS activity.

ÖZET

WGS KATALİZÖRLERİ ÜZERİNE DENEYSEL BİR ÇALIŞMA: GERÇEKÇİ BESLEME KOŞULLARINDA ELDE EDİLEN PERFORMANS İLE OKSİJEN DEPOLAMA KAPASİTESİNİN İLİŞKİLENDİRİLMESİ

Yürütülen çalışma, hâlihazırda devam eden bir çalışmanın parçası olup PEM yakıt pilleri için H_2 üretimi gerçekleştiren demo ölçekli yakıt işlemcilerinde kullanılmak üzere yüksek performanslı, buhar toleransına sahip ve parlayıcı olmayan su-gaz değişimi reaksiyonu (WGS) katalizörleri dizayn etmeyi ve geliştirmeyi amaçlamaktadır. Bu çalışma, IGA-MS analizi ile katalizörlerin oksijen depolama kapasitelerinin (OSC) saptanması için güvenilir bir metot geliştirilmesi üzerine odaklanmış ve katalizörlerin WGS aktiviteleri ile OSC'leri arasında bir bağlantı kurmayı amaçlamıştır. Bu bağlamda, Pt-Re-V/CeO_2 katalizörleri hazırlanmış, karakterize edilmiş ve iki farklı gerçekçi besleme koşulunda ve 300, 350, 400 ve 450 °C sıcaklıklarda besleme hızının katalizör miktarına oranı 120,000 ml $g_{cat}^{-1}h^{-1}$ olarak sabit tutularak test edilmiştir. Taze indirgenmiş ve kullanılmış katalizörler SEM, XPS, Raman Spectroscopy ve CO Chemisorption karakterizasyon metotları kullanılarak incelenmiştir. Katalitik testlerin sonuçları göstermektedir ki 1Pt-1Re-1V katalizörü diğerlerine göre daha iyi aktivite, kararlılık ve seçicilik göstermesi nedeniyle yakıt işlemcilerinde kullanılma potansiyeli yüksektir. Katalizörlerin OSC değerleri, IGA-MS üzerinden geliştirilen yeni metot ile iki gerçekçi besleme koşulu ve 350 °C altında besleme hızının katalizör miktarına oranı 40,000 ml $g_{cat}^{-1}h^{-1}$ olarak sabit tutularak bulunmuştur. En iyi aktivite gösteren katalizör için 400 ve 450 °C'de ek testler gerçekleştirilmiştir. WGS performans testleri sonuçları ile OSC ölçümleri birlikte değerlendirildiğinde görülmektedir ki WGS performansı üzerinde belirleyici etkisi olan iki tip OSC değeri mevcuttur, yapısal OSC (S-OSC) ve efektif OSC (E-OSC). S-OSC ölçümlerinde saptanan yüzey gruplarının, özellikle de reaktif karışım katalizör ile ilk temas ettiğinde, su aktivasyonu için önemli bir rolü olduğu gözlemlenmiştir. Fakat yüzey konsantrasyonları ve redoks mekanizması stabil bir hal aldığında, E-OSC, WGS aktivitesini etkileyen birincil etken konumuna gelmiştir.

TABLE OF CONTENTS

LIST OF FIGURES

LIST OF TABLES

LIST OF SYMBOLS

F	Molar flow rate
$F_{i,in}$	Molar flow rate of species i in the feed stream
$F_{i,out}$	Molar flow rate of species i in the product stream
w_{cat}	Catalyst weight
P_{gas}	Pressure of the gas
R	Universal gas constant
T_{gas}	Temperature of the gas
V_{gas}	Volume of the gas
n_{gas}	Mole of the gas
MW_{gas}	Molecular weight of the gas
wt	Weight
ΔH°_{298}	Standard enthalpy of reaction

LIST OF ACRONYMS/ABBREVIATIONS

ATR	Auto-thermal Reforming
BSE	Back Scattering Electron
CP	Co-precipitation
DFP	Demo-scale fuel processor
DFT	Density Functional Theory
DI	Deionized
DP	Deposition-precipitation
DRF	Diluted Realistic Feed
DSMS	Dynamic Sampling Mass Spectrometer
E-OSC	Effective Oxygen Storage Capacity
FC	Fuel Cell
FP	Fuel Processor
FTIR	Fourier Transform Infrared Spectroscopy
GC	Gas Chromatograph
GHG	Green House Gases
GHSV	Gas Hourly Space Velocity
HPLC	High Performance Liquid Chromatography
HTS	High Temperature Shift
IGA	Intelligent Gravimetric Analyzer
IRAS	Infrared Absorption Reflection Spectroscopy
LPRD	Liquid Phase Reductive Deposition
LTS	Low Temperature Shift
MFC	Mass Flow Controller
MS	Mass Spectroscopy
OD	Outer Diameter
OSC	Oxygen Storage Capacity

OSCC	Oxygen Storage Capacity, Complete
OSR	Oxidative Steam Reforming
PEMFC	Proton Exchange Membrane Fuel Cell
PEM	Proton Exchange Membrane
PGM	Platinum Group Metal
PID	Proportional-integral-derivative
POX	Partial Oxidation
PROX	Preferential Oxidation
RF	Realistic Feed
SEM	Scanning Electron Microscopy
SE	Secondary Electron
S-OSC	Structural Oxygen Storage Capacity
SR	Steam Reforming
SS	Stainless Steel
TEM	Transmission Electron Microscopy
TCD	Thermal Conductivity Detector
TOF	Turn-over Frequency
TOS	Time-on-stream
T-OSC	Total Oxygen Storage Capacity
TOX	Total Oxidation
TPR	Temperature Programmed Reduction
TWC	Three-way Catalyst
WGS	Water-Gas Shift
XP	X-Ray Photoelectron
XPS	X-Ray Photoelectron Spectroscopy

1. INTRODUCTION

It is getting more and more difficult to satisfy the global energy demand in presence of increase in both human population and in their living standards. Fossil fuels, including coal, oil and natural gas, are the primary sources used in satisfying world's energy demand as they provide convenient, storable, transportable and energy-dense form of chemical energy. However, as the emission of greenhouse gases (GHG), such as carbon dioxide, methane and nitrous oxide during conventional fossil fuel based energy production to the atmosphere has been proven responsible for anthropogenic climate change, the fast transformation of conventional energy production routes becomes crucial, and studying alternative energy production technologies has become an important research topic (Sathre, 2014; Höök *et al.*, 2013).

Hydrogen has been regarded as the fuel of future owing to its clean and high energy carrier nature. Water splitting and biogas reforming are some renewable technologies to produce hydrogen however both are not economically feasible to be applied in large scale operations (Gonzales-Castano *et al.*, 2015; LeValley *et al.*, 2014). Considering the technical hurdles and cost of storing and transporting hydrogen; fuel processors, that produce hydrogen on site from hydrocarbons, like metane/bio-methane, can be integrated with fuel cell technology to generate electricity at small scale. The use of fuel cells is a viable option in clean energy production, and the prominent fuel cell type in small scale stationary applications is proton exchange membrane fuel cell (PEMFC), which has many advantages over others such as low operating temperature, low weight, compactness, fast start-up and suitability to discontinuous operation (Ghenciu, 2005).

In FPs suitable to be used in FP-PEMFC systems, there are mainly three catalytic reactions taking place in series: (i) reforming of hydrocarbons; (ii) water-gas shift (WGS) reaction which decreases carbon monoxide while increasing hydrogen concentration, i.e. enriching the reformer outlet; and (iii) preferential carbon monoxide oxidation (PROX) for complete elimination of CO. In the reformer, the hydrocarbon(s) are converted into a H_2-

rich mixture containing H_2, H_2O, CO and CO_2 via steam reforming (SR), partial oxidation (POX) or oxidative steam reforming (OSR). In case of OSR, steam and oxygen are both present in the feed. In the following WGS unit, which conventionally includes two, high- and low-temperature shift, reactors, CO concentration of the reformer outlet is decreased down to 1-1.5 % range, and the following PROX reactor is used to reduce CO concentration further down to 10-50 ppm, the level that guarantees stable operation of PEMFCs (Çağlayan *et al*., 2008; Önsan, 2007).

Water-gas shift reaction, first reported in 1888, is one of the oldest catalytic processes employed in chemical industry which became well-known along with being used in Haber ammonia synthesis. WGS reaction is a reversible and moderately exothermic reaction in which CO reacts with H_2O to generate CO_2 and H_2 (Mond and Langer, 1888; Saeidi *et al.*, 2016). Since WGS is a slightly exothermic reaction, it is kinetically favored at high temperatures while thermodynamically favored at low temperatures. Due to equilibrium constraints, WGS is conventionally conducted in two consecutive reactors called high temperature shift (HTS) and low temperature shift (LTS) reactor. High temperature shift reactor operates at 623-643 K, and the reaction is conventionally conducted over iron/chromium based catalysts. The operation temperature of low temperature shift reactor is 473-493 K, and the use of copper/zinc based catalysts is preferred for catalyzing the reaction (Perez *et al*., 2014). However, this conventional WGS technology imposing the use of two WGS reactors is hard to be downsized and effectively incorporated to small scale FPs due to the requirement of large reactor volume(s) due to low activity, pyrophoric nature and incompatibility to transient state operation. Instead of conventional two stage WGS units, using a single stage WGS unit operating in HTS-LTS transition temperature in FPs is worth to investigate (Zhu *et al*., 2011; Xu *et al*., 2012).

The design and development of efficient WGS catalysts for FP applications and establishing structure-activity relation for WGS catalytic systems have become crucial for proliferated use and success of the FP-PEMFC technology. Hence, many researchers have focused on the design and development of active, stable and non-pyrophoric catalysts with improved redox and reducibility properties (Çağlayan and Aksoylu, 2009). Thus, noble

metal, especially Pt and Au-based, catalysts on reducible oxides has gained great attention due to their non-pyrophoric behavior and high activity (Lee *et al.*, 2007). Moreover, there have been very comprehensive studies on the design and development of catalysts with noble metals on supports having high reducibility and enhanced redox properties which are in a close relation with WGS activity (Kugai *et al.*, 2011).

The present work is a part of an ongoing study aiming to design and develop high performance, steam tolerant, non-pyrophoric WGS catalyst(s) to be used in a demo-scale fuel processor (DFP) producing PEM grade hydrogen for FP-PEMFC applications. The current work mainly focuses on developing a reliable methodology for determination of oxygen storage capacity (OSC) of the catalysts through the use of *operando* IGA-MS analysis; and establishing a relation between WGS activity and OSC. In that context, selected Pt-Re-V systems prepared on CeO_2 were tested by their WGS performance for realistic conditions, an *operando* methodology for the determination of their oxygen storage capacities under the same conditions was proposed, the OSC values of the samples were determined, and -*through a comparative analysis*- a relation between WGS performance and OSCs was established.

Chapter 2 includes a detailed literature survey about fuel processors and fuel cell technology, WGS reaction and the catalysts used in this reaction, followed by the oxygen holding capacity concept and its relationship with WGS activity. In Chapter 3 the experimental work is explained in detail. The results of conducted tests are presented and discussed in Chapter 4. Finally, the conclusions from the current study and the recommendations for the future work are given in Chapter 5.

2. LITERATURE SURVEY

2.1. Fuel Cell and Fuel Processor Technology

In course of time, growing concerns about environmental problems such as climate change, ozone layer depletion and acidic rains, has motivated the studies on fuel cells owing to their clean and efficient mechanism for energy conversion. Fuel cells are the electrochemical devices that provide one-step conversion of chemical energy into electrical energy which ensures no harmful emission; produces only water in case of fueled by hydrogen. Since the overall efficiency in a system decreases by increasing the number of energy conversion steps involved, conversion of chemical energy directly into electrical energy in fuel cells makes them having high efficiency (Zharaf and Orhan, 2014).

Fuel cells are categorized according to the electrolyte used and proton exchange membrane fuel cells have been recognized one of the most promising types for small scale applications due to their easy scale-up, low operating temperature, fast start up and high power density features (Wang *et al.*, 2010).

The most favorable fuel for PEMFCs appears to be hydrogen which is ionized at the anode of the cell. However, technological obstacles still exist to overcome the hydrogen transportation and storage problems which have led fuel processors in which hydrocarbon fuel is converted into hydrogen on board to be used in combined with fuel cells. PEMFCs have platinum-catalyzed electrodes making them intolerant to impurities, especially carbon monoxide which will poison the catalysts in the cell when the level of it above about 1-100 ppm. Therefore, fuel processors must be designed accordingly to meet these CO level requirements (Trimm and Önsan, 2011).

In a fuel processor (FP), there are three catalytic units in series: reformer unit, in which hydrocarbons are converted to hydrogen, water-gas shift reaction (WGS) to reduce the CO amount while enriching the hydrogen concentration, and preferential carbon monoxide

oxidation (PROX) for further elimination of CO amounts to trace levels necessary for stable operation of PEMFCs (Çağlayan *et al.*, 2005).

Reformer unit, the initial catalytic unit of fuel processors, converts hydrocarbon fuels to hydrogen containing mixture which also includes CO, CO_2 and H_2O (Iulianelli *et al.*, 2014). Reforming unit can utilize a broad array of fuels such as methane, ethane, methanol, ethanol, acetone and higher hydrocarbons etc. as feed stocks. Apart from all these, the leading source of hydrogen is reforming of gaseous fuels and lately methane steam reforming (SR) has drawn considerable interest owing to giving highest quantity of hydrogen and preferable byproduct formation taking other feeds into account. The general equation of SR reaction is shown below in Equation 2.1:

$$C_nH_m + nH_2O \rightarrow nCO + \left(n + \frac{m}{2}\right) H_2 \qquad (2.1)$$

Steam reforming is an extremely endothermic reaction being performed at high temperatures between 750 °C and 1450 °C which can be regarded as a disadvantage since it needs high amount of heat to shift the equilibrium to the right in order to produce H_2 and CO. Since it is cheap and quite active, nickel is most widely used metal in steam reforming catalysts. Still Ni-based catalysts have some drawbacks as tendency to sulfur poisoning, carbon formation on surface and sintering due to conditions required for SR (LeValley *et al.*, 2014; Nahar *et al.*, 2017). Although the highest hydrogen amount is obtained by steam reforming, the necessities of high heat, large amount of catalyst loadings and large reactors make this reaction not suitable for on-board FP-FC systems (Avcı *et al.*, 2004).

Partial oxidation (POX) (Equation 2.2) is other reforming reaction to generate H_2 which has exothermic nature and by this reaction using oxygen or air as oxygen source, hydrocarbon fuels are converted to H_2 and CO. In case of total oxidation (TOX) (Equation 2.3) on the other hand, the final products are H_2O and CO_2 (Nahar *et al.*, 2017):

$$C_nH_m + \frac{n}{2}O_2 \rightarrow nCO + \frac{m}{2}H_2 \qquad (2.2)$$

$$C_nH_m + (n + \frac{m}{4})\, O_2 \rightarrow nCO + \frac{m}{2} H_2O \qquad (2.3)$$

Integration of SR and POX processes energetically to reduce the high external energy requirement of endothermic steam reforming reaction by supplying energy from exothermic partial oxidation reaction, called auto-thermal reforming (ATR), has been achieved leading to low energy need due to combination of SR and POX, high gas space velocity and fixed H_2/CO ratio (Escritori *et al.*, 2009; Freni *et al.*, 2000).

In the second unit of a fuel processor fed by the effluent stream of reformer, water-gas shift reaction occurs which is convenient process for further purification capable of not only enriching hydrogen content also reduces CO amount in exit stream (Chen *et al.*, 2017):

$$CO + H_2O \leftrightarrow CO_2 + H_2 \qquad \Delta H^{\circ}_{298} = -41.2\ \mathrm{kJ/mol} \qquad (2.4)$$

WGS reaction is exothermic and reversible reaction and at the end of WGS unit, the CO concentration is reduced to 0.5-1 mole %. Water-gas shift reaction is kinetically favored at high temperatures while the reaction equilibrium shifts to the right and enables the formation of products H_2 and CO_2 at lower temperatures. Thus, the reaction is conducted in two reactors: high-temperature shift (HTS) reactor which converts 90% of CO to H_2 operating at temperature of 623-643 K and low temperature shift (LTS) reactor in which 90% of the remaining CO is converted. The most prevalent catalysts used in industrial applications for HTS and LTS reactions are Fe_2O_3/Cr_2O_3 and $Cu/ZnO/Al_2O_3$, respectively (Haryanto *et al.*, 2005).

Last catalytic unit of the fuel processor is the preferential oxidation unit that is necessary for further purification of hydrogen to feed the stream to the PEMFC as fuel which should not have levels of CO above 50 ppm for stable operation since carbon oxide is toxic to Pt-based electrode. One of the challenges for PROX unit is finding a catalyst which is selective for carbon monoxide oxidation (Equation 2.5) since hydrogen oxidation (Equation

2.6) competes with carbon monoxide oxidation as an undesired phenomenon (Marino *et al.*, 2004; Mohammed *et al.*, 2016).

$$CO + {}^{1}/_{2}\, O_2 \rightarrow CO_2 \qquad \Delta H^{\circ}_{298} = -283\ \text{kJ/mol} \tag{2.5}$$

$$H_2 + {}^{1}/_{2}\, O_2 \rightarrow H_2 \qquad \Delta H^{\circ}_{298} = -242\ \text{kJ/mol} \tag{2.6}$$

The oxidation of carbon monoxide is usually conducted at lower temperatures while the oxidation of hydrogen needs higher temperatures. Therefore, the temperature should be selected carefully, 100-130°C range is ideal, to suppress the undesirable hydrogen oxidation reaction which brings about a decrease in hydrogen amount. The most focused catalysts are Pt-based ones which are the most resistant toward catalyst deactivation (Çağlayan *et al.*, 2011; Romero-Sarria *et al.*, 2016).

2.2. Water Gas Shift Reaction

The water gas shift reaction, -moderately exothermic, reversible and equilibrium-controlled reaction- is of crucial importance since it leads to hydrogen concentration rise while reducing the CO amount in the reformate:

$$CO + H_2O \leftrightarrow CO_2 + H_2 \qquad \Delta H^{\circ}_{298} = -41.2\ \text{kJ/mol} \tag{2.4}$$

WGS was first reported in 1881; however, it became popular with being used in Haber process as source of hydrogen. It has wide usage area in the industry for the production of ethanol, ammonia, hydrogen to be utilized for hydrogenation reactions in the petrochemical industry and hydrocarbons (by Fischer-Tropsch process) (Ratnasamy and Wagner, 2009).

WGS reaction is limited thermodynamically at high temperatures and it is kinetically controlled at low temperatures. In order to handle these thermodynamic and kinetic limitations, WGS is performed in two reactors in series called high temperature shift reactor (HTS) and low temperature shift reactor (LTS) in industrial scale operations, respectively. The high temperature shift reaction is carried out over FeCr-based catalysts at operating

temperatures of 350-500 °C (Jha *et al.*, 2017). The addition of chromium to the iron enhances the stability of catalyst and helps to mitigate of sintering. On the other hand, low temperature shift reaction is conducted over Cu/oxide-based catalysts at 180-250 °C. These catalysts have been recognized as highly selective for WGS reaction and consequently, giving high conversion. But they are not resistant to sulphur, sensitive to temperature and highly pyrophoric in presence of air (LeValley *et al.*, 2014). Conventional Cu based and ferrochrome catalysts are not appropriate for small scale applications owing to their long start-up times, requiring large volume and weight, pyrophoric nature and sensitivity to poison (Miao *et al.*, 2017). Accordingly, there has been progressively increasing interest on developing active, water tolerant, poison resistant, non-pyrophoric, stable and selective to WGS reaction which should not lead to methanation reaction that consumes H_2 (Equation 2.7) catalysts to be used in PEMFC-FP technology (Çağlayan and Aksoylu, 2011):

$$CO + 3H_2 \leftrightarrow CH_4 + H_2O \qquad \Delta H^{\circ}_{298} = -205.81\ \mathrm{kJ/mol} \tag{2.7}$$

2.2.1. Conventional Fe- and Cu-based Catalysts of WGS Reaction

As WGS is of crucial importance for fuel processors since it increases hydrogen yield while decreasing CO content, many studies have been conducted on Fe-based for HTS and Cu-based catalysts for LTS investigating the effects of different parameters on activity.

First step of the WGS unit is the HTS reaction which has been performed generally over Fe-Cr catalysts in which iron acts as the active phase and chromium oxide is the stabilizer at 310-450°C. Chromium oxide has effect to prevent sintering by blocking the thermal agglomeration of Fe_3O_4 particles and provides prolonging activity. Fe_3O_4/Cr_2O_3 catalyst was first used in 1914 by BASF scientists Bosh and Wild who studied different catalysts for HTS reaction and decided Fe-Cr is the best one (Reddy and Smirniotis, 2015). Investigations focusing effect of different parameters on HTS catalysts are clarified in detail at below.

Edwards and co-workers studied the microstructure of an iron oxide based WGS catalysts by different analysis devices. The precursors Fe_3O_4/Cr_2O_3 and $CuO/Fe_3O_4/Cr_2O_3$ were prepared by co-precipitation method. The results showed that the catalysts surface is enriched by Cr ions which are more stable than Fe-rich core and this lessened sintering and diffusion of ions and adding Cu dopant promoted the activity of catalysts (Edwards *et al.*, 2002).

In recent years, the investigations about FeCr and CuO-FeCr catalysts have proceeded and the research driven by Xhu *et al.* (2016) also addressed Cr_2O_3-Fe_2O_3 and CuO- Cr_2O_3-Fe_2O_3 catalysts. At the end, they came into the point that Cr promoter did not engaged in as chemical promoter rather it acted as stabilizer. On the other hand, Cu promoter worked as chemical promoter by enabling high active sites.

Another study stressing on the enhancing effect of Cr on iron oxide catalysts is performed by Natesakhawat *et al.* (2006). The oxidation of Cr^{3+} to Cr^{6+} may allow for better oxidation-reduction cycle leading to promote WGS activity. Accordingly, Cr not only a stabilizer, it has also promoting feature by improving redox function of Fe^{2+} to Fe^{3+}. In this study, aluminum and copper were also suggested as promoter and found that aluminum and copper are promising promoters despite Cu becoming prone to sintering with increasing temperature.

Co-precipitation method has been mostly used while preparing HTS catalysts in which iron oxide is reduced exothermically which can cause undesirable reactions to occur. Therefore, another method -pyrolysis method- was examined by Meshkani and Rezaei (2014). Their results presented that this method provided obtaining the catalysts in the active phase and incorporation of copper and Cu facilitated the activity and stability of the catalysts.

The effect of precursors on the activity of high temperature water gas shift catalysts was investigated by Dofour *et al.* (2013). They prepared FeCr, FeCrCo, FeCrCu and FeCrCuCo by oxidation-precipitation method, utilizing chloride and sulfate metal precursors. The catalysts prepared by using sulfate precursor showed higher activity owing to the decrease of surface basicity which enhanced the reducibility and influenced the CO

chemisorption and hydrogen adsorption. In this study, the effect of Cu or Co presence was observed. Although for the ones prepared by chloride, addition of copper and cobalt increased the CO conversion, for rest prepared by sulfate, did not improve the activity. They claimed that sulfur may poison the copper particles which lead catalyst deactivation.

Increasing concerns about toxicity and safety of chromium has led researchers to study on environmentally friendly Cr-free Fe-based catalysts. Araujo and Rangel (2000) are the ones who have reported Fe-Al-Cu catalysts for the first time. They synthesized Fe-Cu, Fe-Al and Fe-Al-Cu materials by co-precipitation method. They brought about that Cr can be replaced with Al since the Fe-Al-Cu catalyst presented higher activity than the copper- and chromium-doped catalysts.

Zhang *et al.* (2008) maintained a study on Fe-Al-Cu catalysts by changing preparation method from co-precipitation to sol-gel method. The results demonstrated that the catalysts prepared by sol-gel method yielded higher activity than the ones synthesized by one-step and two-step co-precipitation methods. This may be resulted in that this method formed oxygen vacancies in the structure making it a promising Fe-based catalyst preparation method.

In another research conducted by Martos *et al.* (2009), molybdenum was introduced instead of chromium for magnetite based catalysts. The results exhibited that adding molybdenum improved the stability of magnetite active phase and it provided avoiding formation of metallic iron which may cause side reactions such as undesired methanation reaction.

Lin *et al.* (2014) investigated the influence of precipitants used while preparing Cu ferrite-based catalysts. They chose precipitants as KOH, K_2CO_3, Na_2CO_3, NaOH and $NaHCO_3$ and they concluded that copper ferrite catalysts prepared by using KOH has higher activity and better stability among other which can be due to higher Cu dispersion, strong interaction between iron oxides and Cu and weak basicity.

The second step of WGS unit is LTS reaction which has been conducted mostly over $Cu/ZnO/Al_2O_3$ catalyst operating at 150-200 °C and LTS decreases the CO content less than 0.5 % (Reddy and Smirniotis, 2015). First Cu-Zn catalysts were used in 1963 (Moe, 1963). Since then many studies have been conducted on Cu-based LTS catalysts examining the influences of various parameters on activity and some are reviewed briefly at below.

Fue *et al.* (2011) carried out a study analyzing the effect of the Al content in the $Cu/ZnO/Al_2O_3$ catalysts. They synthesized the sample with Cu/Zn ratio of 1 and Al with 4-24 mole % by co-precipitation method. At the end, they concluded that as the Al amount increases in the catalyst, it results in an increase of activity and also stability due to presence of aurichalcite and hydrotalcite phases ascribed to activity and stability, respectively.

The impact of preparation conditions on catalyst activity was explored by Budiman *et al.* (2013). They altered the conventional co-precipitation method by changing synthesis conditions as solvent, pH and precipitation temperature. They obtained catalysts with higher Cu surface area than prepared by the conventional method yielding higher catalytic activity.

Figueriedo and his co-workers (2011) made a research on the effect of alkali cations; Li, K, Rb and Cs, doped on the $Cu/ZnO/Al_2O_3$ catalyst. The samples were prepared by ions impregnation to ternary $Cu/ZnO/Al_2O_3$ catalyst and they were tested at temperature of 177-227 °C. They reached that K ion including catalyst showed the highest CO conversion and they suggested also that adding alkali promoters to ternary catalyst preclude methanol production which allows having higher H_2 selectivity.

Jeong and collaborators (2014) focused on the $Cu\text{-}CeO_2$ catalysts synthesized by co-precipitation method. They have tried to see the effect of Cu loading over this catalyst. They found that 80 wt. % $Cu\text{-}CeO_2$ presented highest activity and stability and they attributed this to the strong support and metal synergy which provides to avoid Cu sintering.

In recent years, the investigations on Cu-based catalysts have been maintained extensively. One of them was performed last year by Santos *et al.* (2017). They have tried to improve the activity of $Cu/ZnO/Al_2O_3$ catalyst by adding gold nanoparticles and they

obtained full conversion of CO. They explained this result with collaboration of Au and Cu and the synergy between them was very promising to accomplish the H_2 purification aims. In addition, they proved the stability of the system for both cyclic and long term operations.

One of the most challenging problems of Cu-based catalysts is that they are not appropriate for portable devices and Price *et al.* (2017) conducted a study on this issue. They developed multicomponent Cu-ZnO catalysts to be able to employ in systems having high space velocities, also means to tackle with residence time limitations. They used different supports and among them CeO_2-Al_2O_3 was remarkable with its activity and stability values.

Despite the fact that Fe-based and Cu-based HTS and LTS catalysts have been well developed and been attained a place in industry, the hassles as requiring particular reduction procedures and concerns about pyrophoric nature of them make these catalysts not viable for PEMFC systems which needs non-pyrophoric, resistant to daily start/stop operations and feasible for small scale application catalysts to be managed in. Hence, lately many search efforts have been spending on designing catalysts noble-metal based; also called Platinum-group metal (PGM) based catalysts, supported on reducible oxides to be able to conduct in single stage WGS reactor (Reddy and Smirniotis, 2015).

2.2.2. Noble Metal-based Catalysts used in WGS Reaction for PEMFC

Many researches have been conducted on noble metal-based catalysts, also called Platinum Group Metals (PGM) in order to overcome the thermodynamic and kinetic limitations owing to the fact that conventional Fe- and Cu-based catalysts are not favorable for single-stage WGS operations. Pt, Au, Ru, Rh and Pd based catalysts supported on oxides like TiO_2, CeO_2, ZrO_2 and mixed oxides have particularly gained importance due to their high activity in WGS reaction. Among these, Pt and Au have been considered as the promising candidates (Reddy and Smirniotis, 2015).

Panagiotopoulou *et al.* (2006) conducted a research on the influence of the support on which noble metals deposited. They compared the catalytic activity of Pt, Rh, Ru and Pd

based catalysts which are supported on either “reducible” (La_2O_3, TiO_2, yttria-stabilized zirconia and CeO_2) or “irreducible” (Al_2O_3, SiO_2 and MgO) oxides and they concluded that Pt catalysts showed higher activity than other metal catalysts especially when supported on reducible oxides. Following year, same group proceeded by extending their study to use of platinum catalysts deposited on composite supports; MO_x/Al_2O_3 and MO_x/TiO_2 (M= Cr, Ti, Fe, V, Co, Mn, Nd, Sm, Gd, Ho etc.). The catalysts were tested with realistic feed composition including 3% CO, 10% H_2O, 20% H_2 and 6% CO_2 at 150-500 °C temperature range and were resulted with improved WGS activity. Hence, they proposed that support was playing directly active role in reaction mechanism and therefore it affected the performance of the catalysts (Panagiotopoulou and Kondarides, 2007).

It is hard to compare the noble metal based catalysts deposited on different supports as they designed and prepared by various groups and tested at different conditions. Accordingly, 20 catalysts have been analyzed for their performance in a commercial reactor using realistic feed composition at 250 °C, 300 °C and 350 °C. Au, Rh, Ru, Cu, Pd and Pt were the metals used and ceria, zirconia, titania, alumina and iron oxide were chosen as supports. Through metals, Pt catalysts was found to be the most promising metal at temperature around 250-350 °C while Au was more active at 150-250 °C (Thinon, 2008).

Santos *et al.* (2017) stated remarkable catalysts in their work. They prepared Au promoted $Cu/ZnO/Al_2O_3$ catalysts synthesized from hydrotalcite precursors and reached full CO conversion at temperature around 180 °C. Au-Cu synergy accounted for the superior catalytic performance of catalyst samples. Using this type of precursor modified microstructures of samples and improved metal oxide synergy. This group tested all catalysts they prepared also for stability during start/stop cycles. Among all, they pointed the catalyst having Cu/Zn ratio of 2.8 as the most robust one that acceptably resists start-up/shut-down cycles.

The effect of synthesis method on catalytic performance and stability of Au/Fe_2O_3 catalysts was investigated by Soria *et al.* (2014). In this work, deposition-precipitation (DP), double impregnation and liquid phase reductive deposition (LPRD) methods were utilized to prepare catalysts with different amount of Au deposited on. The experiments were

performed in a fixed-bed reactor by feeding stream with composition of standard reformer outlet. According to the obtained results, the catalysts synthesized by DP method had highest activity. TPR-H_2 analysis revealed that gold enhanced the redox properties of support which directly affect activity.

Çağlayan *et al.* (2011) observed in her work the influence of Re addition to Au/ceria catalysts. Au-Re/ceria, Re/ceria and Au/ceria catalysts were synthesized, and performance tests were performed at temperature of 200-450 °C. The results showed that Au addition by deposition precipitation technique on impregnated Re/ceria catalysts resulted in high CO conversion while impregnation of Re on Au/ceria catalysts exhibited lower activity in consequence of blockage of active sites.

Comparison of Au and Pt catalysts which both show remarkable catalytic activity in WGS reaction was made by Castaño *et al.* (2014). Pt and Au catalysts dispersed on ceria or mixed CeFe oxide were prepared by aqueous impregnation and direct ionic exchange method, respectively. The performance tests were performed in the temperature range 180-350 °C. At the end, the results indicated that Pt-based catalysts had higher activity at temperatures around 250 °C while Au-based catalysts were more active at 180 °C. In addition to these, Pt-based samples were more endurable to changes in feed stream and have higher TOF.

2.3. Platinum-based PGM Catalysts in WGS Reaction

Recently, Pt-based catalysts supported on reducible oxides have been under intense improvement based upon being highly active and stabile in WGS reaction. The researches have mostly focused on CeO_2, ZrO_2, TiO_2 and Al_2O_3 supports owing to their enhanced redox properties which are particularly significant for WGS mechanism.

2.3.1. Mono and Multi Metallic Platinum-based Catalysts

Hwang *et al.* (2013) investigated the effect of Ti addition to the Pt/ZrO_2 catalysts to improve the activity for single-stage WGS reaction. Results presented that Ti impregnated catalysts have rather superior activity since addition of Ti facilitated Pt dispersion and surface area of support leading increase in 3 times higher CO conversion levels compared to Pt/ZrO_2 catalysts.

A comparative study among Pt/CeO_2, Pt/ZrO_2 and $Pt/Ce_{(1-x)}Zr_{(x)}O_2$, by changing CeO_2/ZrO_2 ratio to optimize catalysts was conducted by Jeong *et al.* (2013). Among them Pt/CeO_2 yield the highest TOF and lowest activation energy in addition to good stability. They have also been found that cubic $Pt/Ce_{(1-x)}Zr_{(x)}O_2$ brought about higher TOF than tetragonal $Pt/Ce_{(1-x)}Zr_{(x)}O_2$ on occasion of easily reducible nature of cubic supports.

Iida *et al.* (2006) studied the impact of precursor type on WGS activity by preparing Pt catalysts with different precursors which are H_2PtCl_6, $Pt(C_5H_7O_2)_2$, $[Pt(NH_3)_4]Cl_2$, $[Pt(NH_3)_4](NO_3)_2$ and *cis*-$[Pt(NO_2)_2(NH_3)_2]$ using impregnation method. The performance tests were performed in a fixed bed flow reactor with H_2O/CO ratio of 1.5. Catalytic activity was obtained highest for the catalysts synthesized from H_2PtCl_6 and they suggested a linear relation between Pt dispersion and activity but altering type of Pt precursors did not incline a big change on performance of the catalysts.

The bimetallic $Pt\text{-}Ni/Al_2O_3$ catalyst was studied by Çağlayan *et al.* (2009). The catalytic activity was tested at temperature range 250-400 °C and being fed with ideal feed composition in a fixed bed micro-reactor. The experimental parameters were H_2O/CO ratio and Ni content in the catalyst samples. Accordingly, increasing H_2O/CO ratio and Ni content enable CO conversion- temperature curve to be shifted to the lower temperatures and $Pt\text{-}Ni/Al_2O_3$ catalysts were stated as one of the promising catalysts due to their highly active and selective behavior.

Lee *et al.* (2007) viewed Ce, Co or Ni deposited Pt/ZrO_2 catalysts to see the effect of second metal on WGS activity. The results exhibited that $Pt\text{-}Ce/ZrO_2$ catalyst yielded the

highest activity and stability. Furthermore, a Pt-Ce/ ZrO_2 catalyst was prepared by sequential impregnation of Pt and Ce on ZrO_2 support to compare the effect of synthesis method. The results pointed out that the co-impregnated Pt-Ce/ZrO_2 catalyst had superior performance than sequential impregnated Pt-Ce/ZrO_2 catalyst.

The influence of alkali metals on WGS activity was examined by Pazmiño *et al.* (2012). They doped Na, Li and K metals on Pt/Al_2O_3 and Pt/TiO_2 by incipient wetness impregnation method and catalytic tests were carried out in plug flow reactors at low temperature range, 200-250 °C. Na addition promoted the CO conversion by changing the properties of support and facilitating formation of new active sites.

2.3.2. Ceria Supported Pt-based WGS Catalysts

Cerium oxide catalysts have been extensively used in catalytic processes, especially in order to purify automobile exhaust gases in three-way catalysts which have been compelled to be used with environmental legislations since late 1980s (Kašpar *et al.*, 1999). Cerium oxide has been proven for being very appropriate support for precious metals by making them well dispersed. CeO_2 has been mostly focused for its easily reducible nature (Ce^{3+}/Ce^{4+}) which eases conversion of CO and hydrocarbons through oxygen stored in. The surface defects, also known as oxygen vacancies, which are introduced to have prime importance being the most active sites on catalysts have close relationship with oxygen storage capacity (OSC) (Vindigni *et al.*, 2011). There has been deep literature data on cerium oxide and its use as support with noble metals, in particular with Pt explained briefly at below.

Ivanov *et al.* (2013) reported an investigation on Pt/CeO_2 catalysts by using low cost extractive-pyrolytic method to prepare samples. Three catalyst samples with Pt loading of 1.2, 2.4 and 4.8 wt. % were synthesized and reaction temperature, space velocity and H_2O/CO ratio were constituted as experimental parameters. The results revealed that the highest activity was obtained with 1.2Pt/CeO_2 catalyst not with the one having highest Pt amount causing cover of Pt particles within the support.

Preparation method of CeO_2 which is another parameter affecting the catalytic activity was analyzed by Roh *et al.* (2012). In this study a simultaneous precipitation/digestion method was used for precipitation of cerium (III) carbonate ($Ce_2(CO_3)_3.8H_2O$). 1 wt. % Pt/CeO_2 catalysts were synthesized by incipient to wetness impregnation method and then samples were tested in fixed-bed micro reactor at temperatures around 200-320 °C. 82% CO conversion and 100% selectivity were obtained with 1 wt. % Pt/CeO_2 catalyst at the end of experiments.

A comparative study about the influence of different ceria supports on activity was carried out by Jain *et al.* (2015). Three different ceria which are the ones prepared by sol-gel and combustion chemical vapor deposition method and bought commercially were used in this study to see the role of modifying surface area and porosities. The 5 wt. % Pt catalysts supported on different ceria were compared at temperature range of 150-450 °C and figured out that the one prepared by sol-gel method gave the highest CO conversion followed by the ones prepared by combustion chemical vapor deposition method and bought commercially. The catalysts of which support synthesized by sol–gel method had promoted activity, and this was explained by small crystallite size leading surface defects and thereby lower energy boundary.

Çavuşoğlu *et al.* (2015) performed a work on Pt and Rh based ceria supported catalysts synthesized by flame spray pyrolysis method and tested in a membrane reactor at atmospheric pressure and 200-450 °C temperature range. Also incipient to wetness impregnation method was used to prepare Pt/CeO_2 catalyst in order to make comparison. Both catalysts prepared by spray pyrolysis method showed high stability, however, catalytic results presented that Pt-based catalysts were more active than Rh-based samples. Moreover, in Rh-based catalysts' experiments, methanation reaction took place which was not the case for Pt-based catalysts making Pt/CeO_2 catalysts outstanding candidates for WGS reactions.

2.3.3. Rhenium and/or Vanadium Promoted Pt-based WGS Catalysts

The bimetallic Pt-Re catalysts have been used successively since being introduced for the sulfur-free naphtha reforming in 1960s (Kluksdahl, 1968). Recently Pt-Re systems have been affirmed to yield remarkably better activity and stability for WGS reaction; however, the reasons behind this superior performance have not been clarified enough, therefore much research effort has been devoted to highlight these causes.

Choung and her co-workers (2006) studied on the addition of Re to $Pt/Ce_{0.46}Zr_{0.54}O_2$ and $Pt/Ce_{0.6}\ Zr_{0.4}O_2$ catalysts. The mixed oxide supports were prepared by co-precipitation process followed by Pt and Re impregnation on them by incipient wetness method. Pt dispersion was analyzed by CO chemisorption. Ultimately, doping Re to Pt $Ce_{0.46}Zr_{0.54}O_2$ revealed higher reaction rate than obtained with Pt $Ce_{0.46}Zr_{0.54}O_2$. According to the CO chemisorption results, enhanced Pt dispersion was observed in Pt-Re systems. Still there may be else reasons to have higher activity with Pt-Re system other than better Pt dispersion.

Radhakrishnan *et al.* (2006) focused on ceria-zirconia oxides supported Pt/Re catalysts. The mixed support was prepared by co-precipitation while Pt and Re were added by ion-exchange. The experimental parameters were chosen as Pt-Re ratio and Re source. The measurements clarified that Re had promotion effect for WGS activity and optimum Pt/Re was decided as 2:1. In addition, the optimum source for Re was rhenium carbonyl $Re_2(CO)_{10}$.

$Pt\text{-}Re/TiO_2$ and $Pd\text{-}Re/TiO_2$ catalysts were examined in study carried out by Sato *et al.* (2005). The samples were prepared by incipient wetness process and the activity tests were performed in fixed-bed reactor with feed composition stimulating reformer outlet. The enhanced activity was provided by Re addition to both system, on the other hand, Re had very remarkable effect on Pd/TiO_2 while the impact was not so explicit in case of Pt/TiO_2.

As stated before, there has been much debate in literature to understand the reasons Re added Pt-based catalysts providing higher activity. One of these researches was carried on

by Iida *et al.* (2006). Pt-Re/TiO_2 (Rutile) and Pt-Re/ZrO_2 catalysts were prepared conventional impregnation method. TEM analysis demonstrated that by addition of Re to Pt/TiO_2, the Pt dispersion was improved and XPS spectra presented that the stronger interaction between Pt-Re in TiO_2 supported catalysts than ZrO_2 supported ones was observed. Re had anchor role for Pt particles which it was strong interaction with and provided Pt particles well dispersed. On the other hand, in case of Pt-Re/ZrO_2 catalysts, the strong interaction was obtained between Re and ZrO_2. Besides the Re redox reaction (Re^{4+}/Re^{7+}) took place during reaction conditions which was attributed to the reason of increase in catalytic activity.

Azzam *et al.* (2013) investigated the role of preparation pathways, the ratio of Pt/Re and contents of metals. Sequential impregnation and co-impregnation techniques were implemented to see the effect of preparation pathways and different amounts of Re and Pt were dispersed on support by employing different Pt/Re molar ratios. In conclusion, they pointed that impregnation of Re before the impregnation of Pt gave better results. Moreover, the optimum molar ratio of Pt/Re was obtained as 1 with 0.5 wt. % Pt content. According to the results acquired from H_2-TPR and in situ FTIR spectroscopy analysis, the idea that oxidation of Re by water leading new OH groups changed the reaction pathway which accelerated activation of water and resulted in high activity and stability.

Lately, the studies on Pt-Re catalysts have been extensively maintained. Duke and her colleagues (2017) performed a research to understand the active sites of Pt-Re/TiO_2 catalysts. The bimetallic clusters were synthesized by the sequential impregnation either Pt on Re and Re on Pt. Both samples showed superior activity rather pure Pt clusters. The DFT and IRAS results represented that CO poisoning was reduced with Re addition since CO attaches Pt more strongly than Pt-Re systems.

A comparative study was performed by Palma *et al.* (2017) about Pt-based bimetallic catalysts where the second metals were La, Re and Rh to achieve single stage WGS reaction. The catalysts were prepared by consecutive wet impregnations. The activity tests were carried on fixed-bed tubular stainless-steel reactor at temperature range of 150-400 °C being fed with ideal feed composition. The results indicated that 1Pt/1Re/$CeZrO_4$ produced better

results either with hydrogen selectivity and CO conversion. Furthermore, the impregnation sequence was also tested and come up with the result that loading Re first introduced higher activity values.

There has not been enough data about the vanadium use in WGS catalysts on literature although it has extensively been participated in oxidation reactions and when partially reduced, it reveals high oxygen mobility owing to the structural defects formed. Therefore, it may be a promising candidate to achieve high activity in WGS reaction (Farias *et al.*, 2008).

Silva *et al.* (2007) conducted a research on hydrogen production from ethanol with partial oxidation integrated WGS reaction system. For purification part, Pt/CeO_2 and V-modified Pt/CeO_2 catalysts were prepared and tested in fixed-bed tubular reactor. The higher activity was attained over $Pt/V\text{-}CeO_2$ catalysts and the result was attributed to the redox properties of V_2O_5.

The vanadium structures formed on Pt/CeO_2 and their effect on changing or acting as active sites were investigated by Farias *et al.* (2008). Four different supports were prepared by altered V loading in the range 1-18 wt. % and then Pt was added to supports by incipient wetness impregnation with constant 1 wt. % Pt amount. The catalytic activity was carried out in fixed-bed U-shaped reactor with feed composition stimulating ethanol reformer outlet at 200-350 °C temperature range. The highest activity was accomplished over $Pt/6VCeO_2$. In this study, the results exhibited that vanadium affected the surface carbonates' structure and the enhancement in WGS activity was correlated with V-O-Ce bonds.

Nguyen-Thanh *et al.* (2008) reported a work on vanadia promoted Pt/ZrO_2 catalysts for WGS reaction. Different amount of V-containing supports (1-13 wt. % V) were prepared and 1 wt. % Pt was impregnated over the samples by incipient wetness impregnation method. In all cases vanadia provided an improvement in activity and the highest results was observed with 3 wt. % V which resulted in the rate about double that of Pt/ZrO_2. The improvement role of monovanadate in WGS was associated with V-O-Zr bonds which were

believed to provide enhanced reducibility making V worth to consider since redox mechanism plays crucial role in WGS reaction.

2.4. Oxygen Storage Capacity

Ceria has been of paramount importance owing to its key roles in several catalytic processes since it improves the WGS activity and stabilizes the alumina support, but most importantly provides oxygen storage capacity (OSC). This term, OSC, has been introduced to define the maximum amount of oxygen "stored" in the oxygen-rich region and released in the oxygen-lean region in order to convert hydrocarbons and CO to CO_2. The ability of cerium to shift between Ce^{3+} and Ce^{4+} oxidation states is intimately connected to surface defects, i.e. oxygen vacancies. The following redox reactions occur under oxidizing conditions (Hilarie *et al.*, 2000; Khossusi *et al.*, 2003):

$$Ce_2O_3 + \frac{1}{2}O_2 \rightarrow 2CeO_2 \quad (2.8)$$

$$2CeO_2 + CO \rightarrow Ce_2O_3 + CO_2 \quad (2.9)$$

It has been widely established that catalytic activity is mostly determined by reducibility of solid and its capability of reproducing itself with molecular oxygen in gas phase (Perdomo *et al.*, 2016). Ceria not only fully meets these expectations also it promotes WGS activity by lowering the barriers of water dissociation step in WGS mechanism and prevents thermal sintering of noble metals. Hence CeO_2 containing materials and measuring their OSCs supplied primarily by cerium itself has been the focus of very intense research (Vindigni *et al.*, 2011; Swanson *et al.*, 2008). Three methods, TPR, chemisorption and pulse injection method have been offered by Yao *et al.* (1983) for OSC measurements. First method was TPR which primes us about the highest amount of transferable oxygen on catalysts surface. The second method was chemisorption, in which oxygen uptake which may enlighten the available sites on catalyst surface was examined by obtaining total and reversible adsorption isotherms of oxygen. Mining the literature, one can see that the most conventional route to detect OSC has been introduced as third method, pulse injection. In this method, the catalyst was exposed to O_2 pulses followed by CO pulses in order to

stimulate the oxidation/reduction phenomena from which CO or O_2 uptake and/or the amount of CO_2 produced were calculated and defined as oxygen storage capacity, OSC. Two measurements were established to explain oxygen storage capacity. First one, the amount of oxidized CO after CO pulses following by O_2 pulse was called as Oxygen Storage Capacity, Complete (OSCC) while OSC was proposed to identify the amount of oxidized CO after one CO pulse again following O_2 pulse (Yao *et al.*, 1983).

Measuring OSC has been receiving a great deal of attention recently and pulse injection method has become the most widely used process to achieve it. Therefore, much literature data is available about oxygen storage capacities of samples. Bedrane *et al.* (2002) performed a study on the oxygen storage process of catalysts supported on ceria and ceria-zirconia. Ten noble metals (Pt, Rh, Pd, Ru and Ir) were impregnated on ceria and ceria-zirconia supports obtained commercially. Oxygen storage capacities were determined by subsequent 2 min pulse injection of CO and O_2 and micromoles of CO_2 produced per gram of catalyst was used for characterization of OSC. In this study, the roles of temperature and metal adding on OSC was also probed and the results clearly indicated that OSC was improved in the presence of metals, especially iridium and ruthenium showed remarkable enhancement in OSC. For temperature change, common trend was observed for all samples. OSC seemed to increase with rise in temperature.

Khossusi *et al.* (2003) studied on determination of oxygen storage capacities for three-way automotive catalysts. Commercial Pt/Rh monolith TWC was used in this research being exposed 1% CO and O_2 in N_2 step changes. The dependence of OSC on temperature was the second part of the investigation resulted in nearly no OSC at low temperatures than 300 °C and the maximum was achieved with 450 °C temperature.

OSC analysis of nanostructured Au-ceria was accomplished by Fu *et al.* (2003) by preparing catalysts with different methods which are deposition-precipitation (DP), co-precipitation (CP) and gelation. OSC measurements were conducted in a flow reactor system having configuration which provides switching valve rapidly to manage step changes of 10 % CO/He, He and 10% O_2/He for 3 min, 6 min and 3 min, respectively for three temperature

values of 100, 200 and 350 °C. The partial pressures were integrated over time to obtain the amount of CO_2 formed. Accordingly, addition of gold promoted the OSC of ceria by easing the interaction between CO and surface oxygen.

Li *et al.* (2013) reported a paper on the effect of support on OSC. For this purpose, supports chosen as CeO_2 ZrO_2 and $Ce_{0.6}Zr_{0.4}O_2$ were prepared by co-precipitation procedure while Pt was deposited on them by incipient to wetness impregnation method. OSCs were obtained by imposing step changes of 5 % CO/He and 5 % O_2/He at 350 °C. The peak area of $Pt/Ce_{0.6}Zr_{0.4}O_2$ was two times higher than that of Pt/CeO_2 which showed more active oxygen species on surface and better coke resistance and this may be the reason behind the notable activity of $Pt/Ce_{0.6}Zr_{0.4}O_2$ catalysts.

Establishing a correlation between OSC of the catalysts and their activities was the objective of research conducted by Perez *et al.* (2015). This study also included the improvement in OSC of ceria when dispersed on carbon. The OSCC analysis was achieved by 10 pulse injection of O_2 and CO, successively and the amount of CO_2 produced referred as OSCC. After 10 min flow of He, the samples were subjected to series of pulses (CO-O_2- CO-O_2- CO-O_2- CO-O_2) at three different temperatures, 150, 250 and 350 °C and the amount of CO_2 produced per pulse was attributed to OSC by assuming CO_2 was coming from the interaction between CO and lattice oxygen of catalysts. The results showed that better OSC was introduced with CeO_2/C rather bulk CeO_2 which was attained to carbon being ideal media for CeO_2 by enabling high surface area though it was not included in chemical processes. The temperature increase was directly correlated with improved OSC and metal-support contact; in this case metal was Ni, facilitated reducibility and presented higher OSC.

Reina *et al.* (2015) made his research on oxygen storage capacities of $Au/CeO_2/Al_2O_3$ and transition metal doped catalysts by preparing supports by co-precipitation method while Au was dispersed by direct anionic exchange process. The catalytic activities were tested at 140-350 °C temperature range with ideal feed composition. OSC was obtained by ten O_2 pulses followed by series of CO-O_2 pulses and the average amount of CO_2 per pulse was ascribed to OSC. According to the results, outstanding WGS activity stemmed from doping Fe since it led improvement in not only structural also redox properties of catalyst.

Same group (Reina *et al.,* 2016) performed a study on following year about multicomponent $Au/Ce_{1-x}Cu_xO_2/Al_2O_3$ catalysts and investigated CeO_2-CuO interaction which may be a key parameter in catalytic performance. Same OSC measurement procedure, pulse injection method, was employed with previous year study. For all samples, the general trend was obtained in which OSC increased with temperature rise. Ce-Cu mixed system showed higher OSC than Ce/Al and Cu/Al samples having similar values which was explained by Ce-Cu synergy. Furthermore, deposition of Au on samples provided an improvement in OSC at all temperatures and this might arise from changing reducibility features of catalysts by Au addition.

A great majority of data obtained for OSC in literature was based on pulse injection method. Reddy *et al.* (2005) had tried a different method to evaluate the OSC of CeO_2, CeO_2-SiO_2, CeO_2-TiO_2 and CeO_2-ZrO_2 samples. Thermogravimetric analysis was completed to examine OSC. The samples were heated to 800 °C in N_2 and cooled to 150 °C in dry air and again heated to 800 °C in N_2 by ramp of 5 K/min. The weight change of sample was used to attain oxygen storage capacities.

3. EXPERIMENTAL WORK

3.1. Materials

3.1.1. Chemicals

The chemicals used for catalyst preparation are all research grade and are listed in Table 3.1.

Table 3.1. Chemicals used for catalyst preparation.

Chemical	Formula	Specification	Source	MW (g/mole)
Ammonium meta-vanadate	NH_4VO_3	99%	Riedel-de Haën	116.98
Ammonium perrhenate	NH_4ReO_4	99.999%	Sigma-Aldrich	268.24
Cerium (III) nitrate hexahydrate	$Ce(NO_3)_3.6H_2O$	99.99%	Sigma-Aldrich	434.23
Oxalic acid dihydrate	$C_2H_2O_4.2H_2O$	98%	Alfa Aesar	126.07
Sodium carbonate	Na_2CO_3	99.9+%	Merck	105.99
Tetraammineplatinum (II) nitrate	$Pt(NH_3)_4(NO_3)_2$	99.995%	Sigma-Aldrich	387.22
Water	H_2O	Deionized	-	18.02

3.1.2. Gases and Liquids

The specifications and applications of the gases and liquids applied in this research are presented in Table 3.2 and 3.3, respectively.

Table 3.2. Specification and application of the liquid used.

Liquid	Specification	Application
Water	Deionized (DI)	Aqueous solutions, Reactant

Table 3.3. Specifications and applications of the gases used.

Gas/Standard	Formula	Specification	Supplier	Application
Argon	Ar	99.995%	Linde	Inert, Reducing agent, GC Carrier Gas
Helyum	He	99.999%	Linde	Inert
Carbon dioxide	CO_2	99.995%	BOS-Linde	Reactant, GC calibration
Carbon monoxide	CO	99.999%	BOS	Reactant, GC calibration
Dry air	-	99.998%	Linde	GC 6-way pneumatic valve
Hydrogen	H_2	99.995%	BOS-Linde	Reactant, GC calibration

3.2. Experimental Systems

The experimental system used in this research consists of five main groups:

- Catalyst Preparation Systems: These systems involve equipment in order to prepare the support and to achieve incipient-to-wetness impregnation steps of catalyst preparation.

- Catalyst Characterization Systems: These systems are used to detect the structural and surface chemical properties of catalyst samples and to view the changes which catalyst samples may undergo during reaction.
- Catalytic Reaction System: This system is used to determine the catalytic activity, selectivity and stability. It is composed of a feed section including mass flow controllers for gases, HPLC pump for water and a mixing zone; a reaction section involving a continuous flow fixed-bed micro reactor embed in a temperature-controlled furnace.
- Product Analysis System: The analysis of the product and reactant streams is performed by using an on-line connected gas chromatograph to micro reactor flow system.
- Gravimetric Gas Sorption Analysis System: This group including a gravimetric sorption analyzer and a mass spectrometer is used to examine the O_2 adsorption properties of catalyst samples.

3.2.1. Catalyst Preparation System

The system used for catalyst preparation by incipient-to-wetness impregnation technique (Figure 3.1) involves a Retsch UR1 ultrasonic mixer, a KNF Neuberger vacuum pump, a Büchner flask and a MasterFlex peristaltic pump.

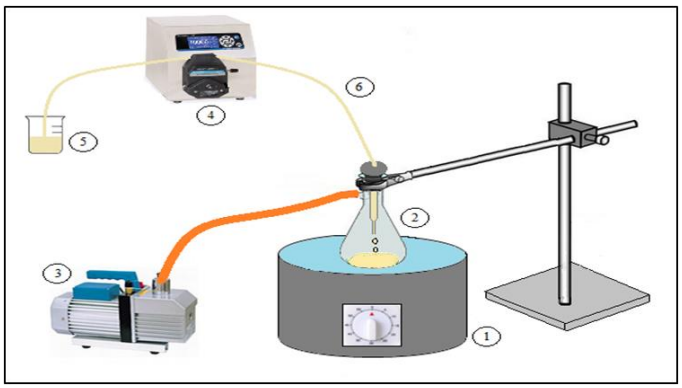

Figure 3.1. Schematic diagram of the impregnation system: 1. Ultrasonic mixer, 2. Büchner flask, 3. Vacuum pump, 4. Peristaltic pump, 5. Precursor solution beaker, 6. Silicone tubing (Başar, 2016).

The system used for support preparation by homogeneous deposition precipitation method including a Julabo ED-13 water bath, the support material beaker, a Heidolph RZR 2021 impeller and a Mettler Toledo FE20 pH-meter is demonstrated in Figure 3.2.

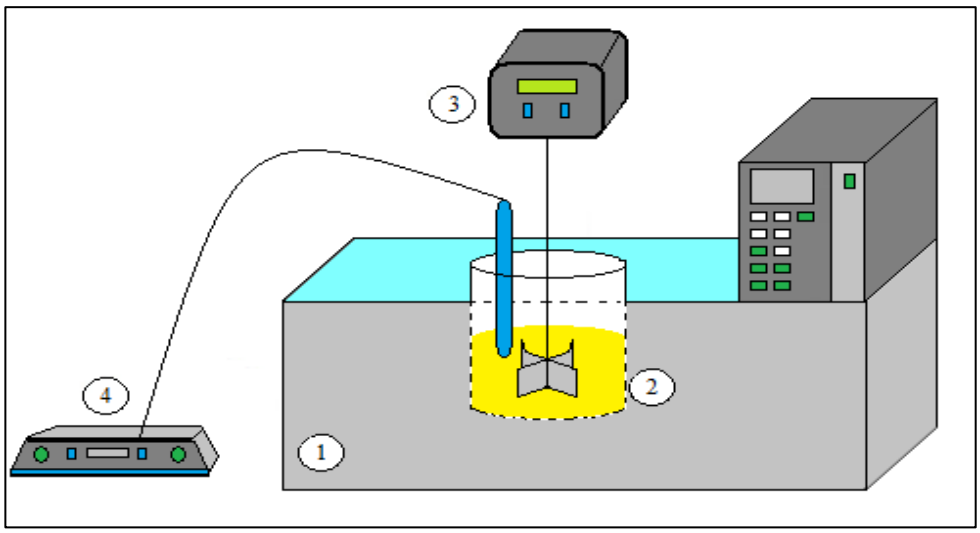

Figure 3.2. Schematic diagram of the deposition precipitation system:
1. Water bath, 2. Beaker, 3. Overhead stirrer, 4. pH meter (Başar, 2016).

3.2.2. Catalyst Characterization Systems

3.2.2.1. Raman Spectroscopy. The possible coke formation on the spent catalysts and extent of V-O-Ce bond formation on samples were analyzed with Raman spectroscopy. A Renishaw in via Raman microscope was used to obtain Raman spectra of the freshly reduced and spent catalysts with 514 nm 20 mW Ar^+ laser as the excitation source, 2 mW laser intensity, 10 s acquisition time and a total of 5 accumulation per spectrum. The analyses were performed at the Advanced Technologies Research and Development Center of Boğaziçi University.

3.2.2.2. X-ray Photoelectron Spectroscopy (XPS). The electronic interactions between the species on the surface and degree of oxidation of metals on freshly reduced and used samples

were examined by X-ray photoelectron spectroscopy (XPS). The analyses were conducted at the Advanced Technologies Research and Development Center of Boğaziçi University.

3.2.2.3. Scanning Electron Microscopy. To analyze the metal dispersion, microstructure and morphology of the freshly reduced and used samples, micrographs were obtained using Philips XL 30 ESEM-FEG system having a maximum resolution of 2 nm. The tests were conducted at the Advanced Technologies Research and Development Center of Boğaziçi University.

3.2.2.4. CO Chemisorption. Pt dispersion was measured with CO Pulse Chemisorption to quantify the total amount of metal available for reaction using Hiden Analytical CATLAB. The samples were reduced in situ prior to CO uptake measurements. The CO uptake analyses were performed at room temperature with 60 ml/min He flow via injecting 0.1 ml pulses involving 5 % CO over the catalyst samples. The amount of CO adsorbed was measured by assuming the ratio of CO to Pt as 1 and metal dispersions were calculated.

3.2.3. Catalytic Reaction System

The catalytic reaction system (Figure 3.3) used in this study was designed and constructed in the Catalysis and Reaction Engineering Laboratory of Chemical Engineering Department, Boğaziçi University. This system comprises of three sections: feed, reaction and product analysis.

The feed section is composed of an Agilent Technologies 1200 series HPLC pump for water feed and the Brook Instrument 0254 series mass flow controllers (MFCs) to adjust the flow rate of the inlet gases via the Brooks Instrument 0254 series control box, 1/4'', 1/8'' and 1/16'' Swagelok stainless steel (SS) tubes, valves and fittings for feeding water and gaseous species, i.e. argon, carbon dioxide, carbon monoxide and hydrogen. The gases involved in this system were procured by pressurized cylinders by passing pressure regulators at the pressure of 2.5 bar. On-off valves were placed right before the mass flow controllers to avoid any possible back-pressure fluctuations. Each gas was fed from an independent line in order to control flow rate of the gases separately.

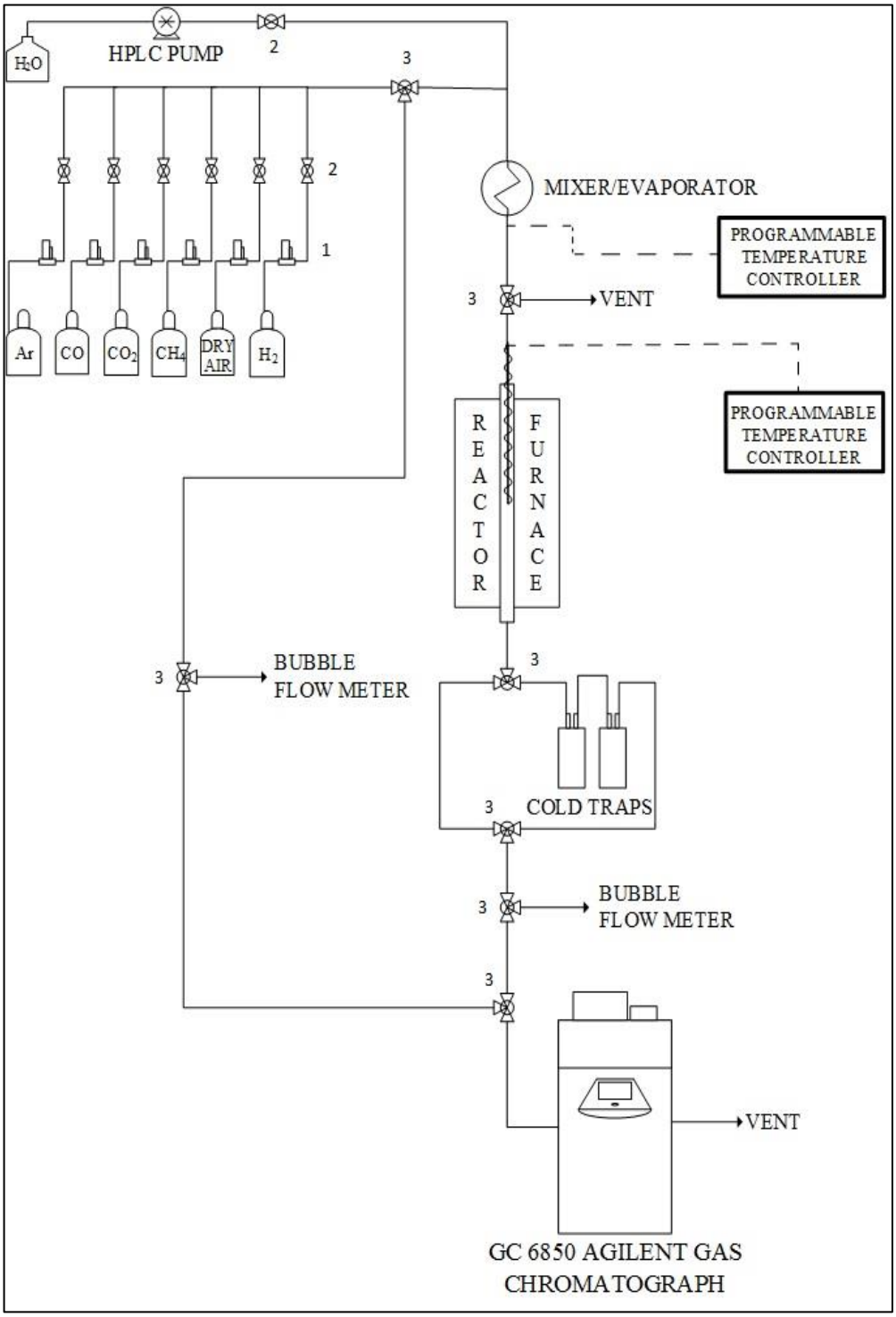

Figure 3.3. Schematic representation of the microreactor flow system:

1. Mass flow controller, 2. On-off valve, 3. Three-way valve (Demirhan, 2015).

The water was sent to the system using an Agilent 1200 series high pressure liquid chromatography pump providing the constant flow rates. The 1/16'' stainless steel tubing was kept at 140 ℃ with the help of a 104 W Cole-Parmer heating tape to ensure that water turns into steam completely. The temperature measurement of the mixing line was achieved by a K-type jacketed thermocouple and was controlled by a Eurotherm 3216 PID temperature controller. In order to avoid heat losses from the heating tape, ceramic wool isolations were implemented through the line where reactants were mixed before entering the reaction section.

The reaction section involved a 71 cm long 1/4'' OD stainless steel fixed bed microreactor placed in a 50 cm x 20 cm x 20 cm furnace, and a K-type jacketed thermocouple and a Shimaden FP23 programmable temperature controller. The catalyst bed was fixed in the middle of the reactor by using silane treated glass wool. Ceramic wool insulation was placed at top and bottom ends of the reactor furnace to avoid heat loss. The reactor was followed by a cold trap including two condensers situated in an ice-water bath to remove steam from the reactant mixture since it causes damages in gas chromatograph column.

3.2.4. Product Analysis System

An Agilent Technologies 6850 gas chromatograph equipped with a HayeSep D column and a Thermal Conductivity Detector (TCD) was used for quantitative determination of dry product and feed streams. The hourly time-on-stream (TOS) data was recorded to evaluate the performance of catalysts. Analysis conditions of the GC are given in Table 3.4 below.

Table 3.4. Product and reactant gas analysis conditions for WGS system.

GC Specifications	**Agilent Technologies 6850**
Carrier gas	Argon
Carrier gas flow rate, ml/min	15
Column temperature (°C)	40

Table 3.4. Product and reactant gas analysis conditions for WGS system (cont.).

GC Specifications	**Agilent Technologies 6850**
Column tubing material	Stainless steel
Column length & Inner diameter	3 m x 3 mm
Column packing material	Hayesep D
Detector type	TCD
Detector temperature (°C)	150
Inlet tempertature (°C)	100
Sample loop (ml)	1

The gas chromatograph was calibrated before starting to the experiments. Calibration was carried out by injecting the known amount of gases under the terms given in Table 3.4. The volume percent versus peak area curves were obtained for each gas and calibration factors were attained by linear regression.

3.2.5. Gravimetric Gas Sorption Analysis System

The gravimetric gas sorption analysis system consisting of a Hiden Isochema Intelligent Gravimetric Analyzer IGA-003 Dynamic Mixed Gas Sorption Analyzer and a Hiden Analytical Dynamic Sampling Mass Spectrometer (DSMS) is shown in Figure 3.4.

The oxygen storage capacities of catalysts samples were determined by IGA system while the volumes of the gases in the outlet stream were measured by DSMS system. Oxygen storage capacity measurements were achieved at reaction conditions applied in WGS performance tests. The calculations were based on observing the change in weight of the sample during WGS tests while increasing temperature of sample under inert atmosphere.

IGA is designed and programmed to work in two modes; that are dynamic and static modes. In static mode, the gases used in the experiments are supplied by pressurized cylinders and sent directly to IGA without adjusting the flow by an MFC. On the other hand,

in dynamic mode, the gases are passed through mass flow controllers which allow setting the desired flow rates before entering IGA system. In the IGA experiments conducted for this study, the dynamic mode was used.

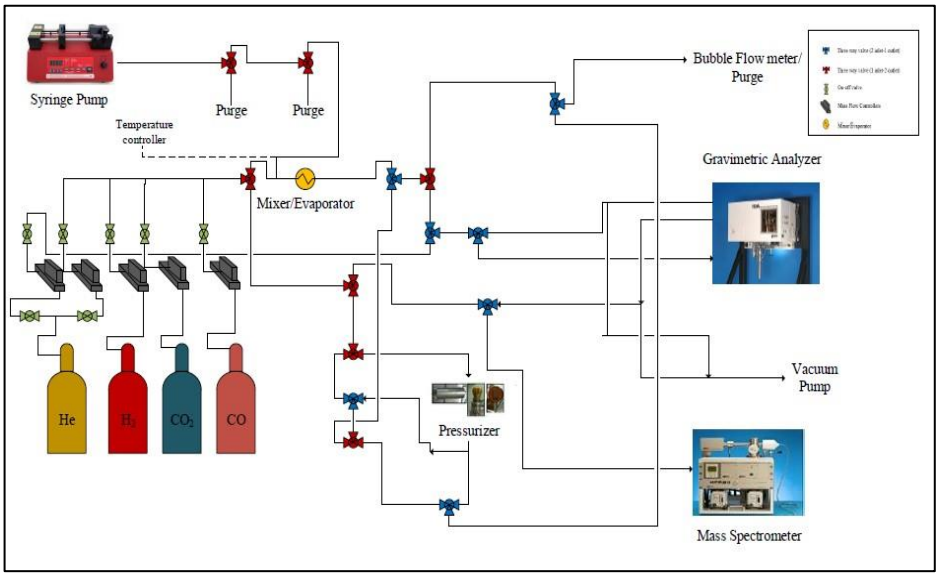

Figure 3.4. Schematic diagram of the gravimetric gas sorption analysis system.

The feed part of the IGA-DSMS system consists of Brooks Instrument 5850E series mass flow controllers and a Teledyne Hastings model mass flow controller to set the desired value for flow rates of gases used in analysis (CO, CO_2, H_2 and He), 1/4", 1/8" and 1/16" Swagelok stainless steel tubing, valves and fittings. The gases supplied by pressurized cylinders were passed through regulators that are adjusted to constant value of 5 bar for all experiments. In order to prevent mass flow controllers from possible back pressure, on-off valves were used between the mass flow controllers and the mixing zone where the gases were mixed homogeneously. In order to send the system trace amount of water, NE-300 model New Era Pump Systems Inc. syringe pump was used. The system also involves pressurizer, Parker ABP1 model back pressure regulator and Keller LEO1 digital manometer to perform high pressure analysis, however, for this study; it was not required due to the pressure range worked in.

The samples were placed in IGA chamber and weighted to see the changes during analyses. The IGA chamber has two outlets: the first one was sent to a vacuum pump to keep the pressure inside the chamber constant at a desired value by opening automatic exhaust valve and the second one was sent to DSMS to detect the amount of gases evolved during experiments.

3.3. Catalyst Preparation and Pretreatment

Ceria support was synthesized by homogeneous precipitation of cerium (III) nitrate hexahydrate by using sodium carbonate as precipitating material. Figure 3.2 presents the set up for support preparation. The aqueous solutions of materials, cerium (III) nitrate hexahydrate and sodium carbonate were obtained by dissolving the precursors in 100 ml of deionized (DI) water. Afterwards, the sodium carbonate solution was slowly added to the cerium nitrate solution until obtaining pH of 8 and the temperature of the solution was kept at 60 ℃ and throughout (stirred at 200 rpm) the procedure. After the pH value was 8, the resulting suspension was left for an hour to be mixed at the specified temperature and pH in the water bath shown in Figure 3.2. The mixture was then filtered by Watman filter paper and washed with DI water several times followed by drying overnight at 110 ℃ and calcination in a muffle furnace at 400 ℃ for 4 hours (Çağlayan, 2011).

The trimetallic Pt-Re-V/CeO_2 catalysts were synthesized by the sequential impregnation of V, Re and Pt precursors to ceria. Accordingly, first V addition to CeO_2 support was accomplished by the incipient to wetness impregnation method using aqueous solution of ammonium metavanadate and oxalic acid dihydrate which was added in order to solve V precursor in DI water with molar ratio of 1:1.5. The calculated amount of CeO_2 support was put in a Büchner flask and kept in ultrasonic mixer for 30 minutes under vacuum. The prepared precursor solution was impregnated over the CeO_2 support which is under vacuum via Masterlex computerized-derive peristaltic pump at a rate of 0.4 ml/min. The obtained slurry stayed in ultrasonic mixer for 1.5 hours under vacuum and then was

dried overnight at 110 °C. Finally, it was subjected to 2 hours calcination in the muffle furnace at 400 °C.

Re-V/CeO_2 catalysts were prepared by the addition of ammonium perrhenate to the V impregnated CeO_2 support by incipient to wetness impregnation technique. The determined amount ammonium perrhenate precursor was dissolved in relevant amount of DI water. The synthesized V/CeO_2 catalyst was placed in a Büchner flask and mixed ultrasonically for 30 minutes under vacuum. The resulting solution was impregnated on the catalyst by the help of Masterlex computerized-derive peristaltic pump at rate of 0.4 ml/min and left for mixing in ultrasonic mixer for 1.5 hours under vacuum. After this step was completed, the catalyst was dried overnight at 110 °C and calcined at 400 °C for 2 hours in the muffle furnace.

Lastly, Pt metal was added to V-Re/CeO_2 catalysts again by following incipient to wetness impregnation method. Accordingly, aqueous solution of tetraammineplatinum (II) nitrate precursor was deposited on V-Re/CeO_2 catalysts which were put in Büchner flask and mixed ultrasonically for 30 minutes under vacuum. After the deposition was achieved by using Masterlex computerized-derive peristaltic pump at rate of 0.4 ml/min, it was dwelled in ultrasonic mixer for 1.5 hours and dried overnight at 110 °C followed by calcination at 400 °C for 4 hours in the muffle furnace.

The catalysts prepared to be tested in this study are demonstrated in Table 3.5. Before conducting the reaction tests, the samples were were reduced in situ by heating from room temperature to the reduction temperature of 375 °C at a rate of 8.75 °C/min under 15 % H_2/Ar flow with total flow rate of 100 ml/min and were kept at 375 °C for 2 hours.

Table 3.5. List of Pt-Re-V/CeO_2 WGS catalysts.

Catalyst Name	**Pt wt.%**	**Re wt.%**	**V wt.%**
0.5Pt-1Re-1V/CeO_2	0.5	1	1
1Pt-1Re-1V/CeO_2	1	1	1
0.5Pt-0.5Re-0.5V/CeO_2	0.5	0.5	0.5

3.4. WGS Performance Tests and Oxygen Storage Capacity Measurements

3.4.1. WGS Performance Tests

In the current study, the WGS perfomance tests were conducted at 300, 350, 400 and 450 °C by using the same two realistic feeds having different H_2O/CO ratio, which are presented in Table 3.6 as RF#1 and RF#2, to investigate the WGS performances of all three catalysts presented in Table 3.5 in 300-450 ^oC temperature range. *Note that the performances of 0.5Pt-1Re-1V/CeO_2 and 1Pt-1Re-1V/CeO_2 catalysts were tested previously by our group members Kesim (2017) and Özer (2016), respectively. By the tests performed in the current work, the performance of those catalysts was analyzed for a wider temperature range, and the previous performance data were confirmed as well.* The tests were carried out on 75 mg freshly reduced catalyst samples with 120,000 ml $g_{cat}^{-1}h^{-1}$ GHSV for 6 hour time-on-stream (TOS). Between the end of reduction step and initiation of reaction, the feed was sent to purge for a period of 1.5 hour aiming to obtain a homogeneous and steady state feed gas composition. In the meantime, the catalyst was trapped in the reactor under Ar atmosphere.

Table 3.6. Realistic feed compositions performed in first part of the study.

Feed Name	**H_2O/CO Ratio**	**Flow Composition**
Realistic Feed #1 (RF#1)	6.7	4.9%CO, 32.7%H_2O, 30%H_2, 10.4%CO_2, 22%Ar
Realistic Feed #2 (RF#2)	16.2	2.1%CO, 34.1%H_2O, 23.7%H_2, 12.3% CO_2, 27.8%Ar

The time-on-stream performance tests was started with the first contact of reactant gases with the freshly reduced catalyst sample, and the first product analysis data was recorded 30 minutes later than the first contact. Three feed analyses were carried out after taking 6 hours TOS data. All the WGS performance experiments conducted for this study are listed in Table 3.7.

Table 3.7. List of the experiments performed for first part of the study.

Catalyst	**H_2O/CO**	**Temperature (°C)**	**Experiment #**
0.5Pt-1Re-1V/CeO_2	6.7	300	1
	6.7	350	2
	6.7	400	3
	6.7	450	4
	16.2	300	5
	16.2	350	6
	16.2	400	7
	16.2	450	8
1Pt-1Re-1V/CeO_2	6.7	300	9
	6.7	350	10
	6.7	400	11
	6.7	450	12
	16.2	300	13
	16.2	350	14
	16.2	400	15
	16.2	450	16
0.5Pt-0.5Re-0.5V/CeO_2	6.7	300	17
	6.7	350	18
	6.7	400	19
	6.7	450	20
	16.2	300	21
	16.2	350	22
	16.2	400	23
	16.2	450	24

3.4.2. Oxygen Storage Capacity (OSC) Measurements

A Hiden Isochema Intelligent Gravimetric Analyzer coupled with Hiden Analytical Dynamic Sampling Mass Spectrometer (IGA-MS or IGA-DSMS) system was used in the *operando* oxygen storage capacity (OSC) measurements. The tests were conducted on 75 mg freshly reduced catalyst with 40,000 ml $g_{cat}^{-1}h^{-1}$ GHSV. Each catalyst was tested at 350 °C, the temperature at which the highest activity was obtained in performance tests, under two diluted realistic feed compositions, DRF#1 and DRF#2, which are the diluted forms of the ones used in performance tests, namely RF#1 and RF#2, respectively. DRF compositions used in the tests were presented in Table 3.8. Additionally, 1Pt-1Re-1V/CeO_2, which had the highest performance in the first part of the study, was tested at three different temperatures, 350, 400 and 450 °C under the flow of DRF #1 in order to clarify the temperature effect.

Table 3.8. Realistic feed compositions performed in second part of the study.

Feed Name	**H_2O/CO Ratio**	**Flow Composition**
Diluted Realistic Feed #1 (DRF#1)	6.7	6.5% RF#1 + 93.5% He *(RF#1: 6.3%CO, 41.9%H_2O, 38.5%H_2, 13.3%CO_2)*
Diluted Realistic Feed #2 (DRF#2)	16.2	5.8% RF#2+ 93.5% He *(RF#2: 2.9%CO, 47.1%H_2O, 32.7%H_2, 17.3% CO_2)*
He	-	100% He

Experiments conducted with pure He flow over each catalyst at all temperature levels were used to determine the "structural" oxygen already exist in the catalysts/their structure. The He experiments revealed the structural oxygen capacity (S-OSC) involving the oxygen in the surface groups and stored oxygen in the ceria lattice. However, the experiments conducted upon diluted realistic feed flow(s) display not only the oxygen stored in lattice and located on surface in the form of surface groups as formate, carbonate and/or carboxyl-carboxylate like intermediates, but also the oxygen emanating from reaction; which can be

called as “total” oxygen storage capacity (T-OSC). The oxygen stored, which is related to the catalytic activity, involves the ones coming from reaction and some surface groups (please see the R&D section on OSC). Table 3.9 illustrates the experiments conducted for OSC measurements.

Table 3.9. List of the experiments performed for determination of OSCs of the catalysts.

Catalyst	**H_2O/CO**	**Temperature (°C)**	**Experiment #**
1Pt-1Re-1V/CeO_2	16.2	350	1
	6.7	350	2
	6.7	400	3
	6.7	450	4
	He	350	5
	He	400	6
	He	450	7
0.5Pt-1Re-1V/CeO_2	16.2	350	8
	6.7	350	9
	He	350	10
0.5Pt-0.5Re-0.5V/CeO_2	16.2	350	11
	6.7	350	12
	He	350	13

The new *operando* methodology utilizing IGA-DSMS system was developed to determine the various types of oxygen storage capacities of the catalyst samples. At the beginning, 75 mg catalyst sample was placed in IGA chamber with certain amount of quartz wool on it to prevent dusting under gas flow. Then, the sample was heated from room temperature to 120 °C under vacuum to degas the system for eliminating gas molecules might be adsorbed on during placement of sample and for removing N_2 from air that might be present in the chamber, which gives partial pressure signal at the same mass value with CO in MS. During degassing, the gas within the system was vacuumed with 50 ml/min rate until the inner pressure decreased down to $5*10^{-3}$ mbar. After degassing, the sample was

reduced *in-situ* under the flow of 50 ml/min '15% H_2-balance He' mixture at 375 °C. Then, WGS reaction was initiated through feeding the system with DRF #1 or #2, and the reaction was conducted for 2 h-TOS. During the reaction step, the oxygen molecules supplied by H_2O as well as oxygen from some surface species participate in WGS reaction. At the end of 2 hours, He was allowed to flow for 1 hour to sweep all of the gases remained inside the large reactor volume. This was followed by a temperature increase to 800 °C in a controlled manner; throughout the temperature ramp the weight change of the sample was recorded at Hiden Isochema Intelligent Gravimetric Analyzer while partial pressures of outlet gases were measured by Hiden Analytical Dynamic Sampling Mass Spectrometer at real-time basis. The only difference between *operando* reaction tests conducted to determine T-OSC and the He experiments through which S-OSC was measured is; instead of feeding the system with DRFs in the reaction step, 50 mL/min pure He was introduced to the chamber in He tests.

All calculations were based on the weight change of the catalyst sample and the volume ratio of outlet gas mixture. Firstly, the inconsistencies in data obtained from mass spectrometer and IGA system due to time shift were detected, and time lag was eliminated via taking the time when WGS reaction was stopped as the basis. Then, the misleading data led by any electrical fluctuations affecting MS signal were corrected. In the next stage, for each of the CO_2 and CO partial pressure data series, a minimum value was determined and subtracted from the whole set; thus that minimum value is zeroed and the whole set is called "zeroed data". Zeroed data was then normalized via dividing the whole set by a maximum signal value measured just before the signal began to drop following the cease of feed mixture, which stops the reaction. Thus, the normalized data set was confined between 0 and 1. Throughout the tests SEM detector, which provides high precision data with higher frequency, was used instead of Faraday detector. The fluctuations due to very high sensitivity of the SEM detector were then smoothed by moving average method -*the average of 20 data before the data itself*-. The areas obtained via OPUS 6.5 Software under the plots of "smoothed data vs. time" for CO_2 and CO signals *measured by MS* and weight change *by IGA* during temperature rise stage of the method were utilized to calculate T-OSC and S-OSC, for the tests conducted under reactive and inert atmosphere, respectively. E-OSC was

then calculated by subtracting S-OSC from T-OSC. A representative smoothed plot of CO_2 at the outlet, obtained under DRF #1 flow at 350 °C, along with the enlarged plot of area under consideration were given in Figure 3.5 a&b. In order to ensure the reliability and sensitivity of the data obtained for OSC studies; the blank tests, during which only the quartz wool was placed in the chamber for the same conditions/methodology mentioned above, were conducted. The results of the blank tests verified that quartz wool was not reactive, and confirmed the reactant gasses were completely swept from the chamber in the sweeping stage of the procedure.

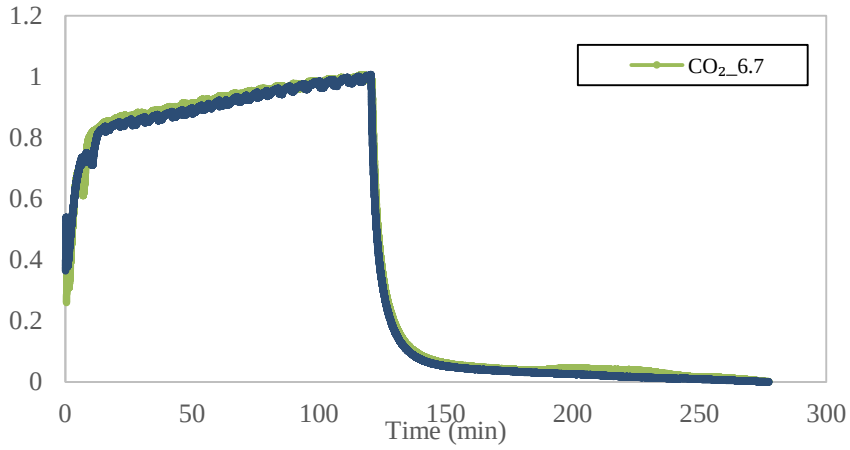

(a)

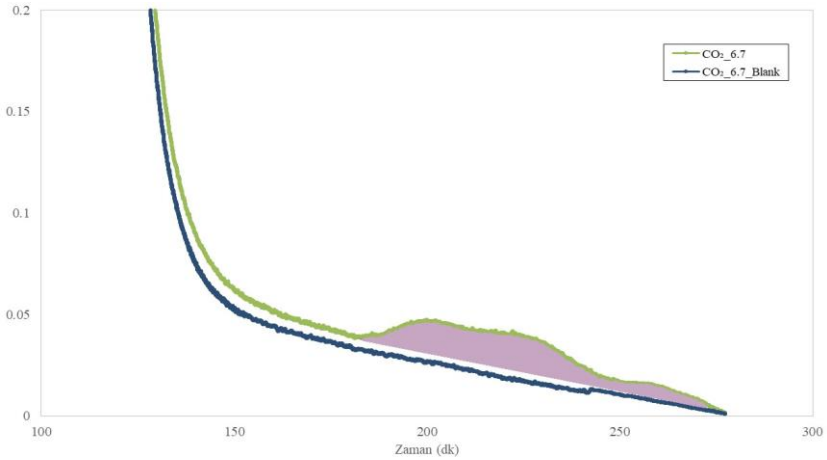

(b)

Figure 3.5. The representative data of smoothed CO_2 MS signal for realistic feed #1 and the blank test (a); and zoomed version of same data (b).

4. RESULTS AND DISCUSSIONS

The present work is a part of an ongoing study aiming to design and develop high performance, steam tolerant, non-pyrophoric WGS catalyst(s) to be used in a demo-scale fuel processor (DFP) producing PEM grade hydrogen for PEM fuel cells. The current work mainly focuses on developing a reliable methodology for determination of oxygen storage capacity (OSC) of the catalysts through the use of *operando* IGA-MS analysis; and establishing a relation between WGS activity and OSC.

The results of this study are presented in three sections. In the first section, the results of WGS performance tests conducted under realistic conditions are reported. The second section comprises the results of the SEM, XPS and Raman Spectroscopy analyses, which were performed to clarify the link between micro physical and (surface) chemical properties of the catalysts and their WGS activity. In the final section, an *operando* methodology proposed for measuring oxygen storage capacity (OSC) of the samples is explained and verified; values of different types of OSC measured/calculated for the samples are presented; then, the relation between OSC and WGS activity for the samples is scrutinized.

4.1. Water Gas Shift Performance Tests

The performances of catalysts prepared were evaluated based on their activity and stability in WGS reaction under the experimental conditions listed in Table 3.7. Catalytic activity was reported as CO conversion and amount of net H_2 produced for both realistic feed compositions. 2 h TOS data were used to make comparison between the catalytic activities of samples (Figure 4.1 and 4.2). Blank tests were previously performed by Çağlayan to verify that stainless steel reactors, glass wool and CeO_2 support have no catalytic activity (Çağlayan, 2011).

CO conversion, *as the percentage of converted CO based on the CO amount sent in feed stream*, and amount of net H_2 produced, *as the net percentage increase in H_2 flow in product stream on the basis of H_2 amount fed in the reactant stream*, are calculated by using Equation 4.1 and 4.2, respectively.

$$\text{CO conversion (\%)} = \left[\frac{F_{CO,in} - F_{CO,out}}{F_{CO,in}}\right] 100 \tag{4.1}$$

$$\text{Net } H_2 \text{ production (\%)} = \left[\frac{F_{H_2,out} - F_{H_2,in}}{F_{H_2,in}}\right] 100 \tag{4.2}$$

The molar flow rate of each species in the feed and product streams is calculated by using Equation 4.3:

$$F_i\ (\mu\text{mol s}^{-1}) = \frac{P\ V_{i,gas}}{R\ T} \tag{4.3}$$

Where P denotes the atmospheric pressure, $V_{i,gas}$ is the volumetric flow rate of the gas, R is the universal gas constant and T is the absolute temperature.

Equation 4.4 and Equation 4.5 are used to calculate CO conversion and the net gas (H_2 and CO_2) production rate, respectively:

$$\text{CO conversion rate } (\mu\text{mol g}^{-1}\text{s}^{-1}) = \frac{F_{CO,in} - F_{CO,out}}{w_{cat}} \tag{4.4}$$

$$\text{Net gas production rate } (\mu\text{mol g}^{-1}\text{s}^{-1}) = \frac{F_{gas,out} - F_{gas,in}}{w_{cat}} \tag{4.5}$$

The stability of catalysts is evaluated on the basis of activity loss which is defined as the percent loss of initial activity and is calculated by Equation 4.6:

$$\text{Activity loss (\%)} = \left[\frac{(\text{CO conversion})_{0.5\text{h}} - (\text{CO conversion})_{6\text{h}}}{(\text{CO conversion})_{0.5\text{h}}}\right] 100 \qquad (4.6)$$

All the TOS activity and stability data obtained from WGS performance tests are provided in Appendix A.

4.1.1. Realistic Feed Tests

The performance tests were carried out under atmospheric pressure at four different temperatures, 300, 350, 400 and 450 °C, over three Pt-Re-V/CeO_2 samples for two realistic feed conditions, which simulate typical reformer outlet presented in Tables 3.5 and 3.6. Throughout the tests, GHSV was kept fixed at 120,000 ml g_{cat}^{-1} h^{-1}. There was no methane formation at any reaction condition, proving that Pt-Re-V system suppressed secondary methanation activity.

The role of temperature on catalytic activity and net H_2 production of the trimetallic Pt-Re-V/CeO_2 catalysts for the RF #1 (H_2O/CO=6.7) are displayed in Figures 4.1 (a) and (b), respectively. Figure 4.1 (a) also involves the equilibrium CO conversions for WGS reaction evaluated by the help of HSC-Chemistry Software.

Experimental results indicate that the conversion levels for each catalyst were relatively lower at 300 °C. On the other hand, the highest conversion values that were achieved on 1Pt-1Re-1V/CeO_2 and 0.5Pt-0.5Re-0.5V/CeO_2 catalysts at 350 °C are 71% and 66%, respectively. Both catalysts generated ca. 10% additional H_2 on the basis of H_2 amount already existed in the feed stream. Similar to the trend in thermodynamic equilibrium conversion change with temperature; as the temperature increased to 400 °C, the catalytic activities of 1Pt-1Re-1V/CeO_2 and 0.5Pt-0.5Re-0.5V/CeO_2 samples both decreased to ca.

64% conversion level, leading to a decrease in net H_2 production from 10% to 9% though 0.5Pt-1Re-1V/CeO_2 catalyst showed its highest catalytic activity at 400 °C with 60% CO conversion value and 7% net H_2 production.

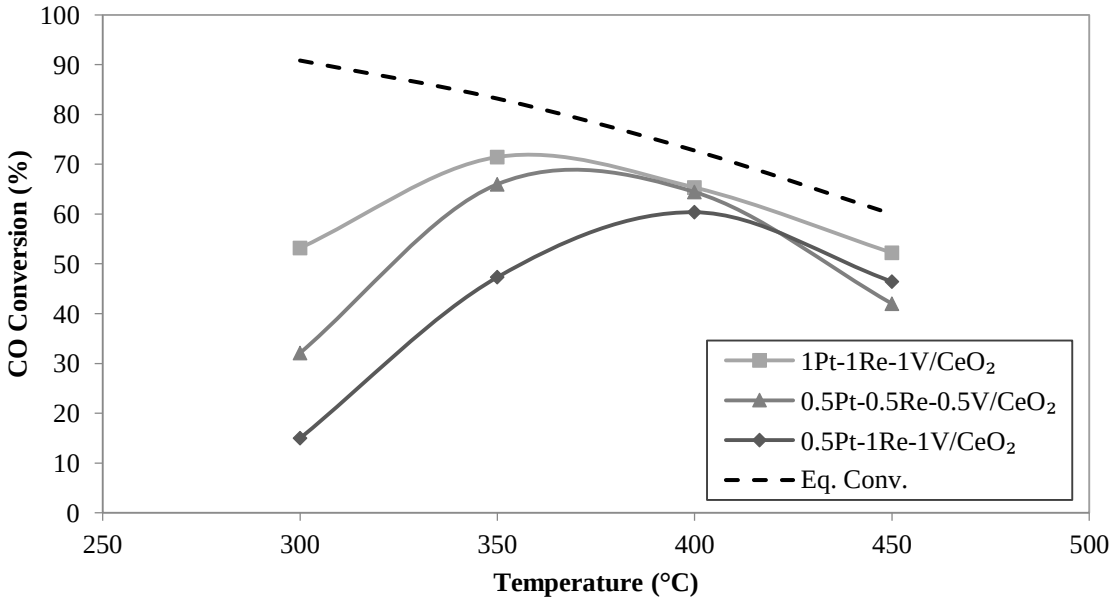

(a)

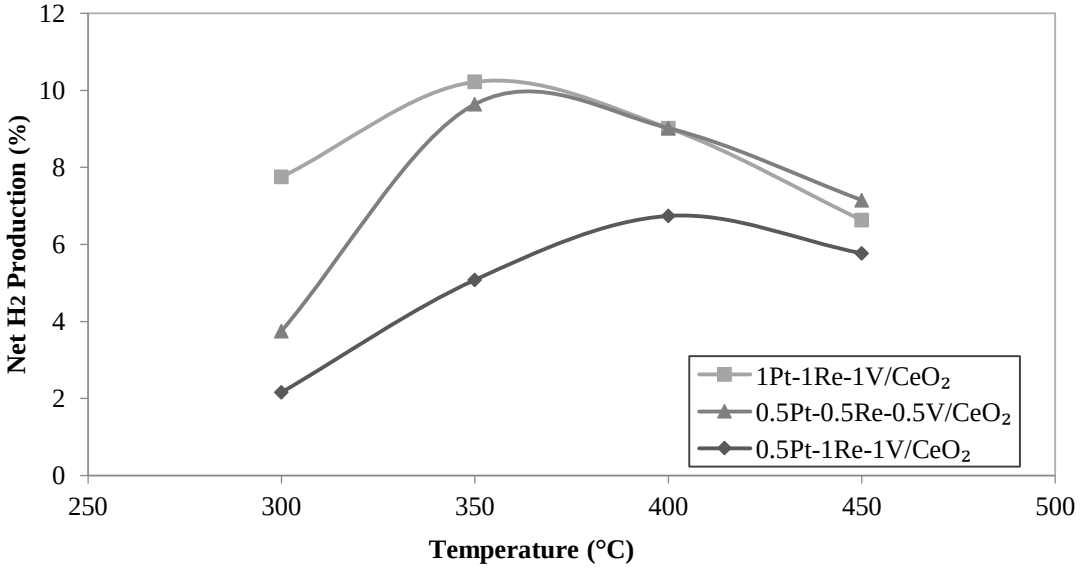

(b)

Figure 4.1. Temperature dependence of (a) catalytic activity and (b) net H_2 production for realistic feed #1, H_2O/CO = 6.7 (4.9% CO, 32.7% H_2O, 30.0% H_2, 10.4% CO_2, 22.0% Ar).

Further increase in temperature, to 450 °C, led to decrease in both CO conversion levels and net H_2 production percentages for all catalysts. At this temperature level, the lowest CO conversion level (42%) was attained over 0.5Pt-0.5Re-0.5V/CeO_2 catalyst although for other temperature levels, 0.5Pt-1Re-1V/CeO_2 catalyst showed inferior conversion values accompanied by its low net H_2 production amounts. Moreover, among three catalysts and for the temperature range tested, the lowest hydrogen production rate (2%) was obtained at 300 °C over 0.5Pt-1Re-1V/CeO_2 along with its 15% CO conversion, which was also the lowest conversion level measured in this experimental set. In all cases except for 300 °C, the CO conversion values for all samples were close to the equilibrium conversions.

The temperature dependence of CO conversion and net H_2 production for the RF#2 (H_2O/CO= 16.2) are presented in Figures 4.2(a) and 4.2(b), respectively. Figure 4.2 (a) also includes the equilibrium conversions for WGS reaction evaluated by HSC-Chemistry Software.

In this part of the performance tests, the feed composition was changed from RF #1 to RF #2, which has higher H_2O/CO feed ratio. For all catalyst samples, the conversion values obtained for both H_2O/CO feed ratios at 350 °C were close to each other whereas for the other temperature values, the difference became apparent. It should be noted that, in general, altering feed composition from RF#1 *having H_2O/CO ratio of 6.7* to RF#2 *having 16.2 H_2O/CO ratio*, caused loss in catalytic activity, i.e. resulted in lower CO conversion and net H_2 production values measured.

The results of this part of the study illustrated that 0.5Pt-0.5Re-0.5V/CeO_2 and 0.5Pt-1Re-1V/CeO_2 catalysts yielded the lowest CO conversion values and 0.5Pt-1Re-1V/CeO_2 catalyst produced the lowest H_2 amount (0.19%) at 300 °C while 1Pt-1Re-1V/CeO_2 catalyst reached relatively higher CO conversion (55%) and H_2 production (3%) values at this temperature level.

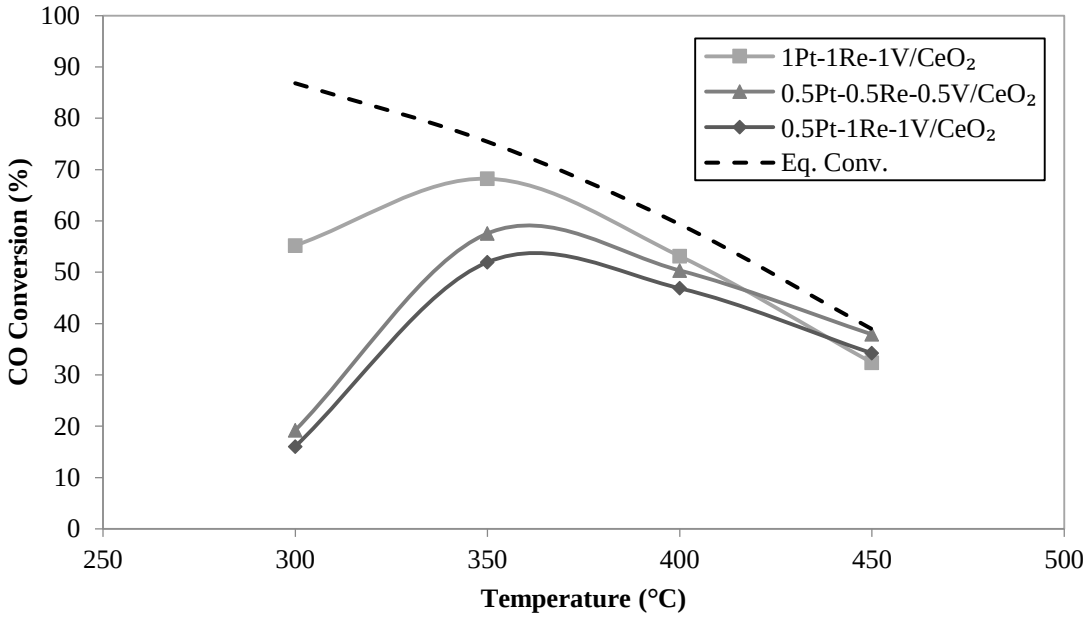

(a)

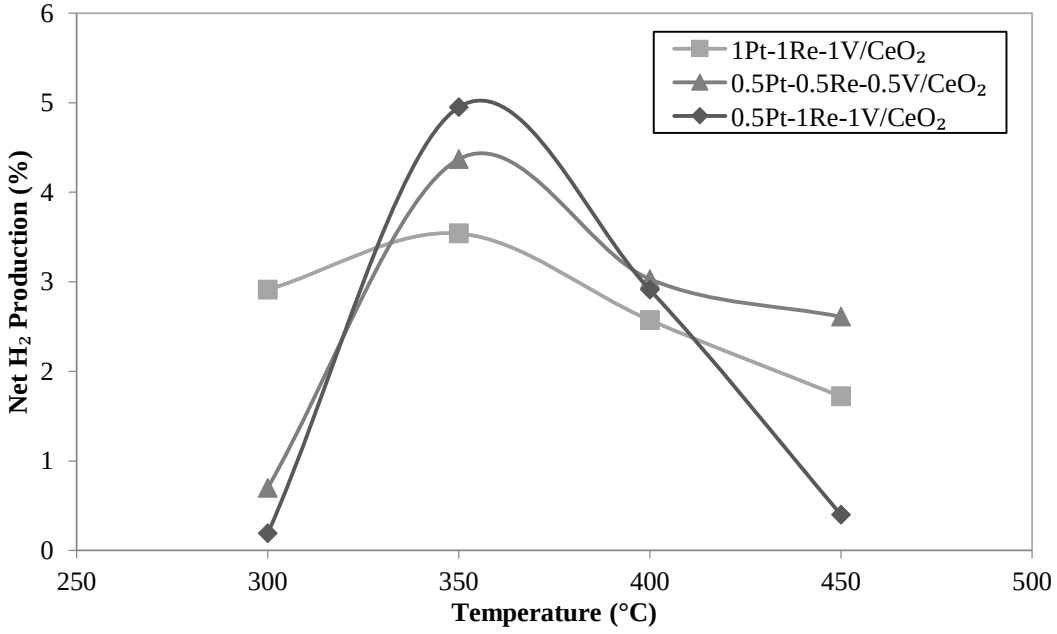

(b)

Figure 4.2. Temperature dependence of (a) catalytic activity and (b) net H_2 production for realistic feed # 2, H_2O/CO = 16.2 (2.1% CO, 34.1% H_2O, 23.7% H_2, 12.3% CO_2, 27.8% Ar).

The highest conversion (68%) was reached again over 1Pt-1Re-1V/CeO_2 at 350 °C with net H_2 production percentage of 3.5% followed by 57% and 52% CO conversion with 4.4% and 5% net H_2 production levels obtained over 0.5Pt-0.5Re-0.5V/CeO_2 and 0.5Pt-1Re-1V/CeO_2, respectively. Increasing temperature led to decrease in both CO conversion and net H_2 production for all catalysts. For 1Pt-1Re-1V/CeO_2 catalyst sample, changing temperature to 400 °C resulted in a decrease in CO conversion and net H_2 production to ca. 53 % and to 2.5%, respectively. Further rise in temperature to 450 °C, brought further decline in catalytic activity. At high temperatures, the CO conversion values approached not only to each other's but also to the equilibrium conversion levels.

The activity losses of the catalysts were evaluated through comparing 0.5 h and 6 h TOS data. The time dependent activity results for RF #1 at 350 °C were presented in Figure 4.3. 1Pt-1Re-1V/CeO_2 having superior performance with respect to conversion revealed also the most stable performance with 2.4 % activity loss among other catalyst samples under these conditions. This highest stability level was followed by 0.5Pt-1Re-1V/CeO_2 catalyst with activity loss of 5.7% even though the CO conversion values of this sample was below that of 0.5Pt-0.5Re-0.5V/CeO_2 catalyst which lost 13% of its activity at the end of 6 h.

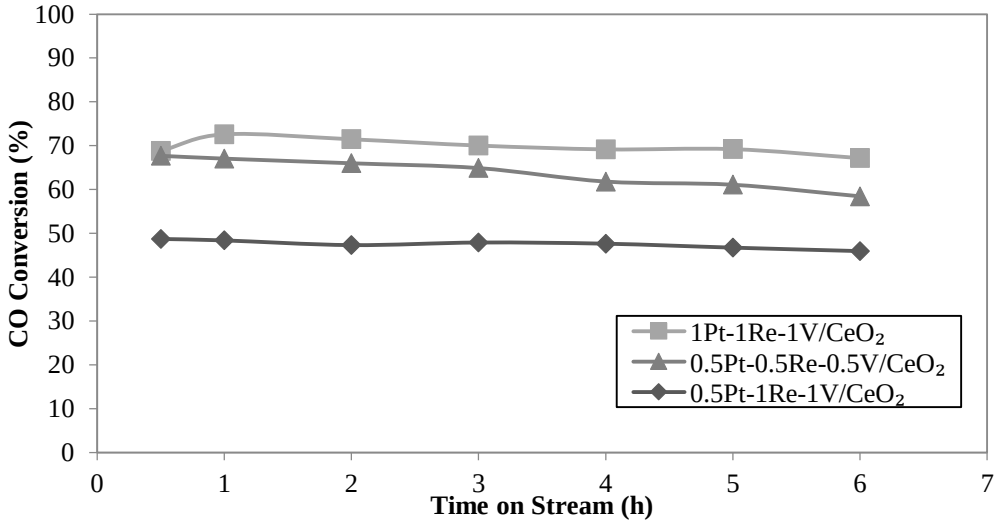

Figure 4.3. Time dependent stability values of catalysts for realistic feed #1, H_2O/CO = 6.7 at 350 °C (4.9% CO, 32.7% H_2O, 30.0% H_2, 10.4% CO_2, 22.0% Ar).

Time dependent stability values evaluated considering 0.5 h and 6 h data for RF #1 at 400 °C are presented in Figure 4.4. The catalytic activities of both 1Pt-1Re-1V/CeO_2 and 0.5Pt-0.5Re-0.5V/CeO_2 catalysts decreased with temperature rise. On the other hand, the activity of 0.5Pt-1Re-1V/CeO_2 showed the exact opposite relationship with temperature; as temperature was raised to 400 °C, its activity was enhanced both in terms of CO conversion and net H_2 production. At this temperature, 1Pt-1Re-1V/CeO_2 and 0.5Pt-0.5Re-0.5V/CeO_2 catalysts had the highest stability with activity losses of 2.9% and 8.8%, respectively. Even though it had higher activity compared to that of obtained at 350 °C, 0.5Pt-1Re-1V/CeO_2 catalyst showed activity loss of 14% at 400 °C.

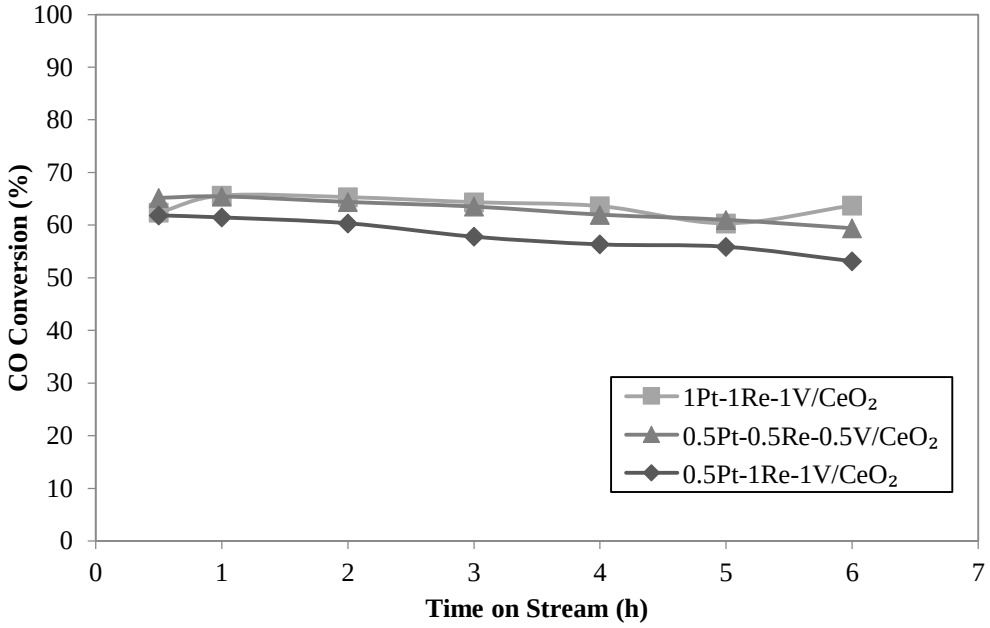

Figure 4.4. Time dependent stability values of catalysts for realistic feed #1, H_2O/CO = 6.7 at 400 °C (4.9% CO, 32.7% H_2O, 30.0% H_2, 10.4% CO_2, 22.0% Ar).

The results of the study revealed that the experiments conducted with RF #1 resulted in higher net H_2 production rate and CO conversion values. Actually, RF #1 differs from RF #2 with its CO concentration; it contains nearly two times the CO amount of RF #2. Since H_2O, H_2 and CO_2 concentrations were almost the same in both feed compositions, lower net H_2 production levels obtained with RF #2 may have been resulted from the limitation in the CO amount.

Besides to catalytic activity and stability, selectivity is another parameter in evaluating the performances of the catalyts studied. WGS catalysts should not only reduce CO concentration, but also produce additional H_2 and therefore they should not have a tendency to form methane through methanation reaction causing H_2 consumption. Throughout the reaction tests, there was no methane formation and all the tests gave positive net H_2 production rates, though for some cases the values are rather low. Figures 4.5 and 4.6 demonstrate the selectivities of three catalysts on the basis of the H_2 and CO_2 poduction rates obtained at 6 h TOS at four different temperature levels under the flow of RF #1 and #2, respectively.

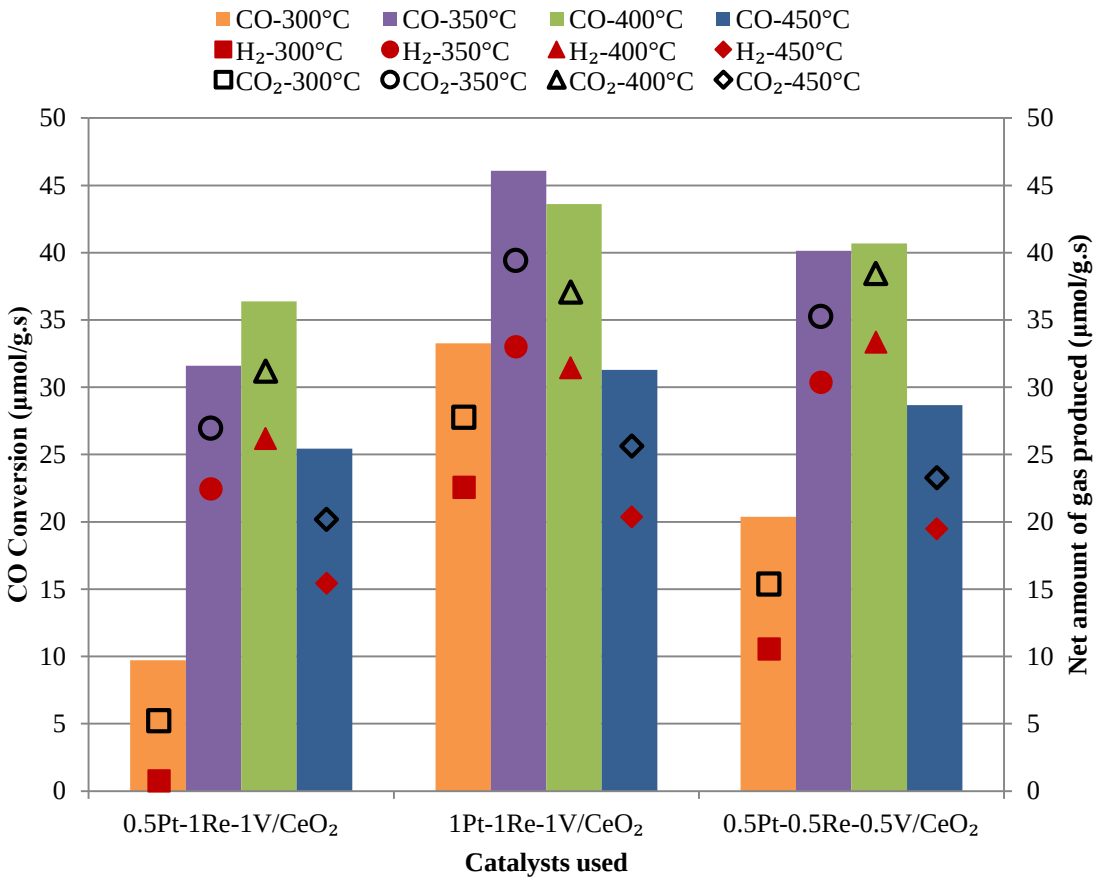

Figure 4.5. The net H_2 and CO_2 production rates and the effect of the catalyst type on the CO conversion for realistic feed #1 (H_2O/CO = 6.7) at the end of 6 h TOS.

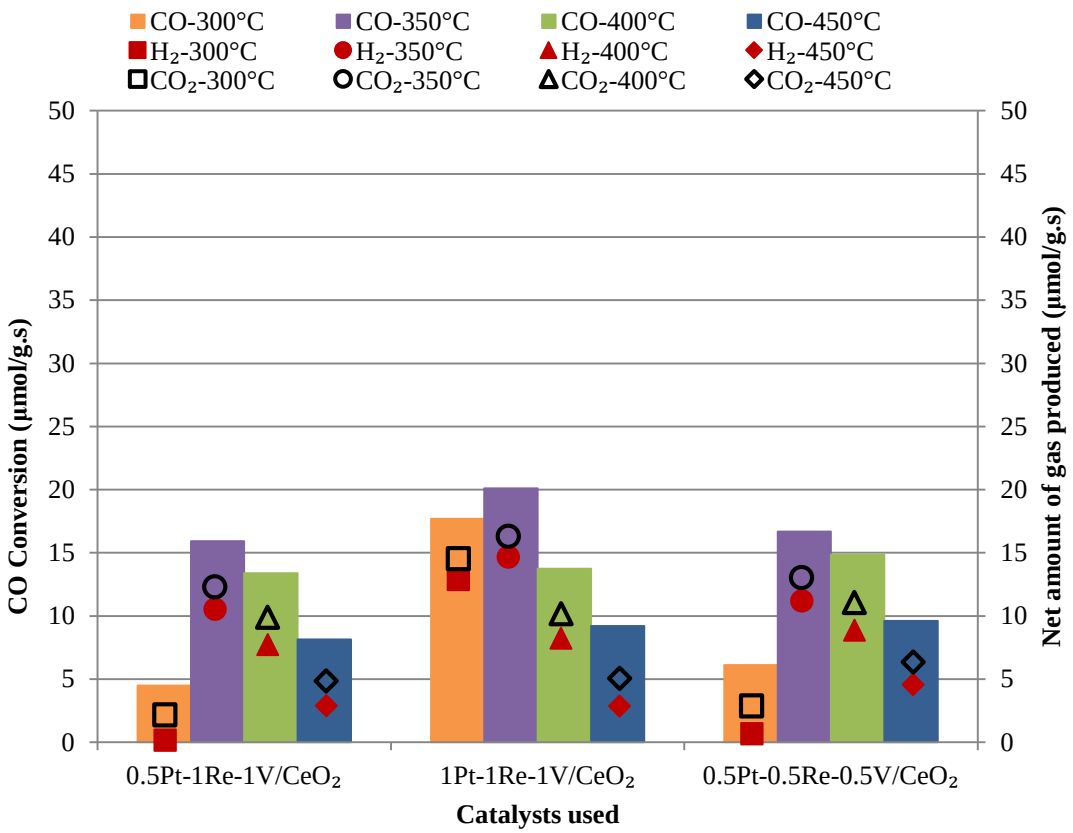

Figure 4.6. The net H_2 and CO_2 production rates and the effect of the catalyst type on the CO conversion for realistic feed #2 (H_2O/CO = 16.2) at the end of 6 h TOS.

The comparative analysis of the results indicated that catalyst composition and reaction conditions have significant effect on WGS performance. The catalysts reached their highest performances at 350 and 400 °C; the highest net H_2 production values were obtained under feed flow having low H_2O/CO ratio, RF#1, over 1Pt-1Re-1V and 0.5Pt-0.5Re-0.5V catalysts at 350 and 400 °C, respectively. The differences between catalysts' performances become apparent under RF #1 with low H_2O/CO ratio while under RF #2 flow, no pronounced differences were observed.

In general, the results revealed that 1Pt-1Re-1V/CeO_2 and 0.5Pt-0.5Re-0.5V/CeO_2 have great potential to be used in a fuel processor as WGS catalysts owing to their high activity, stability and selectivity. Another important point is that those catalysts can make the use of a single stage WGS unit in an FP possible instead of conventional two stage (HTS and LTS) WGS unit.

4.2. Catalyst Characterization

In this section, the characterization results of Pt-Re-V catalyst samples used in this study are presented. For the characterization of samples; SEM was used to detect the microstructural properties, XPS was used to identify the oxidation levels of CeO_x support and metallic components, and Raman Spectroscopy was used to analyze the V-O-V and V-O-Ce bonds, and the changes that these bonds undergo in response to changes in Pt:Re:V loadings.

4.2.1. SEM

The microstructural properties of the freshly reduced catalysts were analyzed by using scanning electron microscopy (SEM). All the samples characterized by SEM presented a very porous, blossom-like morphology. The SEM micrographs of all freshly reduced catalysts; 0.5Pt-0.5Re-0.5V/CeO_2, 0.5Pt-1Re-1V/CeO_2 and 1Pt-1Re-1V/CeO_2, at 100,000x magnification are given Figures 4.7 (a), (b) and (c), respectively. Figure 4.7 indicates that all three catalysts have similar microstructural properties.

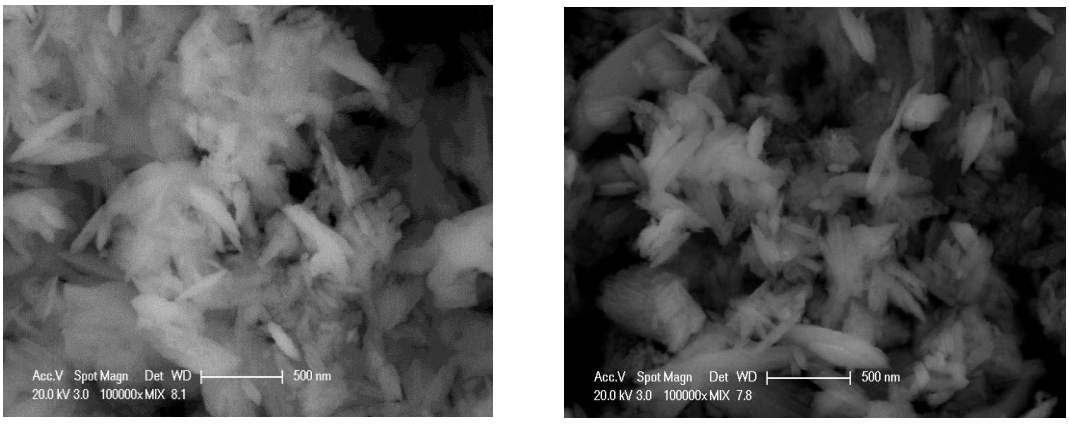

(a) (b)

Figure 4.7. SEM micrographs of freshly reduced catalysts (100,000x) for (a) 0.5Pt-0.5Re-0.5V/CeO_2, (b) 0.5Pt-1Re-1V/CeO_2 and (c) 1Pt-1Re-1V/CeO_2.

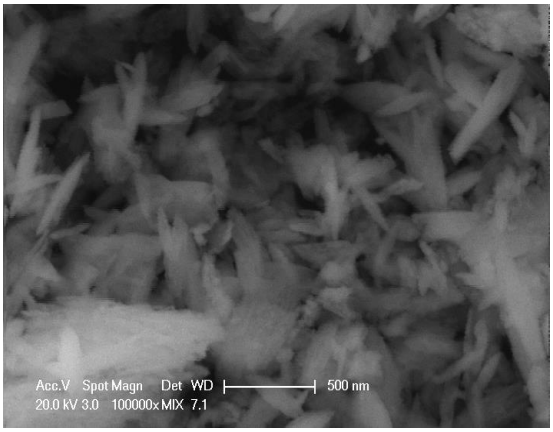

(c)

Figure 4.7. SEM micrographs of freshly reduced catalysts (100,000x) for (a) 0.5Pt-0.5Re-0.5V/CeO_2, (b) 0.5Pt-1Re-1V/CeO_2 and (c) 1Pt-1Re-1V/CeO_2 (cont.).

SEM micrograph for 1Pt-1Re-1V/CeO_2 sample taken at 100,000x magnification is presented in Figure 4.8. The bright areas shown in red circles mainly consist of platinum particles dispersed over CeOx support, which has blossom-like stucture with 30-50 nm width and primarily determines the micro-physical structure of the catalyst.

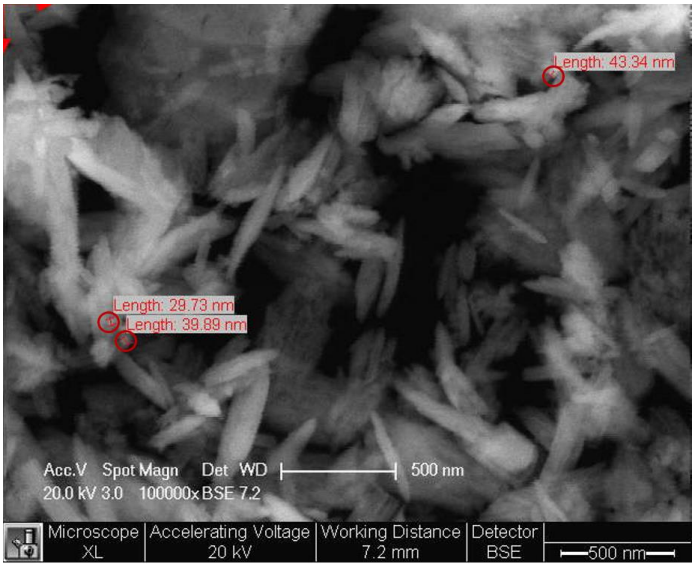

Figure 4.8. SEM micrograph of 1Pt-1Re-1V/CeO_2 catalyst from taken at 100,000x.

Since the number of backscattered electrons (BSE) reaching the BSE detector is proportional to the mean atomic number of the element, V and Ce elements which have close atomic numbers, have nearly the same brightness; hence it is hard to distinguish the V atoms on surface from Ce in BSE images. This is the reason why V atoms are not seen in SEM micrographs. The SEM images of 0.5Pt-0.5Re-0.5V/CeO_2 and 0.5Pt-1Re-1V/CeO_2 samples are shown in Figures 4.9 (a) and (b), respectively.

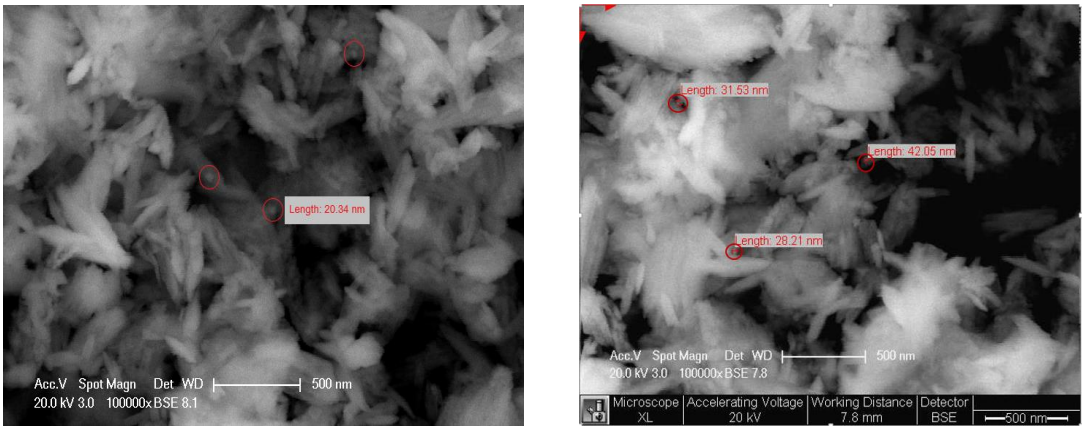

(a) (b)

Figure 4.9. SEM micrographs of (a) 0.5Pt-0.5Re-0.5V/CeO_2 and (b) 0.5Pt-1Re-1V/CeO_2.

4.2.2. XPS

The elemental composition of the catalysts' surface and the oxidation states of the metallic species present on it were analyzed by X-ray photoelectron spectroscopy (XPS). XPS is a meaningful method to analyze both the surface of a freshly reduced sample and that of a spent catalyst subjected to modification(s) during reaction. XP spectra of samples presented the characteristic oxidation states of Ce, Pt, Re, V and O atoms.

The XP spectra for Ce 3d region of freshly reduced catalyst samples including the principal spin-orbit state peaks of $Ce3d_{3/2}$ and $Ce3d_{5/2}$ corresponding to Ce^{3+} and Ce^{4+} oxidation states, labeled as v and u, respectively, are illustrated in Figure 4.10. The spectra of Ce 3d region displayed total of 10 peaks compatible with the literature (Çağlayan and

Aksoylu, 2011; Jardim *et al.*, 2015). The shift observed in XP spectra has resulted from the incorporation of metals into ceria lattice (Çağlayan and Aksoylu, 2011) and the change in catalysts' composition.

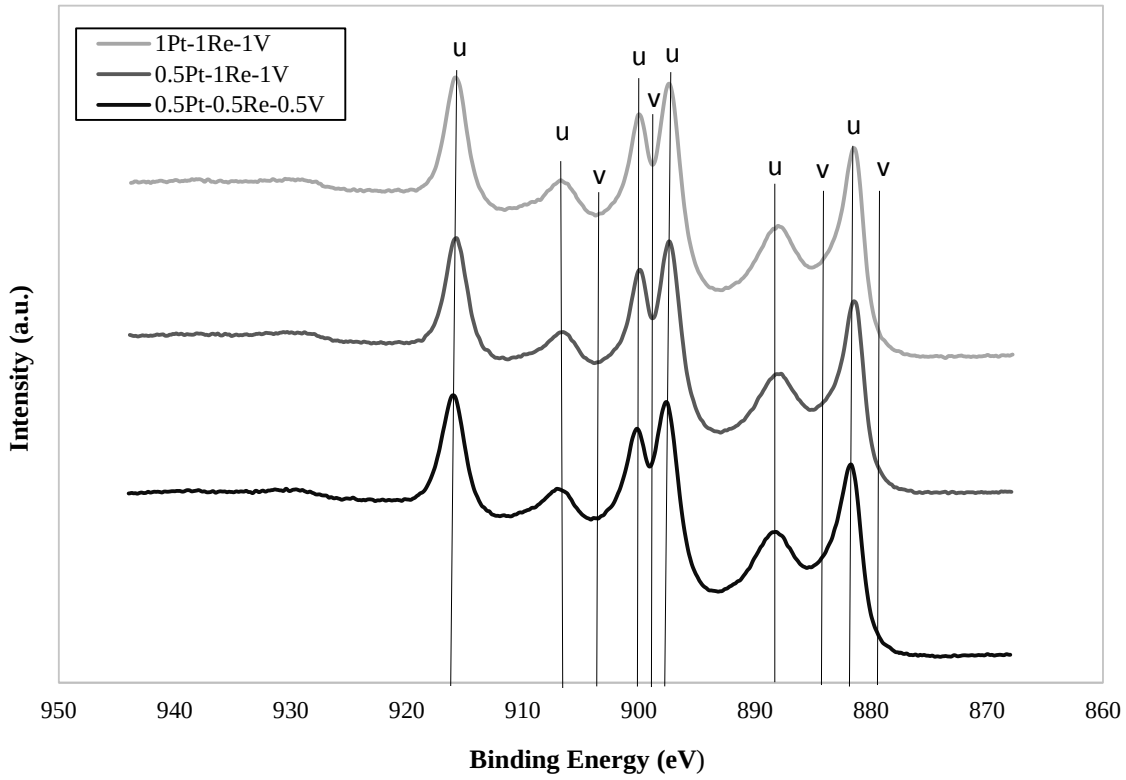

Figure 4.10. XP spectra for Ce 3d region of freshly reduced catalyst samples (v: Ce^{3+}, u: Ce^{4+}).

Figures 4.11 presents the XP spectra of Ce 3d region of freshly reduced and spent catalysts used during performance tests conducted. The spent catalysts were subjected to WGS tests through 6 h TOS at 350 °C under feed flows having H_2O/CO ratio of 6.7 and 16.2, i.e. RF #1 and #2, respectively. The resulting spectra show that the peaks attributed to Ce^{3+} and Ce^{4+} oxidation states were still detected, however with different intensities.

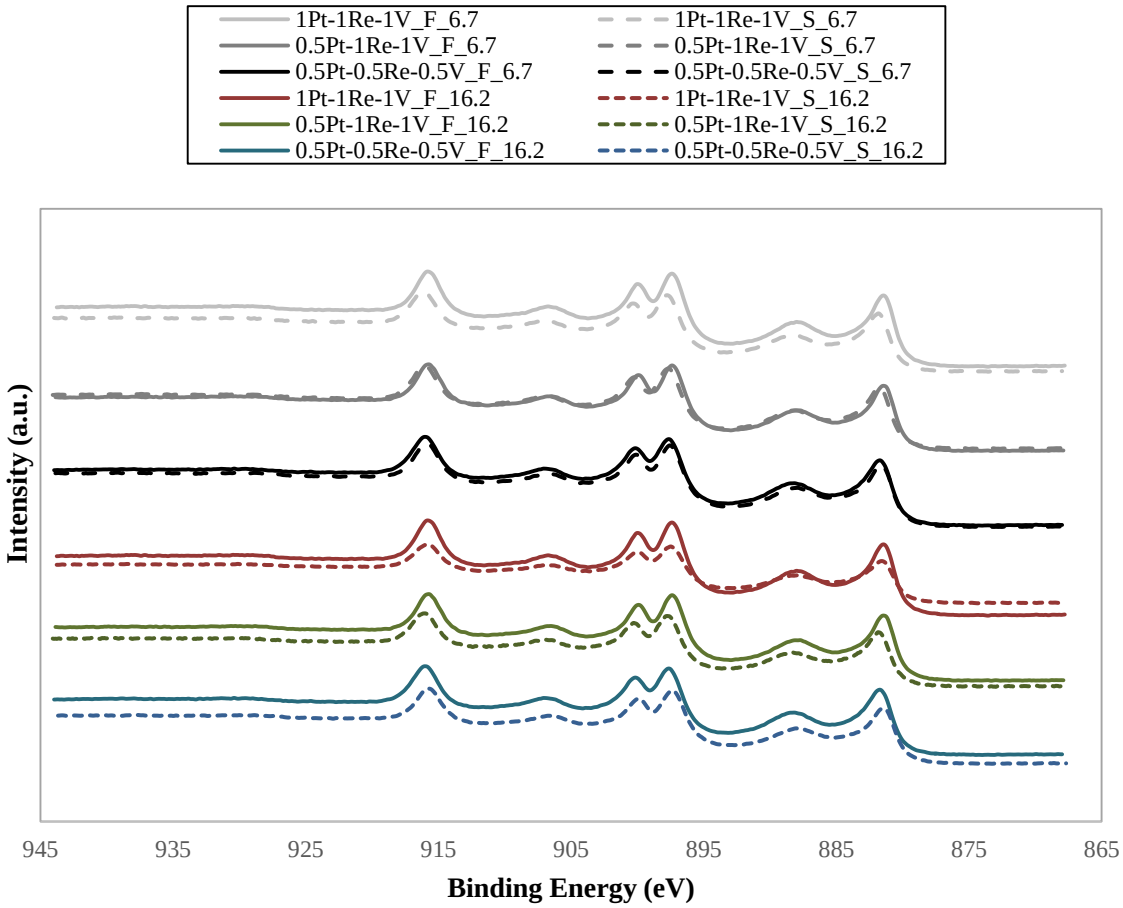

Figure 4.11. XP spectra for Ce 3d region of freshly reduced and spent catalysts at 350 °C under RF #1 and #2.

Deconvolution of the peaks was achieved by using the Avantage software, and the amount of Ce^{3+} was calculated for reduced and spent catalysts considering the given formula below (Jardim *et al.*, 2015; Çağlayan and Aksoylu 2011):

$$[Ce^{3+}] = I - Ce^{3+}/(I - Ce^{3+} + I - Ce^{4+})$$

where, $I - Ce^{3+}$ and $I - Ce^{4+}$ represent the sum of the intensities of two doublets resulting from Ce_2O_3 and three doublets resulting from CeO_2, respectively.

The Ce^{3+} amounts of the catalysts studied in this work were determined for both freshly reduced and spent forms and presented in Table 4.1. The catalyst reached the highest WGS activity, 1Pt-1Re-1V/CeO_2, was found out to contain relatively higher Ce^{3+} content in its freshly reduced form compared to other samples' proving the crucial role of Ce^{3+} content in enhancing electron transfer ability from the support to metallic sites (Çağlayan and Aksoylu, 2011; Tabakova *et al.*, 2003; Andreeva *et al.*, 2007).

Table 4.1. The Ce^{3+} contents (%) of freshly reduced and spent (under realistic feed #1, RF #1 and realistic feed #2, RF #2) catalyst samples.

Catalyst	**Ce^{3+} (%)**		
	Freshly reduced	**Spent (RF#1)**	**Spent (RF#2)**
1Pt-1Re-1V/CeO_2	20.6	14.3	15.9
0.5Pt-1Re-1V/CeO_2	19.0	16.1	16.8
0.5Pt-0.5Re-0.5V/CeO_2	18.5	16.0	16.8

In order to establish a relation between the WGS activity and Ce^{3+} percentage change upon reaction, the Ce^{3+} amounts of the spent catalyst samples were evaluated. As expected, the amount of Ce^{3+} declined during reaction for all samples. Additionally, the spectra belonging to spent samples indicated that Ce^{3+} and Ce^{4+} peaks shifted to higher or lower binding energies. In the literature, it is stated that due to the excess electron generated from the removal of an oxygen atom from CeO_x, Ce^{3+} ions are very reactive to reactants (Campbell and Peden, 2005) and the ability of electron transfer from support material to metallic sites provides high surface concentration and thus high WGS activity (Çağlayan and Aksoylu, 2011). The Ce^{3+} content is expected to decrease owing to the electron transfer during reaction for all samples. The Ce^{3+} content on 1Pt-1Re-1V/CeO_2 catalyst surface which demonstrated highest WGS activity among other samples presented 31% and 23% decrease at 350 °C under RF #1 and #2, respectively. Moreover, the catalysts subjected to RF #1 with lower H_2O/CO feed ratio, yielded lower Ce^{3+} content indicating the extent of the catalyst's electron transfer ability is directly related to the feed composition.

The V 2p XP spectra of freshly reduced and spent catalysts are shown in Figure 4.12. The spectra revealed a peak at 516.2 eV which was attributed to V^{4+} oxidation state (Duarte de Farias *et al*., 2008; Suchorski *et al*., 2005). The V^{4+} ions which belong to VO_2 compound have been reported to enhance WGS activity (Demeter *et al.*, 2000; Junior *et al.*, 2005). Accordingly, the catalysts which have superior WGS activity, 1Pt-1Re-1V/CeO_2 and 0.5Pt-0.5Re-0.5V/CeO_2, have higher peak areas centered at 516.2 eV indicating higher amounts of V^{4+} ions on catalyst. No peaks appeared in the spectra around 523 eV belonging to V_2O_5 compounds which are stated as non-active for WGS reaction owing to the presence of V-O-V bonds (Duarte de Farias *et al.*, 2008; Ballarini *et al.*, 2006).

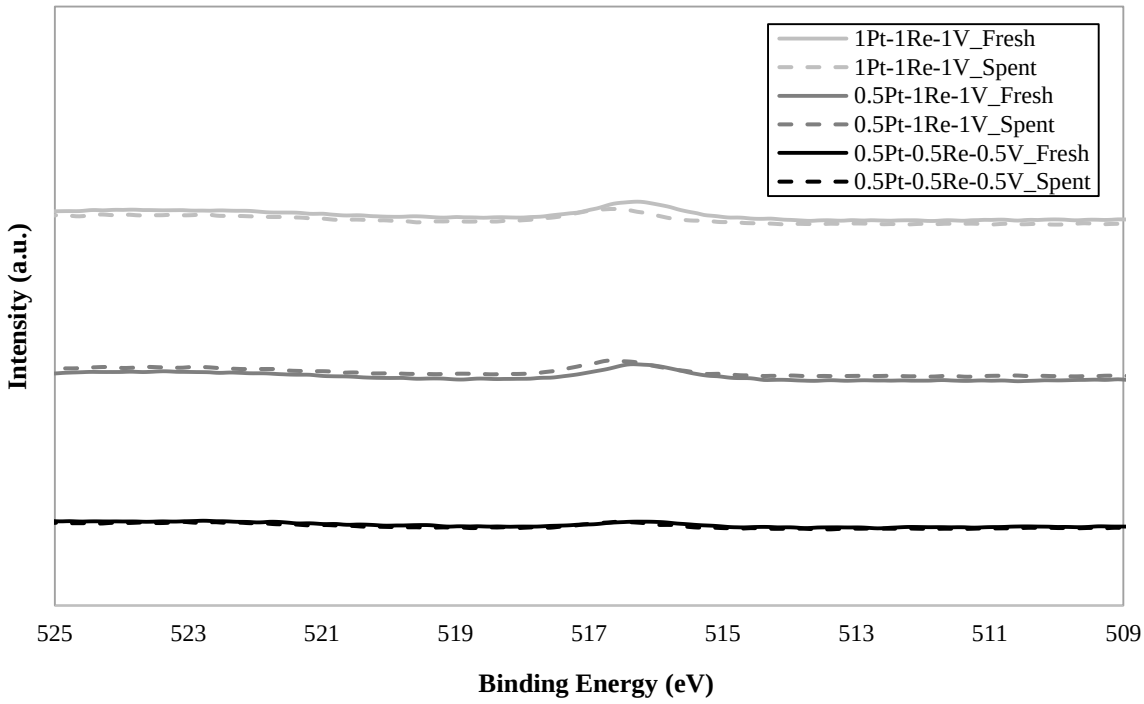

Figure 4.12. XP spectra for V 2p region of freshly reduced and spent catalysts under realistic feed #1 at 350 °C.

The O 1s spectra of freshly reduced and spent catalysts, which were subjected to RF #1 having H_2O/CO ratio of 6.7 at 350 °C, are presented in Figure 4.13. The freshly reduced catalysts illustrated 3 peaks centered at around 528, 530 and 533 eV, which can be attributed

to oxygen in the CeO_x lattice, chemisorbed water and hydroxyls, and weakly adsorbed water only on the CeO_x in oxidized state, respectively (Çağlayan and Aksoylu, 2011). After WGS reaction, the intensities of 528 eV peaks decreased, *which indicates a decline in ceria lattice oxygen*, supporting that CeO_2 have an active role in the reaction. On the other hand, the intensity of 530.5 peak increased, which suggests the step involving hydroxyls may be the rate determining step in the reaction mechanism. In order to see the effect of feed compositions on the type of surface oxygen species, the O 1s spectra of the spent 1Pt-1Re-1V/CeO_2 catalyst tested under RF #2 at 350 °C was also obtained (not shown) and it was observed that the spectra of both samples were alike.

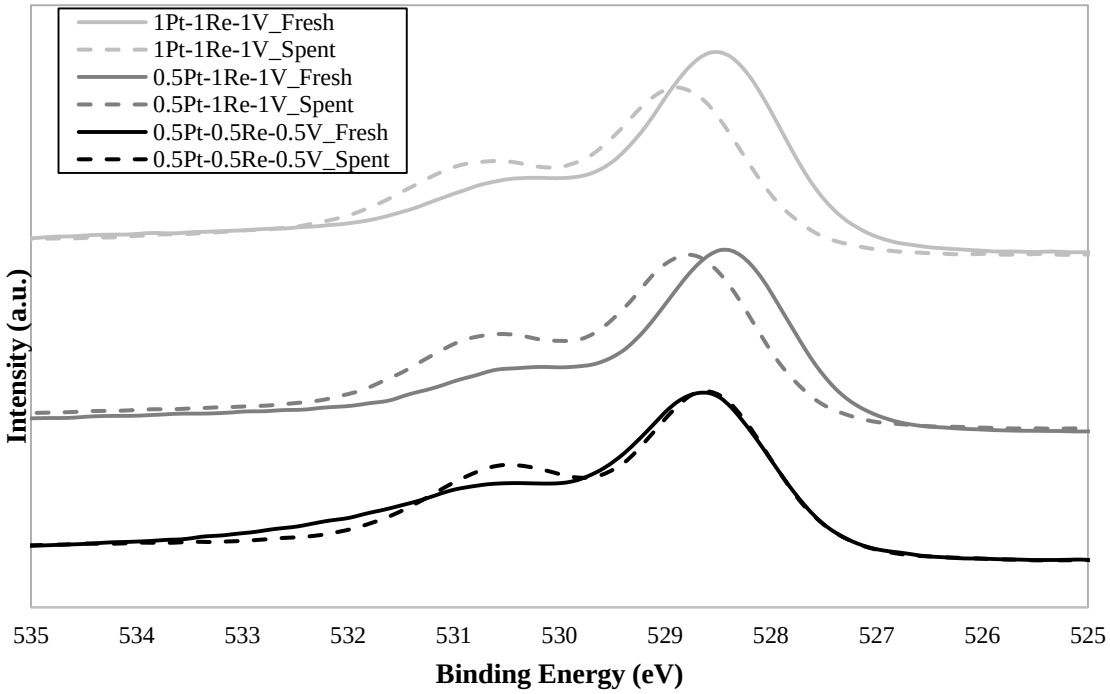

Figure 4.13. XP spectra for O 1s region of freshly reduced and spent catalysts under realistic feed #1 at 350 °C.

Figure 4.14 demonstrates the Pt 4f region spectra of freshly reduced and spent catalyst samples used in the reaction tests conducted with RF#1 at 350 °C. In the literature, the Pt $4f_{7/2}$ peak at 71.0 eV and the Pt $4f_{5/2}$ peak at 74.2 eV are assigned to Pt^0 and the peaks at 71.9 and 75.1 eV corresponds to Pt^{2+} which is reported as active species for WGS reaction while the peaks at 74.3 and 77.5 eV are assigned to Pt^{4+} species (Mei *et al.*, 2015; Yu *et al.*, 2010;

Pierre *et al.*, 2007). The spectra of all samples showed that the majority of Pt existed in +2 oxidation state which have active role in WGS reaction. The 1Pt-1Re-1V/CeO_2 and 0.5Pt-0.5Re-0.5V/CeO_2 samples had slight amounts of Pt^{4+} which was reported as having no effect on catalyst stability. No peak belonging to Pt^0 species, which is known to have no effect on WGS activity, have appeared in the spectra (Pierre *et al.*, 2007).

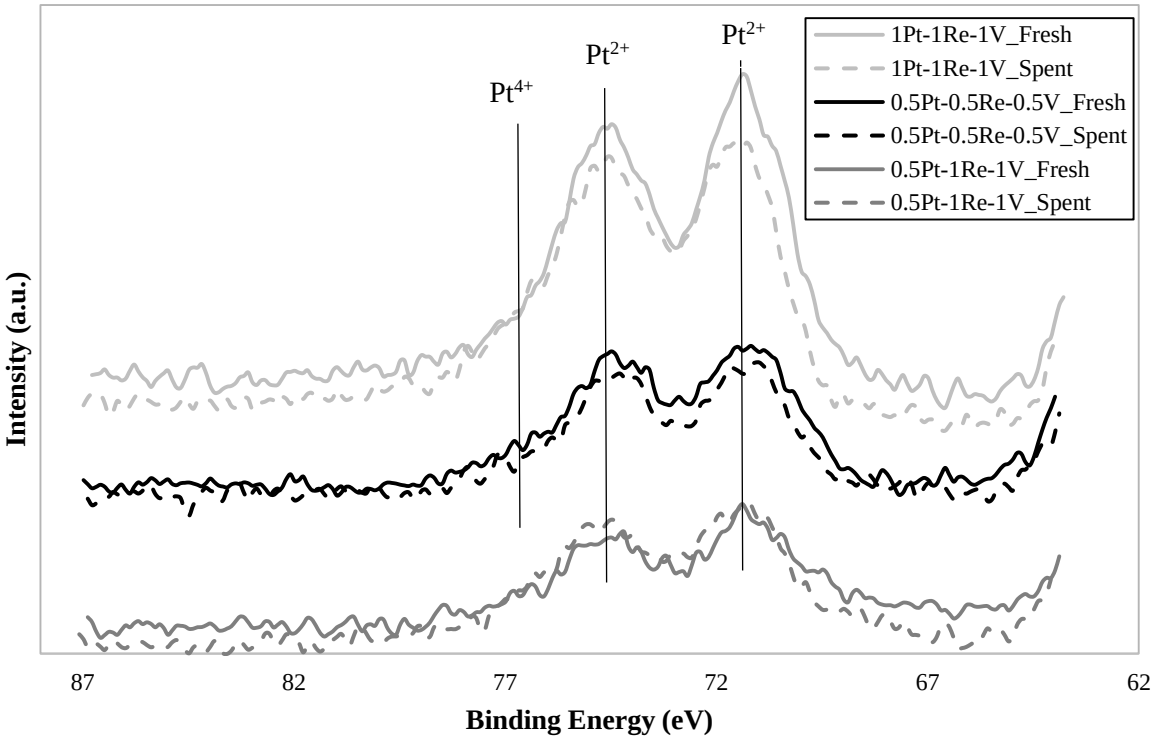

Figure 4.14. XP spectra for Pt 4f region of freshly reduced and spent catalysts under realistic feed #1 at 350 °C.

The spectra for Re 4f region of freshly reduced and spent catalysts (not shown) have illustrated that Re was present in its oxidized form (ReO_x) in accordance with literature (Azzam *et al.*, 2008; Iida *et al.*, 2006).

4.2.3. Raman Spectroscopy

Raman spectroscopy is a method used for investigating the vibrational, rotational, and other low frequency modes in a metal oxide system (Wu *et al.*, 2011). Hence it is used for the analysis of metal oxide systems present in the freshly reduced and spent forms of the catalysts used in this work.

Figure 4.15 (a) and (b) present the Raman spectra of freshly reduced and spent Pt-Re-V/CeO_2 samples; the spent catalysts were tested for WGS reaction through 6 h TOS at 350 °C under the flow of RF #1 and #2 having H_2O/CO= 6.7 and 16.2, respectively. The perfect Raman scattering nature of ceria results in overwhelming the signal from surface vanadium species and since the samples mainly consist of CeO_2, the spectra are dominated by CeO_2 bands (Wu *et al.*, 2011).

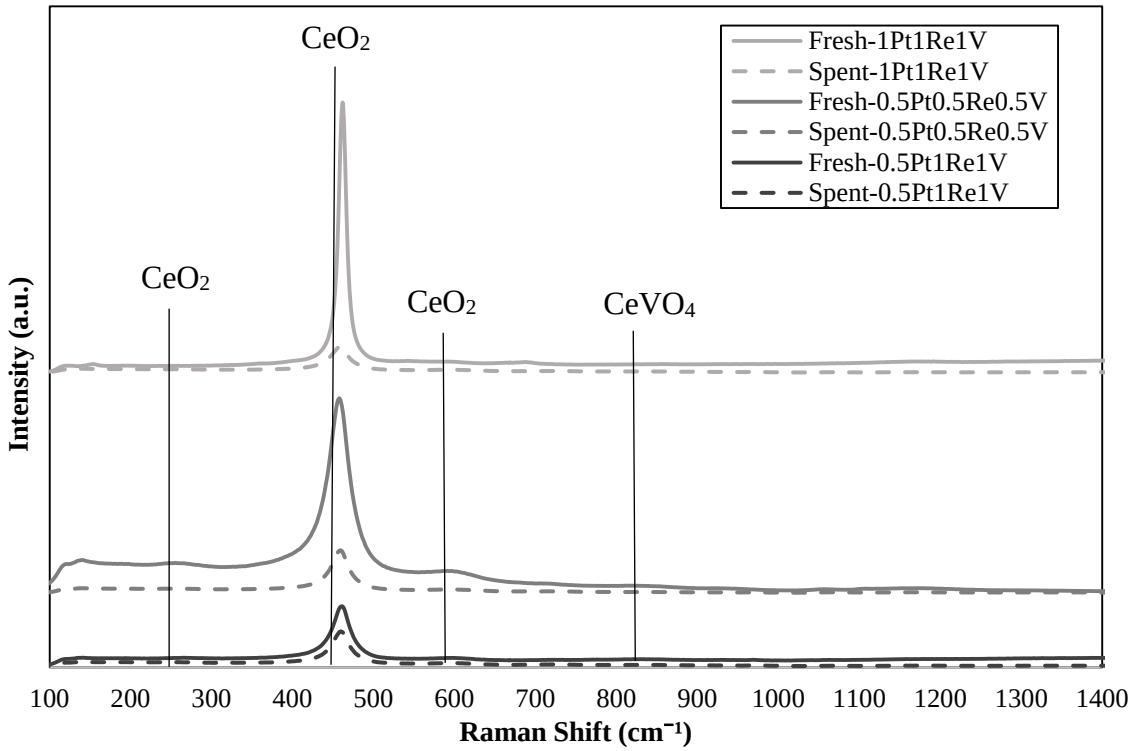

(a)

Figure 4.15. Raman spectra of freshly reduced and spent catalyst samples for (a) realistic feed #1 and (b) realistic feed #2 at 350 °C.

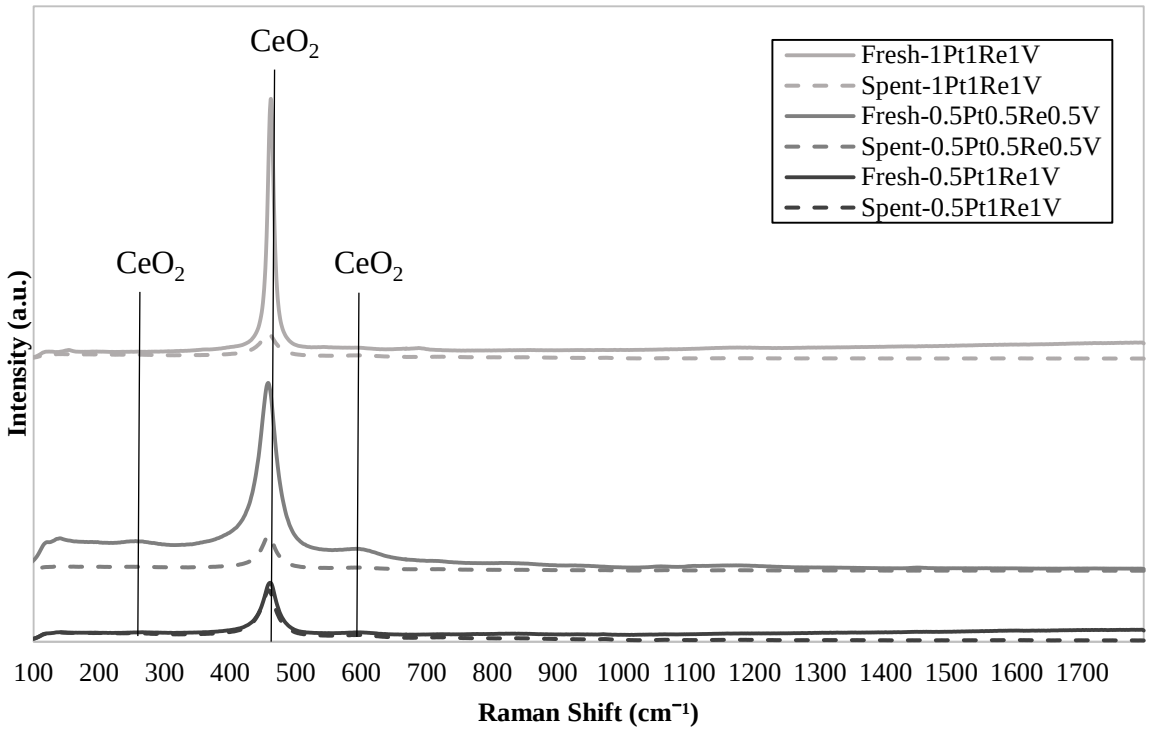

(b)

Figure 4.15. Raman spectra of freshly reduced and spent catalyst samples for (a) realistic feed #1 and (b) realistic feed #2 at 350 °C (cont.).

The sharpest Raman peak at around 460 cm^{-1}, which is attributed to bulk ceria, was detected for freshly reduced and spent forms of all catalysts. Besides the main peak, the samples revealed bands at around 265 cm^{-1} and 590 cm^{-1} resulting from the oxygen vacancies in CeO_2, which are consistent with the literature values (Hwang *et al.*, 2011; Yu *et al.*, 2011). It was reported that higher values of I_{590}/I_{460} ratio shows the extent of oxygen vacancies (Harshini *et al.*, 2014). 1Pt-1Re-1V/CeO_2 catalyst led to a higher I_{590}/I_{460} ratio in its spent form compared to those of other samples', suggesting it has higher oxygen storage capacity (OSC). The decrease in the intensity of the 460 cm^{-1} band for the spent forms of 1Pt-1Re-1V/CeO_2 and 0.5Pt-0.5Re-0.5V/CeO_2 can be attributed to their activity in WGS reaction because no noticeable decrease was detected in the intensity of the same peak for spent form of 0.5Pt-1Re-1V/CeO_2, over which lower CO conversion values obtained in performance

tests. It is worthwhile to mention that a slight shift of 460 cm^{-1} band observed in Raman spectra of the spent catalysts to lower wavenumber levels suggests active role of CeO_2 in WGS reaction (Rico-Frances *et al.*, 2016).

As the peak at 460 cm^{-1} is very dominant, the expanded version of Figure 4.15 (a) was given in Figure 4.16 in order to see the 550-1800 interval clearly. The characteristic peaks at this interval are also valid for spectra of samples subjected to RF #2 (not shown).

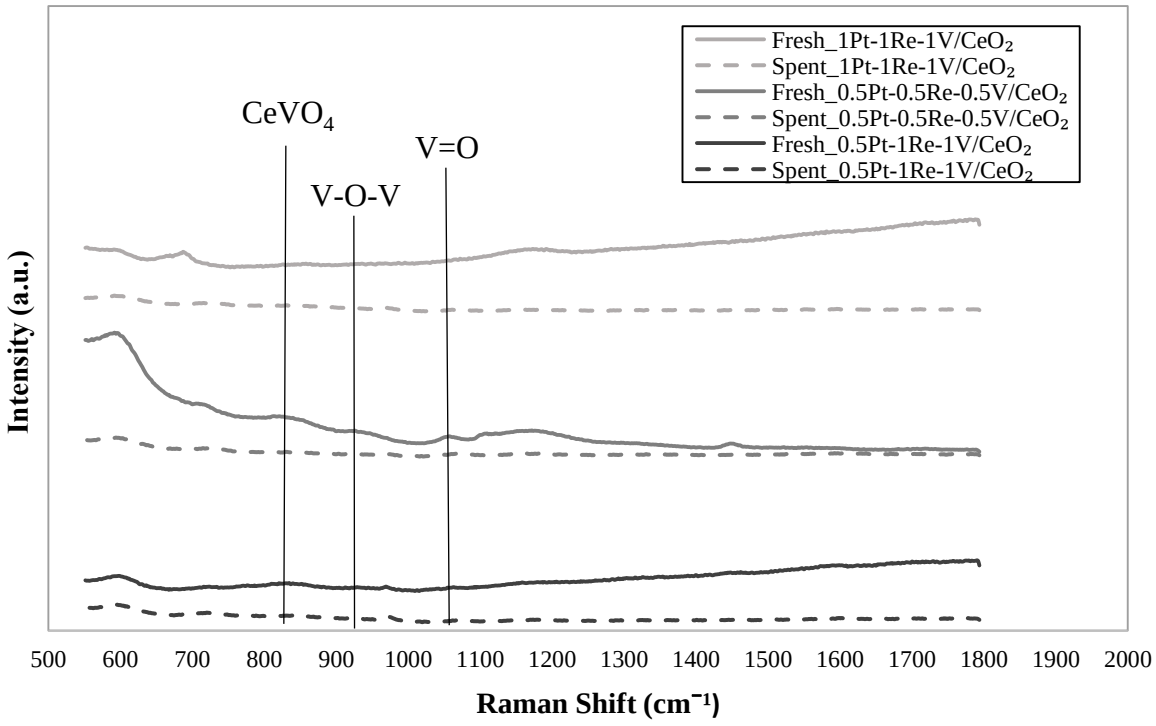

Figure 4.16. The expanded Raman spectra of freshly reduced and spent catalyst samples for realistic feed #1 350 °C.

The band at around 840 cm^{-1} was attributed to $CeVO_4$ species (Wu *et al.*, 2011; Martinez-Huerta *et al.*, 2008). Furthermore, the peaks located at around 930 cm^{-1} and 1060 cm^{-1} belong to V-O-V and V=O modes in polyvanadate surface species, respectively (Wu *et al.*, 2011; Ayandiran *et al.*, 2016). $CeVO_4$ can be formed since CeO_2 support has tendency to react with surface V^{5+} species to generate V^{5+}-O-Ce^{3+} bonds which are known as active formations for selective oxidation and WGS reactions (Martinez-Huerta *et al.*, 2008; Duarte

de Farias *et al.*, 2008). On the other hand, alteration of $CeVO_4$ single crystals to bulk crystalline phase was reported to cause activity decrease due to lessening in the number of V^{5+}-O-Ce^{3+} sites on the support (Martinez-Huerta *et al.*, 2008).

It should be noted that no bulk V_2O_5 crystals was detected corresponding to 180, 285 and 345 cm^{-1} bands implying that vanadium is highly dispersed at the surface (Al-Ghamdi *et al.*, 2014; Ayandiran *et al.*, 2016). Figure 4.17 shows the Raman spectra of spent catalyst samples under both realistic feed conditions at 350 °C. The disordered structural mode of crystalline carbon species and graphitic carbon with high degree of symmetry are denoted as D and G bands corresponding 1360 cm^{-1} and 1600 cm^{-1} modes, respectively (Paksoy *et al.*, 2015). Since these bands showed low intensities except for 0.5Pt-1Re-1V/CeO_2 catalyst tested under realistic feed #1 giving relatively lower CO conversion levels, it can be assumed that nearly no coke formation was formed. Additionally, no observable Pt and Re bonds were detected in all spectra may be an indication of the incorporation of these atoms in the CeO_2 lattice (Rico-Frances *et al.*, 2016).

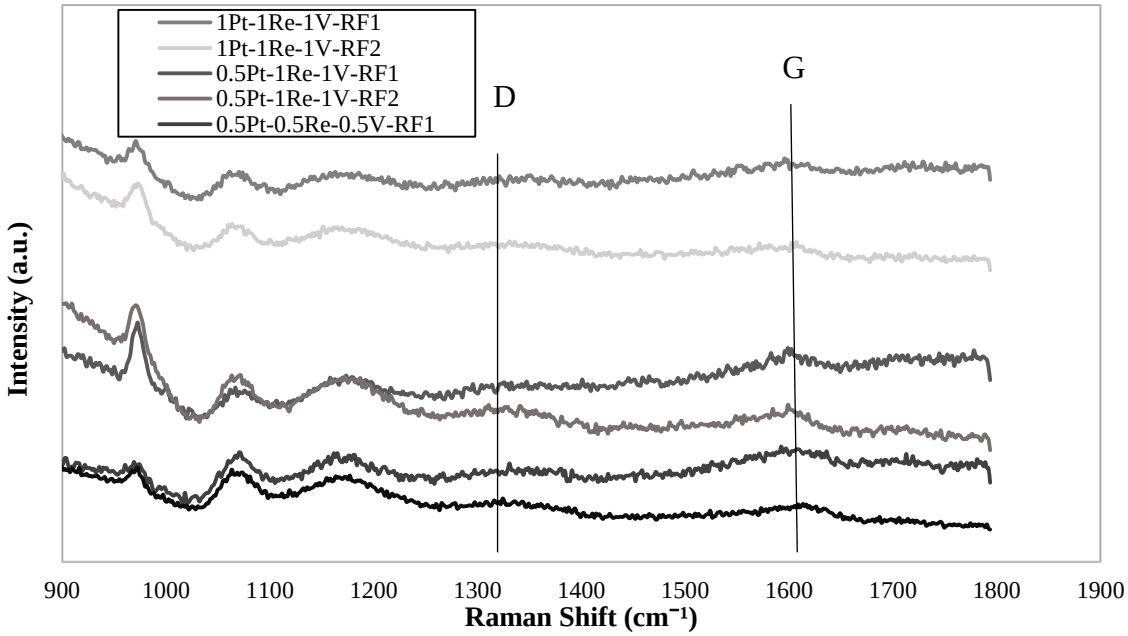

Figure 4.17. Raman spectra of spent catalyst samples tested under realistic feed #1 (RF1) and realistic feed #2 (RF2) at 350 °C.

4.2.4. CO Chemisorption

CO Chemisorption is a method used to quantify the exposed metal amount on the catalyst available for reaction. Pt dispersion measurement was conducted on 75 mg catalyst sample. Each catalyst sample was reduced *in situ* under 15 % H_2 with total flow of 60 ml/min at 375 °C prior to analysis, and then cooled to room T under He flow. The CO uptake analysis was conducted at room temperature through injection of 0.1 ml of pulses of 5% CO to the inert carrier (He) that had 60 ml/min flow rate. The amount of CO adsorbed was obtained and the metal dispersion values were calculated by assuming the "metal atom to adsorbed gas" stoichiometry (CO:Pt) as 1, which is compatible with literature (Bo *et al.*, 2018; Kugai *et al.*, 2015; Lenarda *et al.*, 2018).

The measurements over CeO_2, V/CeO_2 and $Re\text{-}V/CeO_2$ performed previously by our group showed that negligible amount of CO was adsorbed on these samples at room temperature. This result is in accordance with the finding of Peick *et al.* (2005) that CO was adsorbed only on Pt at room T. Therefore, the obtained dispersion values were attributed to Pt metal. Table 4.2 presents the Pt dispersion values over the catalyst samples.

Table 4.2. The Pt dispersion values of catalyst samples.

Catalysts	**Pt Dispersion (%)**
$0.5Pt\text{-}0.5Re\text{-}0.5V/CeO_2$	15
$0.5Pt\text{-}1Re\text{-}1V/CeO_2$	15
$1Pt\text{-}1Re\text{-}1V/CeO_2$	37

4.3. Oxygen Storage Capacity Measurements

The oxygen storage capacities (OSC) of the catalysts used in performance tests were measured by following the methodology described in Section 3.4.2. In the tests, three different types of OSC, namely total (T-OSC), structural (S-OSC) and effective (E-OSC), were determined by using the OSC methodology (Section 3.4.2). As the methodology

requires *operando* reaction over the catalyst samples, the samples were subjected to WGS feed flows DRF#1 and DRF#2, which are the diluted forms of the realistic feeds RF#1 and RF#2, respectively, used in the WGS peformance tests; the detailed compositions of DRF#1 and DRF#2 are presented in Table 3.8. The experimental conditions used in the *operando* OSC studies were listed in Table 3.9

The OSCs were calculated based on the amounts of CO_2 and CO gases leaving catalyst surface, in no. of moles, while increasing sample temperature to 800 °C upon the application of either reactive or inert environments, and were expressed in "mmol O/g_{cat}". There are two OSC definitions in literature; the first one is the total or thermodynamic OSC, which is related to complete reducibility, expresses the maximum amount of oxygen that can be extracted from the sample. The second OSC is termed as dynamic or kinetic OSC, assessing the most reactive and readily accessible oxygen, which is associated to the amount of oxygen renewable in the course of reaction (Porsin *et al.*, 2016; Aneggi *et al.*, 2006; Trovarelli *et al.*, 1997). Similarly, in this study, structural OSC (S-OSC) term is used to define the oxygen storage capacity in the lattice as well as of the species on the catalyst surface, in the form of surface groups as formate, carbonate or carboxyl-carboxylate like species, while effective OSC (E-OSC) term is used to describe the oxygen associated with, i.e. replenished and renewed, through reaction. At this point, it is worth to mention that all the oxygen stored in samples; both 'structural' and 'effective', is assumed to leave surface as CO_2 and CO and this assumption was verified with an experiment conducted in IGA equipment showing when the sample temperature was increased, the desorbing gases were mainly CO_2 and CO. No oxygen, methane or water desorption was detected. Blank tests were conducted to assure that quartz reactor and quartz wool used in experiments had no catalytic activity and did not have any oxygen storage capacity. The OSC calculations were accomplished through the combined use of the weight change of the sample, which was obtained from IGA measurements during the temperature increase from reaction (or inert treatment) temperature to 800 °C, and the volume ratio of CO_2 and CO gases leaving the surface during that time, which was determined from MS data (see Section 3.4.2). The oxygen storage capacities of the samples were evaluated by using equations from 4.7 to 4.12. The ideal gas equation was used to obtain molar ratio of CO_2 and CO:

$$P_{CO_2}V_{CO_2} = \dot{n}_{CO_2}RT_{CO_2} \quad (4.7)$$

$$P_{CO}V_{CO} = \dot{n}_{CO}RT_{CO} \quad (4.8)$$

Where $\dot{n}_{gas}$ denotes the molar flow rate of the gas, P_{gas} is the atmospheric pressure, V_{gas} is the volume of the gas, R is the universal gas constant and T_{gas} is the absolute temperature. From these equations, following relation can be obtained:

$$\frac{V_{CO_2}}{V_{CO}} = \frac{\dot{n}_{CO_2}}{\dot{n}_{CO}} \left(= \frac{n_{CO_2}}{n_{CO}}\right) \quad (4.9)$$

The difference of the sample weight between the time when temperature is started to be increased and at 800 °C was used to obtain the moles of CO_2 and CO gases desorbing from surface according to the formula below:

$$Weight\ change = MW_{co} * n_{co} + MW_{co_2} * n_{co_2} \quad (4.10)$$

Where MW_{gas} shows molecular weight of the gas and n_{gas} is the moles of gas leaving the sample. After calculating the number of moles of each gas, total moles of oxygen was obtained by using Equation 4.11, and OSCs of the samples were found in mmol O/g_{cat} by using Equation 4.12:

$$Total\ O\ mol = 1 * n_{co} + 2 * n_{co_2} \quad (4.11)$$

$$OSC\ (mmol/g_{cat}) = {Total\ O\ mmol}/{w_{cat}} \quad (4.12)$$

where OSC indicates oxygen storage capacity (T-OSC or S-OSC depending on the procedure) and w_{cat} is the weight of sample.

4.3.1. Oxygen Storage Capacity Tests

The oxygen storage capacity tests were conducted under atmospheric pressure. In the tests, all types of OSCs were determined for the 0.5Pt-1Re-1V/CeO_2 and 0.5Pt-0.5Re-0.5V/CeO_2, *which showed relatively lower activity in performance tests at 350 °C*, upon *operando* reaction and inert treatment at 350 ^oC, and for 1Pt-1Re-1V/CeO_2, *which showed the highest activity during the performance tests*, upon *operando* reaction and inert treatment at three different temperatures, 350, 400 and 450 °C. The reactive environments in the OSC tests were generated through the use of two diluted realistic feeds, DRF #1 and DRF #2, whose detailed compositions are presented in Table 3.8, while for inert environment %100 pure helium was used. During the tests, GHSV was kept constant at 40,000 ml g_{cat}^{-1} h^{-1}.

As explained in Section 3.4.2, three types of OSCs were mesured. The OSCs obtained upon reaction under DRF flows and upon inert treatment for specific temperature through following the same procedure were called as total OSCs (T-OSC) and structural OSCs (S-OSC), respectively. Effective OSC (E-OSC) was calculated as the difference between T-OSC and S-OSC for a specific reaction temperature. Figure 4.18 (a) and (b) present T-OSC, S-OSC and E-OSC data of samples subjected to DRF #1 and DRF #2 at 350 °C, respectively.

Figure 4.18 (a) illustrates that , T-OSCs of samples o1Pt-1Re-1V/CeO_2 and 0.5Pt-1Re-1V/CeO_2 were found very close as 0.8693 and 0.8687 mmol O/g_{cat}, respectively, while 0.5Pt-0.5Re-0.5V/CeO_2 was found to have slightly higher T-OSC, ca. 0.8728 mmol O/g_{cat}, under DRF #1 at 350 ^oC. Similar results were achieved under DRF #2 (Figure 4.18 (b)): 1Pt-1Re-1V/CeO_2 and 0.5Pt-1Re-1V/CeO_2 had close T-OSC values (0.8399 and 0.8495 mmol O/$g_{cat,}$ respectively), while 0.5Pt-0.5Re-0.5V/CeO_2 has significantly higher T-OSC (0.8827 mmol O/g_{cat}) compared to others. As stated before, the experiments were also conducted under inert (He) atmosphere at the same temperature to discriminate the effective oxygen resulting from the reaction and the structural oxygen. The outcomes of He experiments imply that 0.5Pt-0.5Re-0.5V/CeO_2 catalyst has higher S-OSC (0.5394 mmol O/g_{cat}) comprising the oxygen in both CeO_2 lattice and surface groups. The lowest S-OSC value (0.4361 mmol O/g_{cat}) was obtained for 1Pt-1Re-1V/CeO_2 catalyst which yielded the highest CO conversion

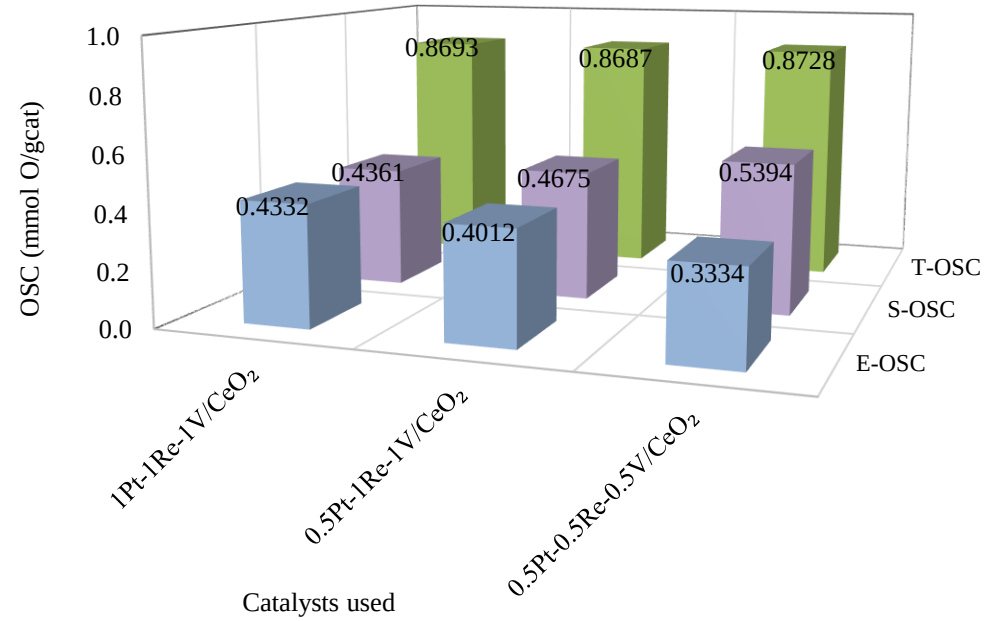

(a)

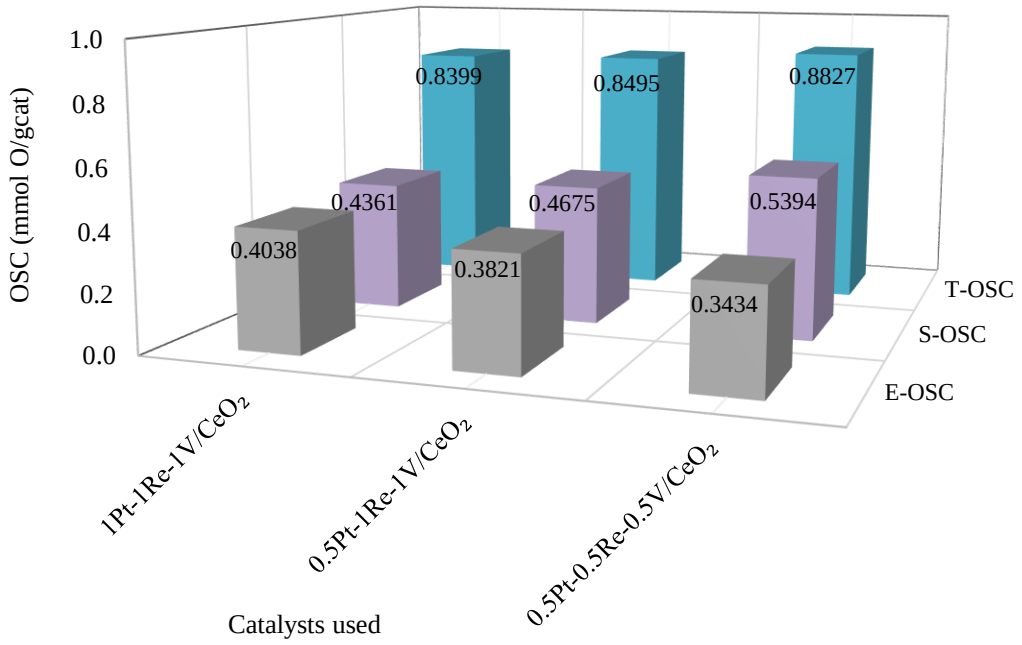

(b)

Figure 4.18. OSCs of samples tested at 350 °C under (a) DRF #1 having $H_2O/CO=6.7$ and (b) DRF #2 having $H_2O/CO=16.2$ (see Table 3.8 for the detailed DRF compositions).

and -*in general*- net H_2 production in performance tests. This clearly points out that the oxygen associated with reaction is of paramount importance in defining WGS activity. Though the effect of S-OSC on WGS activity is rather inferior, the results of He tests yielding S-OSC were subtracted from the T-OSC results in order to isolate its effect on WGS activity; as mentioned above, this difference is called 'effective' OSC (E-OSC), *which represents oxygen formed, used and renewed during the course of reaction*. According to the performance results, the activity of catalysts was roughly following the order: 1Pt-1Re-1V/CeO_2 > 0.5Pt-0.5Re-0.5V/CeO_2 > 0.5Pt-1Re-1V/CeO_2. However, the resulting E-OSCs of samples have the order of 1Pt-1Re-1V/CeO_2 > 0.5Pt-1Re-1V/CeO_2 > 0.5Pt-0.5Re-0.5V/CeO_2. Figure 4.19 displays the E-OSCs and CO conversions of the trimetallic Pt-Re-V/CeO_2 catalysts under diluted feed flows having H_2O/CO ratio of 6.7 and 16.2 at 350 °C.

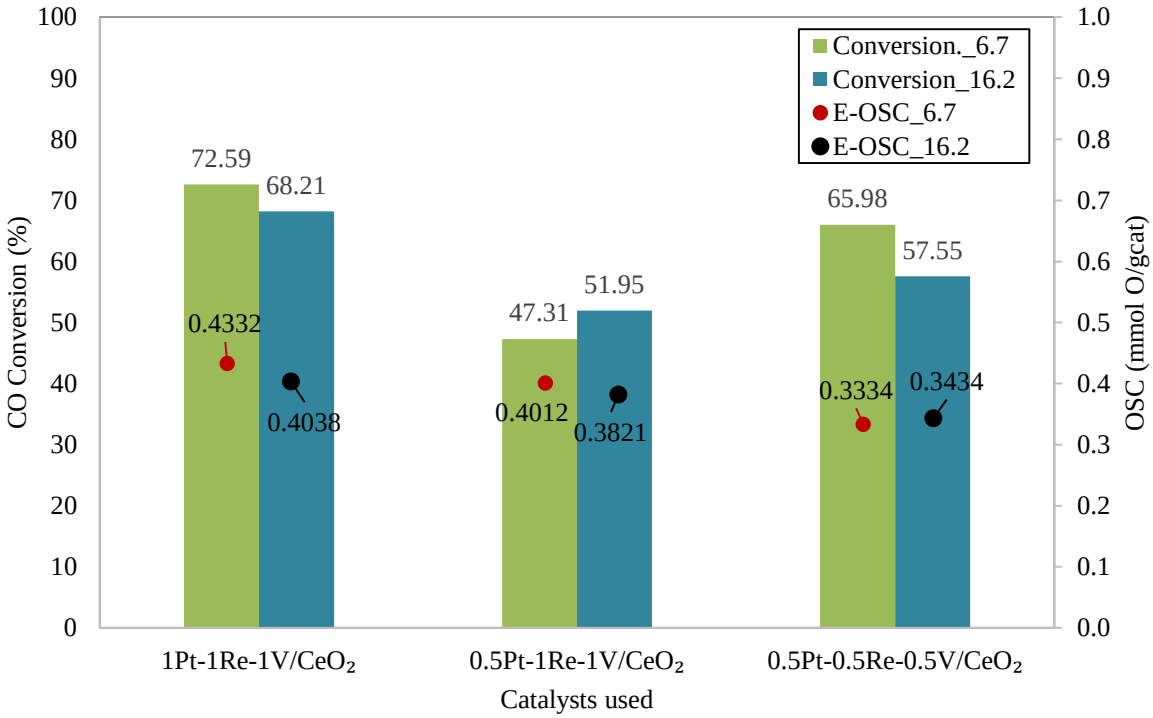

Figure 4.19. CO conversions and effective OSCs of samples subjected to DRF #1 and DRF #2 at 350 °C.

1Pt-1Re-1V/CeO_2 catalyst yielded the highest effective OSCs calculated for both feed conditions. In the literature, oxygen storage capacities of the CeO_2 supported catalysts are

reported to be stemmed from the oxygen vacancies and/or the surface groups generated during reaction which promote redox ability between Ce^{3+} and Ce^{4+} (Montini *et al.*, 2016). The oxygen vacancies created during WGS conditions have been mainly associated with catalytic activity, owing to the fact that these defects promote water activation on sites and facilitate initiation of the reaction (Reina *et al.*, 2015). Consequently, it is not suprising that the samples which had better catalytic activity have higher E-OSCs. Yet, though 0.5Pt-0.5Re-0.5V/CeO_2 catalyst displayed an average catalytic performance, it brought about the lowest E-OSCs for both feed conditions. The catalyst giving the lowest performance in catalytic tests, 0.5Pt-1Re-1V/CeO_2, provided higher effective OSC values compared to that of 0.5Pt-0.5Re-0.5V/CeO_2 sample under both feed conditions. This suggests that while deducing a link between the catalytic activity and the OSC, the oxygen coming from reaction is not the only key parameter; the oxygen present on surface as in the form of surface groups is also taking part in mechanism and influences activity. In the literature, much effort has been made to investigate the rate determining step in WGS reaction mechanism; some research groups have reported that the surface reaction of CO and O is the limiting step rather than diffusion of oxygen ions which leads to the oxygen generation (Porsin *et al.*, 2016; Hori *et al.*, 1998) while others have proposed an associative mechanisms involving the formation of formate, carbonate or carboxyl-carboxylate like intermediates (Ribeiro *et al.*, 2011; Goguet *et al.*, 2004; Chen *et al.*, 2011). Under the light of these, the conclusion that oxygen vacancies formation is not the rate limiting step can be drawn on the basis of the finding that catalytic activity of 0.5Pt-0.5Re-0.5V/CeO_2 was superior to 0.5Pt-1Re-1V/CeO_2 although the latter had higher capacity to generate oxygen vacancies expressing that it is more reducible (Vecchietti *et al.*, 2014).

In order to see the effect of the reaction temperature on oxygen storage capacity, OSC experiments were performed at three different temperatures, 350 °C, 400 °C and 450 °C, with DRF#1 for the sample yielded the highest catalytic activity; 1Pt-1Re-1V/CeO_2. The results are shown in Figure 4.20.

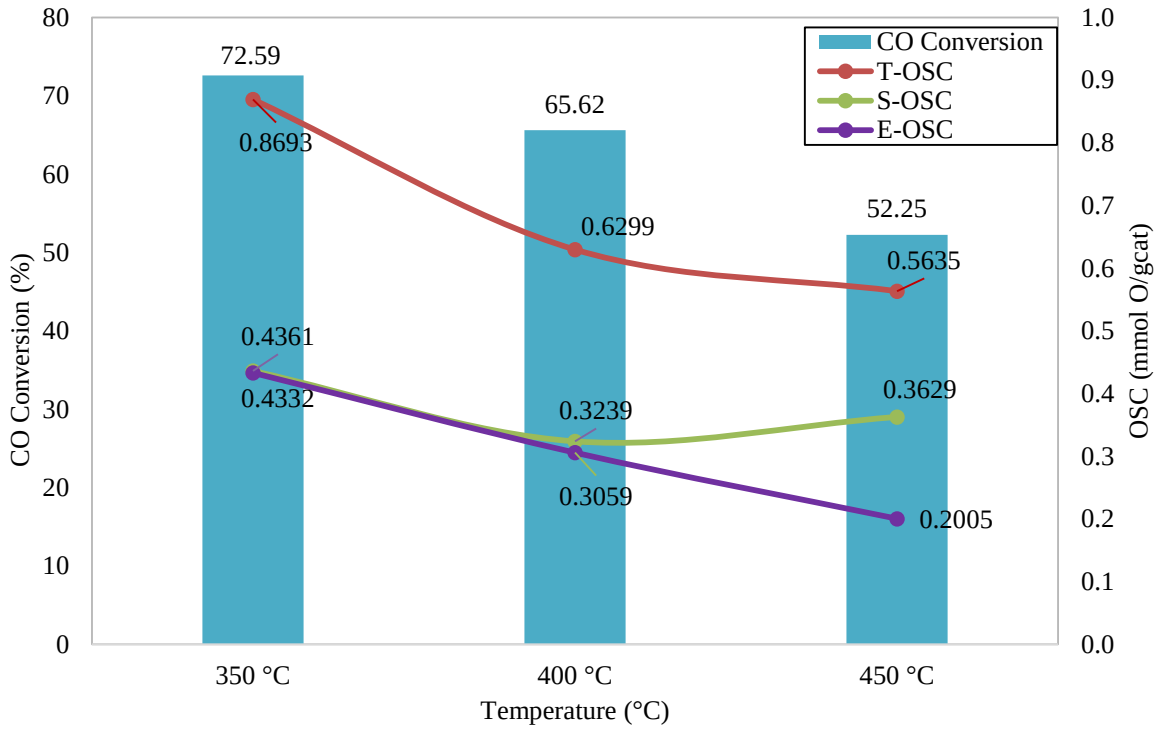

Figure 4.20. CO conversion, and T-OSC, S-OSC, E-OSC data obtained for 1Pt-1Re-1V/CeO_2 catalyst under DRF #1 at different temperatures.

The results demonstrate that there is a hand-in-hand decrease with increasing reaction temperature in both WGS activity (CO conversion) and the E-OSCs values measured under DRF #1. When the obtained data are analyzed, it can be clearly seen that at 350 °C, which is the temperature that superior catalytic activity (72.59 %) of 1Pt-1Re-1V/CeO_2 was achieved, the highest effective OSC value (0.4332 mmol O/g_{cat}) was obtained. Similarly, at the temperature which inferior catalytic performance was obtained, the effective OSC reached its lowest value (0.2005 mmol O /g_{cat}). On the other hand, the experiments conducted under He flow presented a different trend; as temperature was raised from 350 °C to 400 °C, the catalyst gave lower S-OSC, and further increase to 450 °C led higher S-OSC than that at 400 °C but the value was still lower than S-OSC calculated at 350 °C. Thus, it was also confirmed that the relation between S-OSC and WGS activity is important but rather limited, as discussed above for 0.5Pt-0.5Re-0.5V/CeO.

Hence, as a general outcome; the results point out that the surface groups determined in S-OSC measurements have significant roles in the beginning of WGS reaction, especially in water activation at the time when reactive mixture first contacts the catalyst; however, after the concentrations on catalyst surface and redox mechanism reach steady state, E-OSC becomes the determining factor for WGS activity.

5. CONCLUSION

5.1. Conclusions

The main purpose of this study is to design and develop high performance, steam tolerant, non-pyrophoric WGS catalyst(s) to be used in a demo-scale fuel processor (DFP) producing PEM grade hydrogen for PEM fuel cells. This work mainly focuses on developing a reliable methodology for determination of oxygen storage capacity (OSC) of the catalysts through the use of *operando* IGA-MS analysis; and establishing a relation between WGS activity and OSC. The current work involves determination of WGS performance of selected Pt-Re-V systems under realistic conditions at different reaction temperatures; suggesting and confirming an *operando* methodology for measuring oxygen storage capacity (OSC) of the samples, and determination of OSC values of the samples; and establishing a relation between WGS performance and OSCs. The major conclusions of this study can be summarized as follows:

The results of performance tests indicated that 1Pt-1Re-1V/CeO_2 catalyst may be a great candidate to be used in a fuel processor due to its high activity, selectivity and stability. The catalysts showed their highest performances at 350 and 400 °C and the highest net H_2 production values were achieved over 1Pt-1Re-1V and 0.5Pt-0.5Re-0.5V catalysts at 350 and 400 °C, respectively under feed flow having low H_2O/CO ratio, RF#1. No pronounced differences were detected between the catalysts' performances under RF #2 flow. Moreover, all samples presented more stable performance when they were exposed to RF #1 flow having low H_2O/CO ratio.

SEM analysis showed that well dispersed Pt particles on blossom-like CeO_2 formations having 30-50 nm width. XPS results revealed that Ce^{3+} content of 1Pt-1Re-1V/CeO_2 catalyst having superior WGS activity was relatively higher and decreased through reaction for all samples. No bulk V_2O_5 crystals was observed in analyses indicating vanadium was highly dispersed at surface. CO Chemisorption analysis presented the Pt

dispersion value for 1Pt-1Re-1V/CeO_2 catalyst sample as 37%. For the samples having lower Pt which are 0.5Pt-1Re-1V/CeO_2 and 0.5Pt-0.5Re-0.5V/CeO_2, 15% Pt dispersion was obtained.

The OSC values of the catalysts were decided through a novel *operando* IGA-MS methodology under two realistic feed compositions at 350 °C by fixed GHSV as 40,000 ml g_{cat}^{-1} h^{-1}. The sample having superior performance was also tested at 400 and 450 °C. The combined evaluation of WGS performance and OSC results indicates that there are two types of OSC; structural oxygen storage capacity (S-OSC) which defines the oxygen in surface groups and effective (E-OSC) having noticeable effect on WGS performance and increase in reaction temperature have negative effect on it. Hence, S-OSC including surface groups have key role in water activation at the time when reactive mixture first contacts with the catalyst, while E-OSC becomes primary factor affecting WGS activity after the surface concentrations reach steady state.

5.2. Recommendations

Following topics are recommended for future studies on Pt-Re-V/CeO_2 system:

- *operando* FTIR-DRIFTS studies under realistic conditions should be performed to investigate WGS reaction mechanism(s);

- The robustness of WGS catalysts during transient fuel processor operations, especially during testing cycles involving exposure of catalyst to air and liquid water, should be studied in detail;

- Additional OSC tests should be performed for reference systems, like Pt/CeO_2, Re/CeO_2, V/CeO_2, Pt-Re/CeO_2, Pt-V/CeO_2 and Re-V/CeO_2, to form a reliable reference basis/benchmarks in investigating the effect of adding metal or promoter on OSC;

- New and different catalyst preparation methodologies should be parametrically investigated to see their effects on OSC.

REFERENCES

Andreeva, D., I. Ivanov, L. Ilieva, J. W. Sobczak, G. Avdeev and T. Tabakova, 2007, "Nanosized gold catalysts supported on ceria and ceria-alumina for WGS reaction: Influence of the preparation method", *Applied Catalysis A: General*, Vol. 333, pp. 153-160.

Aneggi, E., M. Boaro, C. Leitenburg, G. Dolcetti and A. Trovarelli, 2006, "Insights into the redox properties of ceria-based oxides and their implications in catalysis", *Journal of Alloys and Compounds*, Vol. 408-412, pp. 1096-1102.

Araujo, G. C. and M. C. Rangel, 2000, "An environmental friendly catalyst for the high temperature shift reaction", *Studies in Surface Science and Catalysis*, Vol. 130, pp. 1601-1606.

Avcı, A. K., D. L. Trimm, A. E. Aksoylu and Z. İ. Önsan, 2004, "Hydrogen production by steam reforming of n-butane over supported Ni and Pt-Ni catalysts", *Applied Catalysis A: General*, Vol. 258, pp. 235-240.

Ayandiran, A. A., I. A. Bakare, H. Binous, S. Al-Ghamdi, S. A. Razzak and M. M. Hossain, 2016, "Oxidative dehydrogenation of propane to propylene over VO_x/CaO–γ-Al_2O_3 using lattice oxygen", *Catalysis Science and Technology*, Vol. 6, pp. 5154-5167.

Azzam, K. G., I. V. Babich, K. Seshan, B. L. Mojet and L. Lefferts, 2013, "Stable and Efficient Pt-Re/TiO_2 catalysts for Water-Gas Shift: Effect of Rhenium", *Chemistry & Catalysis*, Vol. 5, pp. 557-564.

Azzam, K. G., I. V. Babich, K. Seshan and L. Lefferts, 2008, "Role of Re in Pt-Re/TiO_2 Catalyst for Water Gas Shift Reaction: A Mechanistic and Kinetic Study", *Applied Catalysis B: Environmental*, Vol. 80, pp. 129-140.

Ballarini, N., A. Battisti, F. Cavani, A. Cericola, C. Lucarelli, S. Racioppi and P. Arpentinier, 2006, "The Oxygen-Assisted Transformation of Propane to CO_x/H_2 through Combined Oxidation and WGS Reactions Catalyzed by Vanadium-Oxide Based Catalysts", *Catalysis Today*, Vol. 116, pp. 313-323.

Başar, M.S., 2016, *A Study on Co-Free Hydrogen Production and Adsorbent Design for Selective Carbon Dioxide Removal*, Ph. D. Thesis, Boğaziçi University.

Bedrane, S., C. Descorme and D. Duprez, 2002, "Investigation of the oxygen storage process on ceria and ceria–zirconia-supported catalysts", *Catalysis Today*, Vol. 75, pp. 401-405.

Bo, Z., S. Ahn, M.A. Ardagh, N.M Schweitzer, C. P. Canlas, O. K. Farha and J. M. Notestein, 2018, "Synthesis and stabilization of small Pt nanoparticles on TiO_2 partially masked by SiO_2", *Applied Catalysis A: General*, Vol. 551, 122-128.

Budiman, A., M. Ridwan, S. M. Kim, J. Choi, C. W. Yoon, J. Ha, D. J. Suh and Y. Suh, 2013, "Design and preparation of high-surface-area $Cu/ZnO/Al_2O_3$ catalysts using a modified co-precipitation method for the water-gas shift reaction", *Applied Catalysis A: General*, Vol. 462-463, pp. 220-226.

Campbell, C. T., and C. H. F. Peden, 2005. "Oxygen Vacancies and Catalysis on Ceria Surface", *Science*, 309, pp. 713-714.

Chen, W., C. Tsai, Y. Lin, R. Chein and C. Yu, 2017, "Reaction phenomena of high-temperature water gas shift reaction in a membrane reactor", *Fuel*, Vol. 199, pp. 358-371.

Chen, Y., H. Wang, R. Burch, C. Hardacre and P. Hu, 2011, "New insight into mechanisms in water-gas-shift reaction on Au/CeO_2 (111): A density functional theory and kinetic study", *Faraday Discussions*, Vol. 152, pp. 121-133.

Choung, S. Y., M. Ferrandon and T. Krause, 2005, "Pt-Re bimetallic supported on CeO_2-ZrO_2 mixed oxides as water–gas shift catalysts", *Catalysis Today*, Vol. 99, pp. 257-262.

Çağlayan, B. S. and A. E. Aksoylu, 2009, "Water-Gas Shift Reaction over Bimetallic Pt-Ni/Al_2O_3 Catalysts", *Turkish Journal of Chemistry*, Vol. 33, pp. 249-256.

Çağlayan, B. S. and A. E. Aksoylu, 2011, "Water-gas shift activity of ceria supported Au-Re catalysts", *Catalysis Communications*, Vol. 12, pp. 1206-1211.

Çağlayan, B. S., İ. I. Soykal and A. E. Aksoylu, 2011, "Preferential oxidation of CO over Pt–Sn/AC catalyst: Adsorption, performance and DRIFTS studies", *Applied Catalysis B: Environmental*, Vol. 106, pp. 540-549.

Çağlayan, B. S., Z. İ. Önsan and A. E. Aksoylu, 2005, "Production of hydrogen over bimetallic Pt-Ni/δ-Al_2O_3: II. Indirect partial oxidation of LPG", *Catalysis Letters*, Vol. 102, pp. 63-67.

Çavusoglu, G., D. Miao, H. Lichtenberg, H. W. P. Carvalho, H. Xu, A. Goldbach and J. Grunwaldt, "Structure and activity of flame made ceria supported Rh and Pt water gas shift catalysts", *Applied Catalysis A: General*, Vol. 504, pp. 381-390.

Demeter, M., M. Neumann and W. Reichelt, 2000, "Mixed-Valence Vanadium Oxides Studied By XPS", *Surface Science*, Vol. 454-456, pp. 41-44.

Demirhan C. D., 2015, *Design and Development of WGS Catalysts for Small Scale Hydrogen Production Units*, M. S. Thesis, Boğaziçi University.

Duarte de Farias, A. M., P. Bargiela, M. G. C. Rocha and M. A. Fraga, 2008, "Vanadium-promoted Pt/CeO_2 catalyst for water–gas shift reaction", *Journal of Catalysis*, Vol. 260, pp. 93-102.

Dufour, J., C. Martos, A. Ruiz and F. J. Ayuela, 2013, "Effect of the precursor on the activity of high temperature water gas shift catalysts", *International Journal of Hydrogen Energy*, Vol. 38, pp. 7647-7653.

Duke, A. S., K. Xie, A. J. Brandt, T. D. Maddumapatabandi, S. C. Ammal, A. Heyden, J. R. Monnier and D. A. Chen, 2017, "Understanding Active Sites in the Water–Gas Shift Reaction for Pt–Re Catalysts on Titania", *American Chemical Society Catalysis*, Vol. 7, pp. 2597-2606.

Edwards, M. A., D. M. Whittle, C. Rhodes, A. M. Ward, D. Rohan, M. D. Shannon, G. J. Hutchings and C. J. Kiely, 2002, "Microstructural studies of the copper promoted iron oxide/chromia water-gas shift catalyst", *Physical Chemistry Chemical Physics*, Vol. 4, pp. 3902-3908.

Escritori, J. C., S. C. Dantas, R. R. Soares and C. E. Hori, 2009, "Methane autothermal reforming on nickel–ceria–zirconia based catalysts", *Catalysis Communications*, Vol. 10, pp. 1090-1094.

Figueiredo, R. T., M. S. Santos, H. M. C. Andrade and J. L. G. Fierro, 2011, "Effect of alkali cations on the $CuZnOAl_2O_3$ low temperature water gas-shift catalyst, *Catalysis Today*, Vol. 172, pp. 166-170.

Frenia, S., G. Calogeroa and S. Cavallarob, 2000, "Hydrogen production from methane through catalytic partial oxidation reactions", *Journal of Power Sources*, Vol. 87, pp. 28-38.

Fu, Q., S. Kudriavtseva, H. Saltsburg and M. Flytzani-Stephanopoulos, 2003, "Gold–ceria catalysts for low-temperature water-gas shift reaction", *Chemical Engineering Journal*, Vol. 93, pp. 41-53.

Fu, W., Z. Bao, W. Ding, K. Chou and Q. Li, 2011, "The synergistic effect of the structural precursors of $Cu/ZnO/Al_2O_3$ catalysts for water–gas shift reaction", *Catalysis Communications*, Vol. 12, pp. 505-509.

Ghenciu, A. F., 2002, "Review of fuel processing catalysts for hydrogen production in PEM fuel cell systems", *Current Opinion in Solid State and Materials Science*, Vol. 6, pp. 389-399.

Goguet, A., F. C. Meuiner, D. Tibiletti, J. P. Breen and R. Burch, 2004, "Spectrokinetic Investigation of Reverse Water-Gas-Shift Reaction Intermediates over a Pt/CeO_2 Catalyst", *Journal of Physical Chemistry B*, Vol. 108, pp. 20240-20246.

Gonzáles-Castaño, M., T. R. Reina, S. Ivanova, L. M. Martinez Tejada, M.A. Centeno and J. A. Odriozola, 2016, "O_2-assisted Water Gas Shift reaction over structured Au and Pt catalysts", *Applied Catalysis B: Environmental*, Vol. 185, pp. 337-343.

Gonzáles-Castaño, M., T. R. Reina, S. Ivanova, M. A. Centeno, J. A. Odriozola, 2014, "Pt vs. Au in water–gas shift reaction", *Journal of Catalysis*, Vol. 314, pp. 1-9.

Harshini, D., D. H. Lee, J. Jeong, Y. Kim, S. W. Nam, H. C. Ham, J. H. Han, T. Lim and C. W. Yoon, 2014, "Enhanced oxygen storage capacity of $Ce_{0.65}Hf_{0.25}M_{0.1}O_{2-\delta}$ (M = rare earth elements): Applications to methane steam reforming with high coking resistance", *Applied Catalysis B: Environmental*, Vol. 148-149, pp. 415-423.

Haryanto, A., S. Fernando, N. Murali and S. Adhikari, 2005, "Current Status of Hydrogen Production Techniques by Steam Reforming of Ethanol: A Review", *Energy & Fuels*, Vol. 19, pp. 2098-2106.

Hilarie, S., S. Sharma, R. J. Gorte, J. M. Vohs and H. Jen, 2000, "Effect of SO_2 on the oxygen storage capacity of ceria-based catalysts", *Catalysis Letters*, Vol. 70, pp. 131-135.

Hori, C. E., H. Permana, K. Y. S. Ng, A. Brenner, K. More, K. M. Rahmoeller and D. Belton, 1998, "Thermal stability of oxygen storage properties in a mixed CeO_2-ZrO_2 system", *Applied Catalysis B: Environmental*, Vol. 16, pp. 105-117.

Höök, M., and T. Xu, 2013, "Depletion of fossil fuels and anthropogenic climate change", *Energy Policy*, Vol. 52, pp. 797-809.

Hwang, K., J. Park and S. Ihm, 2011, "Si-Modified Pt/CeO_2 Catalyst for a Single-Stage Water-Gas Shift Reaction", *International Journal of Hydrogen Energy*, Vol. 36, pp. 9685-9693.

Hwang, K., S. Ihm, S. Park and J. Park, 2013, "Pt/ZrO_2 catalyst for a single-stage water-gas shift reaction: Ti addition effect", *International Journal of Hydrogen Energy*, Vol. 38, pp. 6044-6051.

Iida, H., A. Igarashi, 2006, "Structure characterization of Pt-Re/TiO_2 (rutile) and Pt-Re/ZrO_2 catalysts for water gas shift reaction at low-temperature", *Applied Catalysis A: General*, Vol. 303, pp. 192-198.

Iida, H., K. Kondo, A. Igarashi, 2006, "Effect of Pt precursors on catalytic activity of Pt/TiO_2 (rutile) for water gas shift reaction at low-temperature", *Catalysis Communications*, Vol. 7, pp. 240-244.

Iulianelli, A., P. Ribeirinha, A. Mendes and A. Basile, 2014, "Methanol steam reforming for hydrogen generation via conventional and membrane reactors: A review", *Renewable and Sustainable Energy Reviews*, Vol. 29, pp. 355-368.

Ivanov, I., P. Petrova, V. Georgiev, T. Batakliev, Y. Karakirova, V. Serga, L. Kulikova, A. Eliyas and S. Rakovsky, 2013, "Comparative Study of Ceria Supported Nano-sized Platinum Catalysts Synthesized by Extractive-Pyrolytic Method for Low-Temperature WGS Reaction", *Catalysis Letters*, Vol. 143, pp. 942-949.

Jain, R., A. S. Poyraz, D. P. Gamliel, J. Valla, S. L. Suib and R. Maric, 2015, "Comparative study for low temperature water-gas shift reaction on Pt/ceria catalysts: Role of different ceria supports", *Applied Catalysis A: General*, Vol. 507, pp. 1-13.

Jardim, E. O., S. Rico-Francés, F. Coloma, J. A. Anderson, J. Silvestre-Albero, and A. Sepúlveda-Escribano, 2015, "Influence of the metal precursor on the catalytic behavior of Pt/Ceria catalysts in the preferential oxidation of CO in the presence of H_2", *Journal of Colloid and Interface Science*, Vol. 443, pp. 45-55.

Jeong, D., H. Na, J. Shim, W. Jang, H. Roh, U. H. Jung and W. L. Yoon, 2014, "Hydrogen production from low temperature WGS reaction on co-precipitated Cu-CeO_2 catalysts: An optimization of Cu loading", *International Journal of Hydrogen Energy*, Vol. 39, pp. 9135-9142.

Jeong, D., H. S. Potdar, J. Shim, W. Jang and H. Roh, 2013, "H_2 production from a single stage water gas shift reaction over Pt/CeO_2, Pt/ZrO_2, and Pt/$Ce_{(1-x)}Zr_{(x)}O_2$ catalysts", *International journal of Hydrogen Energy*, Vol. 38, pp. 4502-4507.

Jha, A., Y. Lee, W. Jang, J. Shim, K. Jeon, H. Na, H. Kim, H. Roh, D. Jeong, S. G. Jeon, J. Na, W. L. Yoon, 2017, "Effect of the redox properties of support oxide over cobalt-based catalysts in high temperature water-gas shift reaction", *Molecular Catalysis*, Vol. 433, pp. 145-152.

Júnior, I. L., J. M. Millet, M. Aouine and M. C. Rangel, 2005, "The Role of Vanadium on the Properties of Iron Based Catalysts for the Water Gas Shift Reaction", *Applied Catalysis A: General*, Vol. 283, pp. 91-98.

Kašpar, J., P. Fornasiero and M. Graziani, 1999, "Use of CeO_2-based oxides in the three-way catalysis", *Catalysis Today*, Vol. 50, pp. 285-298.

Kesim, B., 2017, *An Experimental Study on Optimization of Pt-Based Trimetallic WGS Catalysts*, M. S. Thesis, Boğaziçi University.

Khossusi, T., R. Douglas and G. McCullough, 2003, "Measurement of oxygen storage capacity in automotive catalysts", *Journal of Automobile Engineering*, Vol. 217, pp. 727-733.

Kluksdahl, 1968, "Reforming a sulfur-free naphtha with a platinum-rhenium catalyst", *US Patent*, 3415737 A.

Kugai, J., E. B. Fox and C. Song, 2015, "Kinetic characteristics of oxygen-enhanced water gas shift on CeO_2-supported Pt-Cu and Pd-Cu bimetallic catalysts", *Applied Catalysis A: General*, Vol. 497, pp. 31-41.

Kugai, J., J. T. Miller, N. Guo and C. Song, 2011, "Oxygen-enhanced water gas shift on ceria-supported Pd–Cu and Pt–Cu bimetallic catalysts", *Journal of Catalysis*, Vol. 277, pp. 46-53.

Lee, H. C., D. Lee, O. Y. Lim, S. Kim, Y. T. Kim, E. Ko and E. D. Park, 2007, "ZrO_2-supported Pt catalysts for water gas shift reaction and their non-pyrophoric property", *Studies in Surface Science and Catalysis*, Vol. 167, pp. 201-206.

Lenarda, A., M. Bellini, A. Marchionni, H. A. Miller, T. Montini, M. Melchionna, F. Vizza, M. Prato and P. Fornasiero, 2018, "Nanostructured carbon supported Pd-ceria as anode catalysts for anion exchange membrane fuel cells fed with polyalcohols", *Inorganica Chimica Acta*, Vol. 470, pp. 213-220.

LeValley, T. L., A. R. Richard and M. Fan, 2014, "The Progress in Water Gas Shift and Steam Reforming Hydrogen Production Technologies–A Review", *International Journal of Hydrogen Energy*, Vol. 39, pp. 16983-17000.

Li, H., Y. Bi, J. Yan, L. Zhang and X. Yin, 2013, "Bulk oxygen promoted water–gas shift reaction activity over $Pt/Ce_{0.6}Zr_{0.4}O_2$ catalyst", *Catalysis Communications*, Vol. 42, pp. 45-49.

Lin, X., Y. Zhang, L. Yin, C. Chen, Y. Zhan and D. Li, 2014, "Characterization and catalytic performance of copper-based WGS catalysts derived from copper ferrite", *International Journal of Hydrogen Energy*, Vol. 39, pp. 6424-6432.

Mariño, F., C. Descorme and D. Duprez, 2004, "Noble metal catalysts for the preferential oxidation of carbon monoxide in the presence of hydrogen (PROX)", *Applied Catalysis B: Environmental*, Vol. 54, pp. 59-66.

Martinez-Huerta, M. V., G. Deo, J. L. G. Fiberro and M. A. Bañares, 2008, "Operando Raman-GC Study on the Structure-Activity Relationships in V^{5+}/CeO_2 for Catalyst Ethane Oxidative Dehydrogenation: The Formation of $CeVO_4$", *The Journal of Physical Chemistry C*, Vol. 112, pp. 11441-11447.

Martos, C., J. Dufour and A. Ruiz, 2009, "Synthesis of Fe_3O_4-based catalysts for the high-temperature water gas shift reaction", *International Journal of Hydrogen Energy*, Vol. 34, pp. 4475-4481.

Mei, Z., Y. Li, M. Fan, L. Zhao and J. Zhao, 2015, "Effect of the interactions between Pt species and ceria on Pt/ceria catalysts for water gas shift: The XPS studies", *Chemical Engineering Journal*, Vol. 259, pp. 293-302.

Meshkani, F. and M. Rezaei, 2014, "A facile method for preparation of iron based catalysts for high temperature water gas shift reaction", *Journal of Industrial and Engineering Chemistry*, Vol. 20, pp. 3297-3302.

Miao, D., G. Cavusoglu, H. Lichtenberg, J. Yu, H. Xu, J. Grunwaldt and A. Goldbach, 2017, "Water-gas shift reaction over platinum/strontium apatite catalysts", *Applied Catalysis B: Environmental*, Vol. 202, pp. 587-596.

Mohammed, Z., V. D. B. C. Dasireddy, S. Singh and H. B. Friedrich, 2016, "The preferential oxidation of CO in hydrogen rich streams over platinum doped nickel oxide catalysts", *Applied Catalysis B: Environmental*, Vol. 180, pp. 687-697.

Mond, L. and C. Langer, 1888, "Improvements in Obtaining Hydrogen", *British Patent,* 12608.

Montini, T., M. Melchionna, M. Monai, and P. Fornasiero, 2016, "Fundamentals and catalytic applications of CeO_2-based materials", *Chemical Reviews,* 116, 5987-6041.

Nahar, G., D. Mote and V. Dupont, 2017, "Hydrogen production from reforming of biogas: Review of technological advances and an Indian perspective", *Renewable and Sustainable Energy Reviews,* Vol. 76, pp. 1032-1052.

Natesakhawat, S., X. Wang, L. Zhang and U. S. Ozkan, 2006, "Development of Chromium-Free Iron-Based Catalysts for High-Temperature Water-Gas Shift Reaction", *Journal of Molecular Catalysis A: Chemical,* Vol. 260, pp. 82-94.

Nguyen-Thanh, D., A. M. Duarte De Farias and M. A. Fraga, 2008, "Characterization and activity of vanadia-promoted Pt/ZrO_2 catalysts for the water–gas shift reaction", *Catalysis Today,* Vol. 138, pp. 235-238.

Önsan, Z. İ., 2007, "Catalytic Processes for Clean Hydrogen Production from Hydrocarbons", *Turkish Journal of Chemistry,* Vol. 31, pp. 531-550.

Özer, Ö., 2016, *Design and Development of Pt-Based Trimetallic WGS Catalysts*, M. S. Thesis, Boğaziçi University.

Paksoy, A. İ., B. S. Çağlayan and A. E. Aksoylu, 2015, "A Study on Characterization and Methane Dry Reforming Performance of $Co\text{-}Ce/ZrO_2$ Catalyst", *Applied Catalysis B: Environmental,* Vol. 168-169, pp. 164-174.

Palma, V. and M. Martino, 2017, "Pt-Re Based Catalysts for the Realization of a Single Stage Water Gas Shift Process", *Chemical Engineering Transactions,* Vol. 57, pp. 1657-1662.

Panagiotopoulou, P. and D. I. Kondarides, 2006, "Effect of the nature of the support on the catalytic performance of noble metal catalysts for the water–gas shift reaction", *Catalysis Today*, Vol. 112, pp. 49-52.

Panagiotopoulou, P. and D. I. Kondarides, 2007, "A comparative study of the water-gas shift activity of Pt catalysts supported on single (MO_x) and composite (MO_x/Al_2O_3, MO_x/TiO_2) metal oxide carriers", *Catalysis Today*, Vol. 127, pp. 319-329.

Pastor-Perez, L., R. B. Sierra and A. S. Escribano, 2014, "CeO_2-Promoted Ni/Activated Carbon Catalysts for the Water-Gas Shift (WGS) Reaction", *International Journal of Hydrogen Energy*, Vol. 39, pp. 17589-17599.

Pastor-Perez, L., T.R. Reina, S. Ivanova, M. Á. Centeno, J. A. Odriozola and A. Sepúlveda-Escribano, 2015, "Ni-CeO_2/C Catalysts with Enhanced OSC for the WGS Reaction", *Catalysis*, Vol. 5, pp. 298-309.

Pazmiño, J. H., M. Shekhar, W. D. Williams, M. C. Akatay, J. T. Miller, W. N. Delgass and F. H. Ribeiro, 2012, "Metallic Pt as active sites for the water–gas shift reaction on alkali-promoted supported catalysts", *Journal of Catalysis*, Vol. 286, pp. 279-286.

Perdomo, C., A. Pérez, R. Molina and S. Moreno, 2016, "Storage capacity and oxygen mobility in mixed oxides from transition metals promoted by cerium", *Applied Surface Science*, Vol. 383, pp. 42-48.

Pieck, C.L., C.R. Vera, J.M. Perera, G.N. Gimenez, L.R. Serra, L.S. Carvalho and M.C. Rangel, 2005, "Metal dispersion and catalytic activity of trimetallic Pt-Re-Sn/Al_2O_3 naphtha reforming catalysts", *Catalysis Today*, Vol. 107-108, pp. 637-642.

Pierre, D., W. Deng and M. F. Stephanopoulos, 2007, "The Importance of Strongly Bound Pt-CeO_x Species for the Water-gas Shift Reaction: Catalyst Activity and Stability Evaluation", *Topics in Catalysis*, Vol. 46, pp. 363-373.

Porsin, A. V., E. A. Alikin and V. I. Bukhtiyarov, 2016, "A low temperature method for measuring oxygen storage capacity of ceria-containing oxides", *Catalysis Science and Technology*, Vol. 6, pp. 5891-5898.

Pozdnyakova, O., D. Teschner, A. Wootsch, J. Kröhnert, B. Steinhauer, H. Sauer, L. Toth, F. C. Jentoft, A. Knop-Gericke, Z. Paál and R. Schögl, 2006, "Preferential CO oxidation in hydrogen (PROX) on ceria-supported catalysts, part I: Oxidation state and surface species on Pt/CeO_2 under reaction conditions", *Journal of Catalysis*, Vol. 237, pp. 1-16.

Price, C., L. Pastor-Pérez, E. le Saché, A. Sepúlveda-Escribano, and T. R. Reina, 2017, "Highly active Cu-ZnO catalysts for the WGS reaction at medium high space velocities: Effect of the support composition", *International Journal of Hydrogen Energy*, Vol. 42, pp. 10747-10751.

Radhakrishnan, R., R. R. Willigan, Z. Dardas and T. H. Vanderspurt, 2006, "Water gas shift activity and kinetics of Pt/Re catalysts supported on ceria-zirconia oxides", *Applied Catalysis B: Environmental*, Vol. 66, pp. 23-28.

Ratnasamy, C. and J. P. Wagner, 2009, "Water Gas Shift Catalysis", *Catalysis Reviews: Science and Engineering*, Vol. 51, pp. 325-440.

Reddy, B. M. and A. Khan, 2005, "Nanosized CeO_2–SiO_2, CeO_2–TiO_2, and CeO_2–ZrO_2 Mixed Oxides: Influence of Supporting Oxide on Thermal Stability and Oxygen Storage Properties of Ceria", *Catalysis Survey from Asia*, Vol. 9, pp. 155-171.

Reddy, G. K. and P. G. Smirniotis, 2015, *Water Gas Shift Reaction: Research Developments and Applications*, Elsevier, Amsterdam.

Reina, T. R., S. Ivanova, M. A. Centeno and J. A. Odriozola, 2015, "Boosting the activity of a $Au/CeO_2/Al_2O_3$ catalyst for the WGS reaction", *Catalysis Today*, Vol. 253, pp. 149-154.

Reina, T. R., S. Ivanova, M. A. Centeno and J. A. Odriozola, 2016, "The role of Au, Cu & CeO_2 and their interactions for an enhanced WGS performance", *Applied Catalysis B: Environmental*, Vol. 187, pp. 98-107.

Ribeiro, M. C., G. Jacobs, L. Linganiso, K. G. Azzam, U. M. Graham and B. H. Davis, 2011, "Low Temperature Water Gas Shift: Evaluation of Pt/HfO_2 and Correlation between Reaction Mechanism and Periodic Trends in Tetravalent (Ti, Zr, Hf, Ce, Th) Metal Oxides", *American Chemical Society Catalysis*, Vol. 1, pp. 1375-1383.

Rico-Frances, S., E. O. Jardim, T. A. Wezendonk, F. Kapteijn, J. Gascon, A. S. Escribano and E. V. Ramos-Fernandez, 2016, "Highly Dispersed $Pt^{\delta+}$ on $Ti_xCe_{(1-x)}O_2$ as an Active Phase in Preferential Oxidation of CO", *Applied Catalyst B: Environmental*, Vol. 180, pp. 169-178.

Roh, H., H. S. Potdar, D. Jeong, K. Kim, J. Shim, W. Jang, K. Y. Koo and W. L. Yoon, 2012, "Synthesis of highly active nano-sized (1 wt.% Pt/CeO_2) catalyst for water gas shift reaction in medium temperature application", *Catalysis Today*, Vol. 185, pp. 113-118.

Romero-Sarria, F., S. Garcia-Dali, S. Palma, E.M. Jimenez-Barrera, L. Oliviero, P. Bazin and J. A. Odriozola, 2016, "The role of carbon overlayers on Pt-based catalysts for H_2-cleanup by CO-PROX", *Surface Science*, Vol. 648, pp. 84-91.

Saeidi, S., F. Fazlollahi, S. Najari, D. Iranshahi, J.J. Klemeš, and L.L. Baxter, 2017, "Hydrogen Production: Perspectives, separation with special emphasis on kinetics of WGS reaction: A state-of-the-art review", *Journal of Industrial and Engineering Chemistry*, Vol. 49, pp. 1-25.

Santos, J. L., T. R. Reina, S. Ivanova, M. A. Centeno and J. A. Odriozola, 2017, "Gold promoted Cu/ZnO/Al_2O_3 catalysts prepared from hydrotalcite precursors: Advanced materials for the WGS reaction", *Applied Catalysis B: Environmental*, Vol. 201, pp. 310-317.

Sathre, R., 2014, "Comparing the heat of combustion of fossil fuels to the heat accumulated by their lifecycle greenhouse gases", *Fuel*, Vol. 115, pp. 674-677.

Sato, Y., K. Terada, S. Hasegawa, T. Miyao and S. Naito, 2005, "Mechanistic study of water–gas-shift reaction over TiO_2 supported Pt–Re and Pd–Re catalysts", *Applied Catalysis A: General*, Vol. 296, pp. 80-89.

Sharaf, O. Z. and M. F. Orhan, 2014, "An overview of fuel cell technology: Fundamentals and applications", *Renewable and Sustainable Energy Reviews*, Vol. 32, pp. 810-853.

Silva, A. M., A. M. Duarte de Farias, L. O. O. Costa, A. Barandas, L. V. Mattos, M. A. Fraga and F. B. Noronha, 2008, "Partial oxidation and water-gas shift reaction in an integrated system for hydrogen production from ethanol", *Applied Catalysis A: General*, Vol. 334, pp. 179-186.

Soria, M. A., P. Pérez, S. A. C. Carabineiro, F. J. Maldonado-Hodar, A. Mendes and L.M. Madeira, 2014, "Effect of the preparation method on the catalytic activity and stability of Au/Fe_2O_3 catalysts in the low-temperature water–gas shift reaction", *Applied Catalysis A: General*, Vol. 470, pp. 45-55.

Suchorski, y. L.R. Struckmann, F. Klose, Y. Ye, M. Alandjiyska, K. Sundmacher and H. Weiss, 2005, "Evolution of Oxidation States in Vanadium-based Catalysts under Conventional XPS Conditions", *Applied Surface Science*, Vol. 249, pp. 231-237.

Swanson, M., V. V. Pushkarev, V. I. Kovalchuk and J. L. D'ıtri, 2008, "Evidence for CO Disproportionation over Ceria during Oxygen Storage Capacity Measurements: an in Situ Raman Spectroscopic Investigation", *Journal of Siberian Federal University*, Vol. 1, pp. 24-34.

Tabakova T., F. Boccuzzi, M. Manzoli and D. Andreeva, 2003, "FTIR study of low-temperature water-gas shift reaction on gold/ceria catalyst", *Applied Catalysis A: General*, Vol. 252, pp. 385-397.

Thinon, O., F. Diehl, P. Avenier and Y. Schuurman, 2008, "Screening of bifunctional water-gas shift catalysts", *Catalysis Today*, Vol. 137, pp. 29-35.

Trimm, D. L. and Z. İ. Önsan, 2001, "Onboard Fuel Conversion Hydrogen-Fuel-Cell-Driven Vehicles", *Catalysis Reviews: Science and Engineering*, Vol. 43, pp. 31-84.

Trovarelli, A., F. Zamar, J. Llorca, C. Leitenburg, G. Dolcetti and J. T. Kiss, 1997, "Nanophase Fluorite-Structured CeO_2-ZrO_2 Catalysts Prepared by high Energy Mechanical Milling: Analysis of Low Temperature Redox Activity and Oxygen Storage Capacity", *Journal of Catalysis*, Vol. 169, pp. 490-502.

Vecchietti, J., A. Bonivardi, W. Xu, D. Stacchiola, J. J. Delgado, M. Calatayud and S. E. Collins, 2014, "Understanding the Role of Oxygen Vacancies in the Water Gas Shift Reaction on Ceria-Supported Platinum Catalysts", *American Chemical Society Catalysis*, Vol. 4, pp. 2088-2096.

Vindigni, F., M. Manzoli, A. Damin, T. Tabakova and A. Zecchina, 2011, "Surface and Inner Defects in Au/CeO_2 WGS Catalysts: Relation between Raman Properties, Reactivity and Morphology", *Chemistry – A European Journal*, Vol. 17, pp. 4356-4361.

Wang, T., K. S. Chen, J. Mishler, S. C. Cho and X. C. Adroher, 2011, "A review of polymer electrolyte membrane fuel cells: Technology, applications, and needs on fundamental research", *Applied Energy*, Vol. 88, pp. 981-1007.

Wu Z., A. J. Rondinone, I. N. Ivanov and S. H. Overbury, 2011, "Structure of Vanadium Oxide Supported on Ceria by Multiwavelength Raman Spectroscopy", *The Journal of Physical Chemistry C*, Vol. 115, pp. 25368-25378.

Xu, W., R. Si, S. D. Senanayake, J. Llorca, H. Idriss, D. Stacchiola, J. C. Hanson, and J. A. Rodriguez, 2012, "In situ studies of CeO_2-supported Pt, Ru, and Pt–Ru alloy catalysts for the water–gas shift reaction: Active phases and reaction intermediates", *Journal of Catalysis*, Vol. 291, pp. 117-126.

Yao, H. C. and Y. F. Y. Yao, 1984, "Ceria in Automotive Exhaust Catalysts: I. Oxygen Storage", *Journal of Catalysis*, Vol. 86, pp. 254-265.

Yu, Q., W. Chen, Y. Li, M. Jin and Z. Suo, 2010, "The Action of Pt in Bimetallic Au-Pt/CeO_2 Catalyst for Water-Gas Shift Reaction", *Catalysis Today*, Vol. 158, pp. 324-328.

Yu, Q., X. Wu, C. Tang, L. Qi, B. Liu, F. Gao, K. Sun, L. Dong and Y. Chen, 2011, "Textural, Structural, and Morphological Characterizations and Catalytic Activity of Nanosized CeO_2-MO_x (M=Mg^{2+}, Al^{3+}, Si^{4+}) Mixed Oxides for CO Oxidation", *Journal of Colloid and Interface Science*, Vol. 354, pp. 341-352.

Zhang, L., X. Wang, J. M. Millet, P. H. Matter and U. S. Ozkan, 2008, "Investigation of highly active Fe-Al-Cu catalysts for water-gas shift reaction", *Applied Catalysis A: General*, vol. 351, pp. 1-8.

Zhu, M., T. C. R. Rocha, T. Lunkenbein, A. Knop-Gericke, R. Schlögl and I. E. Wachs, 2016, "Promotion Mechanisms of Iron Oxide-Based High Temperature Water−Gas Shift Catalysts by Chromium and Copper", *American Chemical Society Catalysis*, Vol. 6, pp. 4455-4464.

Zhu, X., M. Shen, L. L. Lobban and R. G. Mallinson, 2011, "Structural Effects of Na Promotion for High Water Gas Shift Activity on Pt-Na/TiO_2", *Journal of Catalysis*, Vol. 278, pp. 123–132.

APPENDIX A: TIME-ON-STREAM ACTIVITY DATA

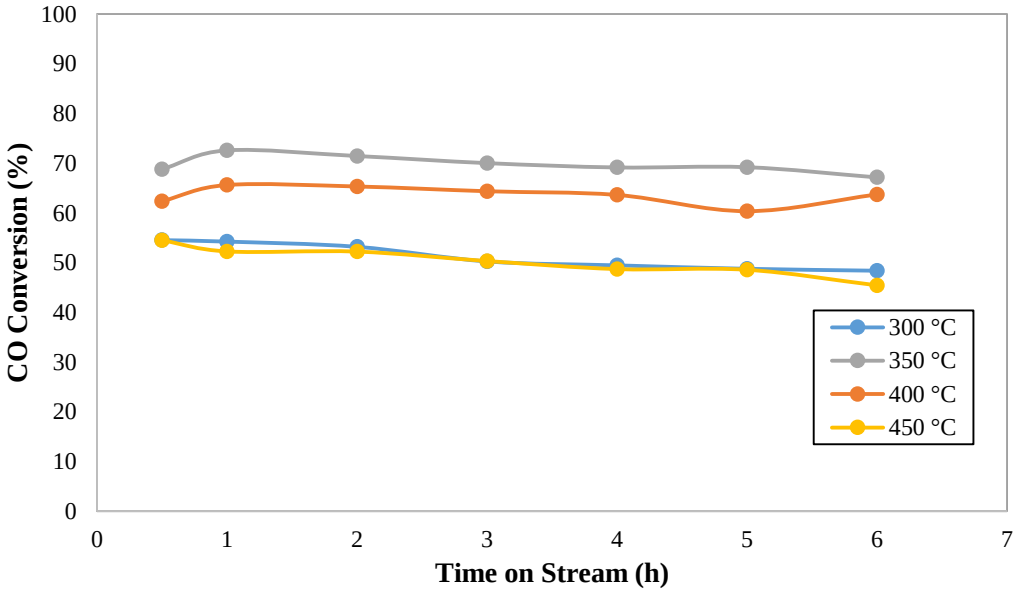

Figure A.1. Temperature dependence of time-on-stream activity data of 1Pt-1Re-1V/CeO_2 for realistic feed #1.

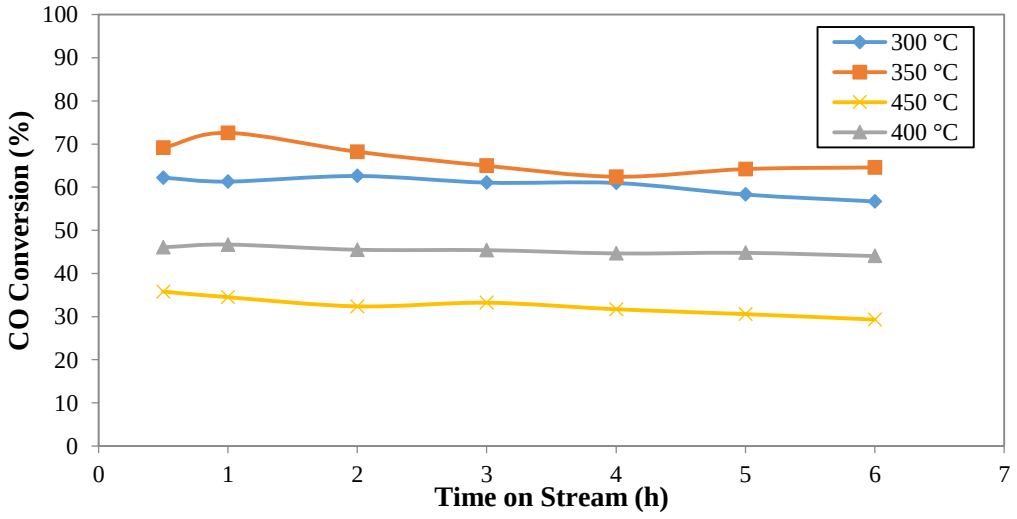

Figure A.2. Temperature dependence of time-on-stream activity data of 1Pt-1Re-1V/CeO_2 for realistic feed #2.

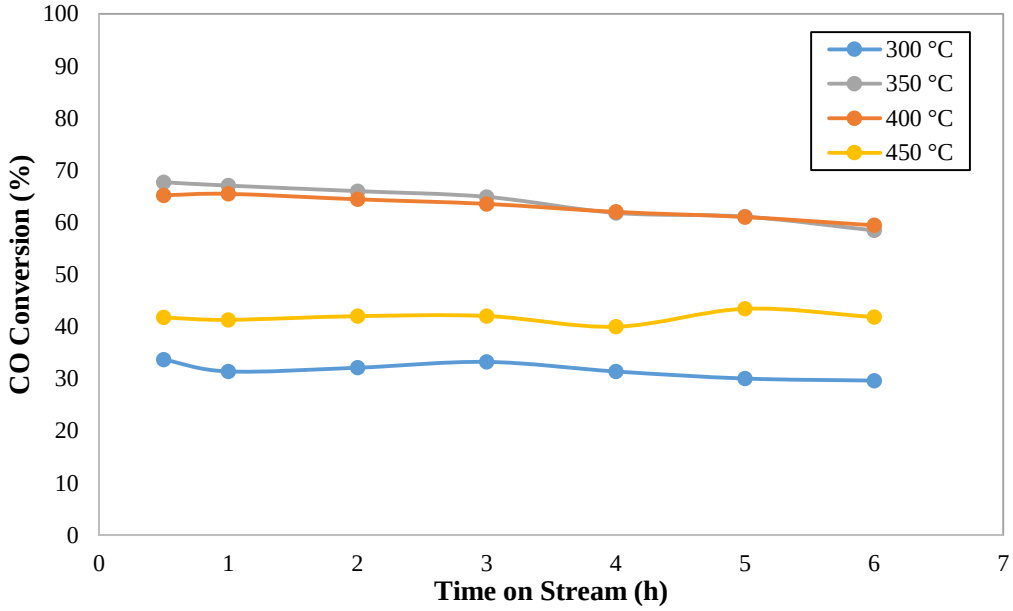

Figure A.3. Temperature dependence of time-on-stream activity data of 0.5Pt-0.5Re-0.5V/CeO_2 for realistic feed #1.

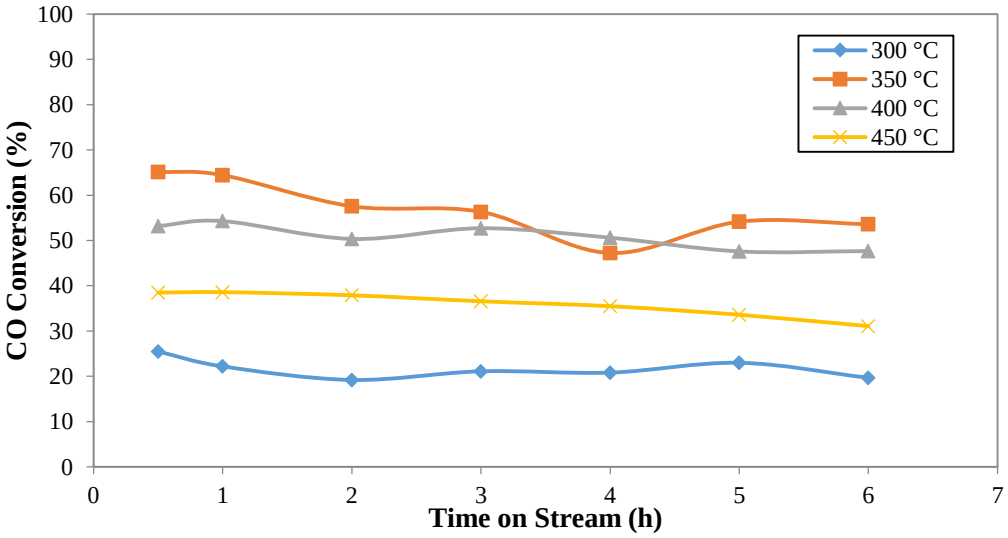

Figure A.4. Temperature dependence of time-on-stream activity data of 0.5Pt-0.5Re-0.5V/CeO_2 for realistic feed #2.

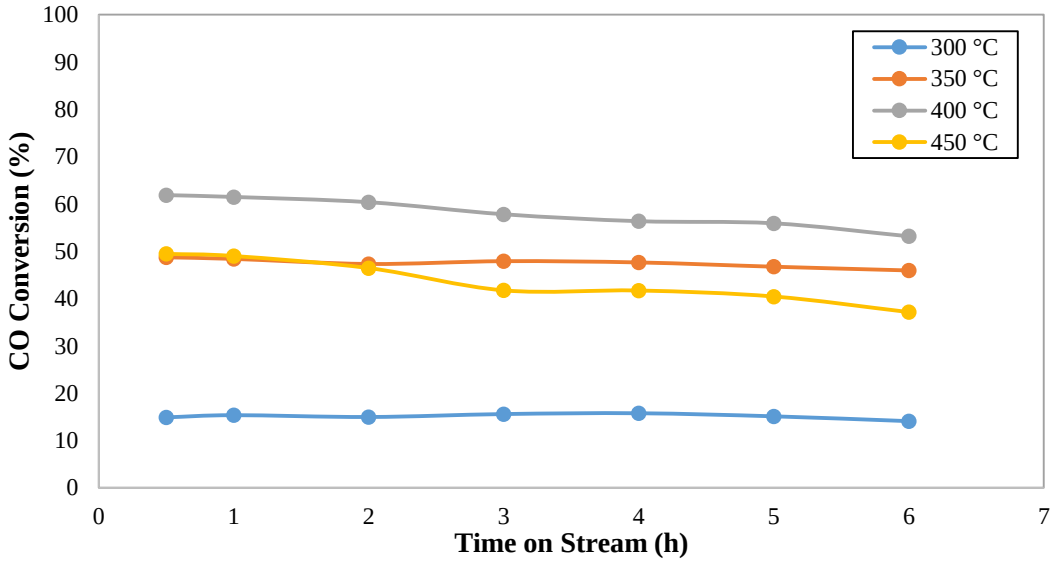

Figure A.5. Temperature dependence of time-on-stream activity data of 0.5Pt-1Re-1V/CeO_2 for realistic feed #1.

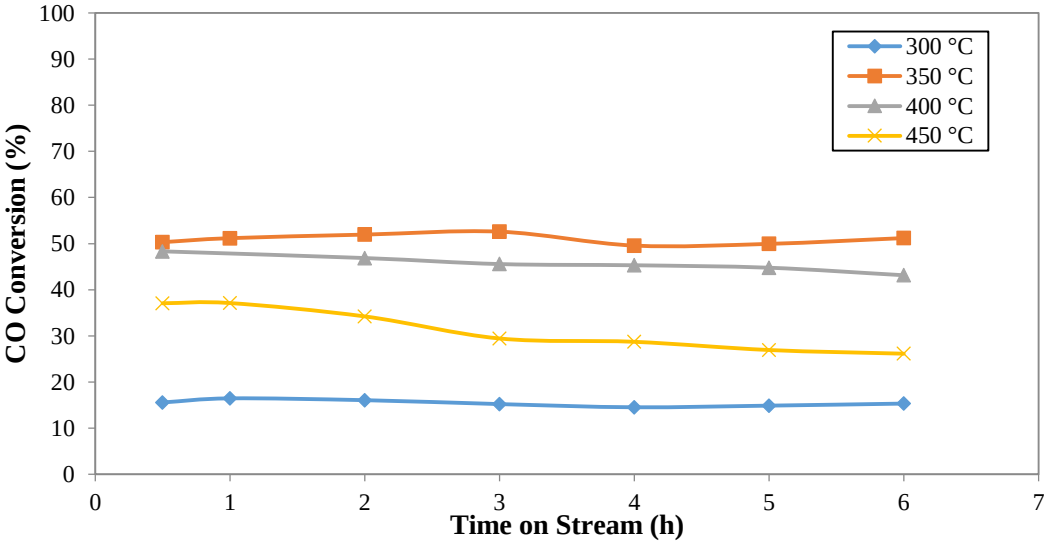

Figure A.6. Temperature dependence of time-on-stream activity data of 0.5Pt-1Re-1V/CeO_2 for realistic feed #2.